NON-EQUILIBRIUM THERMODYNAMIC STUDIES ON TRANSPORT PROCESSES OF RELEVANCE IN WATER DESALTING AND IN BIOPHYSICS

A THESIS SUBMITTED
IN PARTIAL FULFILMENT OF THE REQUIREMENTS
FOR THE DEGREE OF
DOCTOR OF PHILOSOPHY
(CHEMISTRY)

By
SAROJ YADAV

BIRLA INSTITUTE OF TECHNOLOGY AND SCIENCE
PILANI (RAJASTHAN)
MAY 1979

BIRLA INSTITUTE OF TECHNOLOGY AND SCIENCE
PILANI (RAJASTHAN)

CERTIFICATE

This is to certify that the thesis entitled "Non-Equilibrium Thermodynamic Studies on transport processes of relevance in water desalting and in Biophysics" submitted by Miss Saroj Yadav, ID No. 75S83501, for the award of Ph.D. degree of the Institute embodies original work done by her under my supervision.

R.C.Srivastava
Professor of Chemistry

PILANI
Dated: May 3, 1979.

ACKNOWLEDGEMENTS

I express my sincere thanks to Professor R.C.Srivastava, M.Sc., Ph.D., F.R.I.C.(London), Professor of Chemistry, Birla Institute of Technology and Science, Pilani, for his guidance and constant encouragement throughout the course of present investigation.

Thanks are due to the authorities of the Birla Institute of Technology and Science for making available the facilities needed for this work.

I express my thanks to Professor S.S. Mathur, Group Leader, Pharmacy Discipline, who was always very helpful.

I would also like to thank Mr S. Yashonath and Mr. Shishir Srivastava for valuable discussions I had with them. The help rendered by several other friends and colleagues is also gratefully acknowledged. I would in particular mention the names of Dr K.L. Madhok, Dr M. George Abraham, Mr A.K. Thukral, Mr. Vijay Sapra and Miss Shobha Dutt.

Financial assistance received from the Indian Council of Agricultural Research and from the Council of Scientific and Industrial Research, New Delhi is gratefully acknowledged.

I am also thankful to Mr G.D. Sharma (glass blowing section) for the fabrication of the apparatus, to Mr Ram Kumar for typing the thesis and to Messers H.C.Pant and K.N. Sharma for drawing the figures.

Last but not the least my thanks are due to my parents for their blessings.

Saroj Yadav 3.5.1979
(Saroj Yadav)

C O N T E N T S

****

PREFACE

As the title of the thesis indicates, the non-equilibrium thermodynamic studies contained in this thesis can be put in two broad categories, namely, (a) studies relevant to water desalination problem and (b) studies relevant to biophysics. The studies relevant to water desalting are described in Chapters II to IV and the studies having biophysical relevance are contained in Chapters V to VII.

One of the major problems in the area of reverse osmosis has been the search for suitable membranes. Since clays are known to possess salt rejection properties when aqueous solutions of electrolytes are forced through them, it is worth while to explore the possibility of using compacted clays as membranes in reverse osmosis operation. The studies contained in Chapter II have been conducted with this aim in view.

The Kesting's liquid membrane hypothesis is of great significance from the point of view of reverse osmosis technology. The studies contained in Chapter III lend support to the Kesting's hypothesis and also reveal certain novel properties of the Poly vinyl methyl ether (PVME) liquid membranes which had hitherto gone unnoticed.

Chapter IV describes experiments on electro-osmosis of saline waters through a cellulose nitrate membrane with a view to studying the efficiency of electro-kinetic energy conversion.

In Chapter V Kesting's liquid membrane hypothesis has been extended to the case of bile salts which are excellent surfactants of biochemical importance. These studies are expected to be of significance in physiology.

In Chapter VI the experiments and the data of Dainty and Ginzburg on the trans-cellular osmosis of internodal characean cells have been re-examined. It has been concluded that the experiments of Dainty and Ginzburg represent a suituation where the linear formalism of non-equilibrium thermodynamics which has thitherto been considered good enough for the description of transport processes in biological systems, breaks down and the anomalous results are better explained on the basis of Li's non-linear phenomenological equations.

The Chapter VII contains studies on network thermodynamic modelling. The two cases considered are (i) transport through composite membranes and (ii) an enzyme catalysed reaction. In both these cases expression for relaxation times have been deduced. In the case of enzyme catalysed reaction

the expression for steady state reaction velocity has also been deduced. The deductions especially of relaxation times based on network thermodynamics are much simpler in comparison to the corresponding deductions based on Kinetic and statistical methods.

The Chapter I is introductory to the studies reported in subsequent Chapters and contains a summary of the non-equilibrium thermodynamic theory of osmotic and electro-osmotic phenomena. The basic tenets and methodology of network thermodynamics have also been summarized in this chapter.

Saroj Yadav 3.5.1979

(Saroj Yadav)

CHAPTER I

NON-EQUILIBRIUM THERMODYNAMICS OF COUPLED FLOW PROCESS - A GENERAL INTRODUCTION

NON-EQUILIBRIUM THERMODYNAMICS OF COUPLED FLOW PROCESSES - A GENERAL INTRODUCTION

The non-equilibrium thermodynamic studies contained in the subsequent chapters of this thesis can be put in two broad categories:

a) Studies relevant to water desalting

b) Studies relevant to biophysics.

In both the cases mentioned above the phenomena studied are either the simultaneous transport of matter and electricity or simultaneous transport of solute and solvent through relevant membranes. In this chapter therefore we will briefly summarize the non-equilibrium thermodynamic theory of both electro-osmosis and osmosis including the frictional interpretation of the phenomenological coefficients.

Since the studies reported in chapter VII relate to network thermodynamic modelling of some irreversible transport processes, the basic tenets and postulates of network thermodynamics which is relatively a recent development, have also been included in this chapter.

I.1 SIMULTANEOUS FLUXES OF VOLUME, CHARGE AND SOLUTE THROUGH A MEMBRANE - THE DISSIPATION FUNCTION[1,2]

Let us consider an isothermal system consisting of two well stirred compartments (say I and II) and separated

by a membrane. Different concentrations, pressures and electrical potentials are allowed on both sides of membrane so as to give rise to three fluxes, namely the flow of water, the flow of the cation and the flow of the anion through the membrane. The non-equilibrium thermodynamic theory of such an isothermal system in which three flows and three conjugate forces operate simultaneously, has been discussed by Kedem and Katchalsky.[1,2]

The dissipation function ϕ for such a discontinuous system is given by the equation

$$\phi = J_1 \Delta\tilde{\mu}_1 + J_2 \Delta\tilde{\mu}_2 + J_w \Delta\tilde{\mu}_w \quad \ldots\ldots\ldots (1)$$

where J's represent the flows of the species denoted by the subscript and the difference in electrochemical potential across the membrane ($\Delta\tilde{\mu} = \tilde{\mu}^{I} - \tilde{\mu}^{II}$) represent the corresponding conjugate driving forces. The subscript 1,2 and w respectively stand for the cation, the anion and water respectively. Equation (1) can be changed into a more convenient form: if the electrolyte be a salt composed of a Z_1 valent cation and a Z_2- valent anion which dissociates into ν_1 cations and ν_2 anions.

The condition of electroneutrality for the salt is written as

$$\nu_1 Z_1 + \nu_2 Z_2 = 0 \qquad (2)$$

The difference in the chemical potential $\Delta\mu_s$ of the salt (electrolyte) is related to the difference in the electrochemical potentials of the cations and the anions by the relation

$$\Delta\mu_s = \nu_1 \Delta\tilde{\mu}_1 + \nu_2 \Delta\tilde{\mu}_2 \qquad (3)$$

The electro-motive force ΔE acting across a pair of electrodes reversible to one of the ions, say ion 2, can be given as,

$$\Delta E = \frac{\Delta\tilde{\mu}_2}{z_2 F} \qquad (4)$$

where F is the Faraday.

The electrical current I through the membrane is related to the ionic flows by the equation

$$I = (z_1 J_1 + z_2 J_2) F \qquad (5)$$

For the electrodes reversible towards ion 2, the flow of ions 1 can be related with the flow of salt J_s as

$$\nu_1 J_s = J_1 \qquad (6)$$

Introducing the last expression and equation (2) into (5) one can write

$$J_2 = \frac{I}{Z_2 F} + \nu_2 J_s \qquad (7)$$

Now, on substituting the value of J_1 and J_2 from equation (6) and (7) and of $\Delta\tilde{\mu}_2$ from equation (4) into equation (1) and rearranging terms, the dissipation function becomes[3]

$$\phi = J_w \Delta \mu_w + J_s \Delta \mu_s + I \Delta E \qquad (8)$$

Since $\Delta \mu_w$ and $\Delta \mu_s$ can be defined as

$$\Delta \mu_w = \overline{V}_w (\Delta P - \Delta \pi) \qquad (9)$$

and

$$\Delta \mu_s = \overline{V}_s \Delta P + \frac{\Delta \pi}{\overline{C}_s} \qquad (10)$$

where $\overline{V}_w$ and $\overline{V}_s$ denote the partial molar volume of water and solute respectively, ΔP is the hydrostatic pressure across the membrane, $\Delta \pi$ is the difference in the osmotic pressure of the permeable solute and $\overline{C}_s$ is the average of the solute concentration in the two compartments, the equation (8) can be conveniently be transformed into

$$\phi = J_v \Delta P + J_D \Delta \pi_s + I \Delta E \qquad (11)$$

with

$$J_v = J_w \overline{V}_w + J_s \overline{V}_s \qquad (12)$$

and

$$J_D = \frac{J_s}{\bar{c}_s} - J_w \bar{V}_w \qquad (13)$$

In equation (12) and (13), J_v represents the volume flow and the exchange flow J_D represents velocity of the solute relative to that of the solvent.

I.2 ELECTRO-KINETIC PHENOMENA

The classical equipment for the study of electro-kinetic phenomena consisted of a two-compartment system separated by a plug of porous charged material, such as wet clay or a fritted glass filter. Modern experiments could also use an ion-exchange membrane separating two salt solutions of equal concentration ($\Delta\pi_s=0$) and subjected to various pressure differences and electromotive forces. The interest in the coupling of volume flow and electric driving force or of electric flow and hydrostatic pressure goes back to the early 19th century, and through the decades a wealth of experimental material has accumulated for many combinations of flows and forces. The first theoretical explanations of the phenomena, advanced at the end of the 19th century, were based on the theory of the electrical double layer developed by Helmholtz[4], Smoluchowski[5], Gouy[6] and Perrin[7]. All classical theories

treated a simplified model which still serves as a very good approximation to the behavior of loose membranes such as glass filters or clay. The advantage of this approach is that it permits a direct evaluation of the coefficients and gives a tangible picture of the processes in the membrane. However, the theories reach their limit when dealing with very dense membranes containing a low percentage of water. In later years, Saxen[8] observed that several relations between coupled phenomena, derived from the simple theory, also remain valid in the region in which the theory itself fails to describe the experimental data. These Saxen's relations attracted the attention of thermodynamicists, and in 1951 Mazur and Overbeek[9] proved that they may be deduced in a general way from the phenomenological equations of non-equilibrium thermodynamics.[10-14] This is what has been summarized in the following lines.

If in the system $\Delta\pi_s=0$ which means that the concentration of the solutions in the two compartments is uniform, the equation (11) for the dissipation function ϕ simplifies to

$$\phi = J_v \Delta P + I\Delta E \qquad (14)$$

The transport equations in the linear range can be written as

$$J_v = L_{11} \Delta P + L_{12} \Delta E \qquad (15)$$

$$I = L_{21} \Delta P + L_{22} \Delta E \qquad (16)$$

where L_{ik} are phenomenological coefficients goverened by the following conditions

a) $L_{12} = L_{21}$ (Onsager's reciprocity relations[15])

b) $L_{11} L_{22} > L_{21} L_{12}$ (on account of the positive definite character of entropy production)

Expressions for various electro-kinetic effects in the steady state can be derived from equation (15) and (16). These are:

For Electro-osmosis

$$(J_v)_{\Delta P=0} = L_{12} \Delta E; \quad (J_v/I)_{\Delta P=0} = L_{12}/L_{22} \qquad (17)$$

For Electro-osmotic pressure

$$(\Delta P)_{J_v=0} = - (L_{12}/L_{11}) \Delta E \qquad (18)$$

For Streaming potential

$$(\Delta E)_{I=0} = - (L_{21}/L_{22}) \Delta P \qquad (19)$$

For Streaming current

$$(I)_{\Delta E=0} = L_{21} \Delta P \; ; \quad (I/J_v)_{\Delta E=0} = L_{21}/L_{11} \qquad (20)$$

These phenomena are inter-related on account of Onsager

relations. Thus

$$(\Delta P/\Delta E)_{J_v=0} = -(I/J_v)_{\Delta E=0} \tag{21}$$

$$(\Delta E/\Delta P)_{I=0} = -(J_v/I)_{\Delta P=0} \tag{22}$$

which are well known Saxen's relations.[8]

The linear phenomenological equations (15) and (16) can alternatively be written as

$$\Delta P = R_{11}J_v + R_{12}I \tag{23}$$

$$\Delta E = R_{21}J_v + R_{22}I \tag{24}$$

where R_{ik} are the resistance coefficients and are related to the phenomenological coefficient L_{ik} in the following manner

$$R_{11} = \frac{L_{22}}{|L|} \tag{25}$$

$$R_{12} = -\frac{L_{12}}{|L|} \tag{26}$$

$$R_{21} = -\frac{L_{21}}{|L|} \tag{27}$$

$$R_{22} = \frac{L_{11}}{|L|} \tag{28}$$

in which the determinant $|L| = L_{11}L_{22} - L_{12}L_{21}$. In general,

$$R_{ik} = \frac{|L|_{ik}}{|L|}$$

in which $|L|$ is the determinant of the matrix of the coefficients L_{ik} and $|L|_{ik}$ is the minor of the determinant corresponding to the term L_{ik}. The equality

$$R_{12} = R_{21} \qquad (29)$$

follows on account of Onsager's theorem.[15] Counterparts of equations (17) to (20) for various electro-kinetic effects in terms of resistance coefficients R_{ik} can be easily deduced from equations (23) and (24) by applying the condition for appropriate steady states.

Extensive amount of work on electro-kinetic phenomena is both charged and uncharged membranes, ascertaining the domain of validity of the phenomenological equations, their form in the non-linear region and the nature of various phenomenological coefficients has recently been reported in literature.[16-27]

I.3 SIMULTANEOUS TRANSPORT OF SOLUTE AND SOLVENT

If in the system described by the equation (11) $\Delta E=0$ or $I=0$ the dissipation function reduces to

$$\phi = J_v \Delta P + J_D \Delta \pi \tag{30}$$

The phenomenological equation relating the flows and forces defined by the equation (30) are

$$J_v = L_P \Delta P + L_{PD} \Delta \pi \tag{31}$$

$$J_D = L_{DP} \Delta P + L_D \Delta \pi \tag{32}$$

For this system, the Onsager reciprocal relations are

$$L_{PD} = L_{DP} \tag{33}$$

The significance of equation (31) and (32) may be clarified by examination of several common physical situations. In an experiment in which the concentration of the solute is the same on both sides of the membrane, i.e. $\Delta \pi = 0$, if a pressure difference is maintained across the membrane, there will be volume flow J_v, which is a linear function of ΔP. The proportionality coefficient relating J_v to ΔP is L_P which is the mechanical filteration capacity of the membrane. The filteration coefficient has the character of a mobility and represents the velocity of fluid per unit pressure difference. An inspection of equations (31)

and (32) further reveals that a hydrostatic pressure at $\Delta\pi=0$ can produce not only a volume flow but also a diffusional flow.

$$(J_D)_{\Delta\pi=0} = L_{DP}\,\Delta P \qquad (34)$$

The coupling coefficient L_{DP} is a measure of the ultra-filteration properties of the membrane.

An alternative experimental arrangement is if we have different solute concentration in the two compartments ($\Delta\pi \neq 0$) and the pressure is uniform ($\Delta P=0$). In such a situation the difference in osmotic pressure causes a diffusional flow characterized by the coefficient L_D, which represents a diffusional mobility per unit osmotic pressure

$$(J_D)_{\Delta P=0} = L_D\,\Delta\pi \qquad (35)$$

Another effect implied in equation (31) and (32) is a volume flow caused by an osmotic pressure difference at $\Delta P=0$

$$(J_v)_{\Delta P=0} = L_{PD}\,\Delta\pi \qquad (36)$$

The coefficient L_{PD} is the coefficient of osmotic flow.

Thus the phenomenological equations (31) and (32) give an adequate description of the phenomena of membrane

transport and correlate in a consistent manner different experimental observations. On account of Onsager's law a quantitative relation between the phenomena of ultrafilteration and osmotic flow can be given i.e.

$$\left(\frac{J_v}{\Delta \pi}\right)_{\Delta P=0} = L_{PD} = L_{DP} = \left(\frac{J_D}{\Delta P}\right)_{\Delta \pi=0} \qquad (37)$$

Equation (37) shows that the volume flow per unit osmotic pressure should be equal to the diffusional velocity per unit pressure difference.

The introduction of the cross coefficients is not arbitrary but is required by the very nature of the phenomena taking place in the membrane. Moreover, if we disregard the existence of cross relation, we would miss one of the most interesting aspects of membrane function, the selectivity. The use of L_P alone would lead to prediction of mechanical filteration but would make no distinction between a membrane so selective as to give rise to a maximal flow under the action of an osmotic gradient and one so coarse as to make the establishment of an osmotic flow impossible. In the same way, a diffusional or exchange flow will take place in a free solution without the presence of a membrane. It is, however, the coefficient

L_{DP} that introduces membrane characteristics and takes into account the phenomenon of ultrafilteration.

In an osmometeric situation when $J_v=0$ the equation (31) yields

$$(\Delta P)_{J_v=0} = - \frac{L_{PD}}{L_P} \Delta\pi \qquad (38)$$

or that $\Delta P=\Delta\pi$ only if $- L_{PD}= L_P$. This condition is satisfied for an ideal semipermeable membrane, that prevents the transport of solute whatever ΔP or $\Delta\pi$ may be, so that $J_s=0$ for all values of forces.

Staverman[28] recognized that the ratio $- L_{PD}/L_P$ is an adequate measure of membrane selectivity. He called it the reflection coefficient,

$$\sigma = - \frac{L_{PD}}{L_P} \qquad (39)$$

to indicate that when $\sigma = 1$ all the solute is reflected from the membrane, while $\sigma < 1$ means that part of the solute penetrates and is not reflected. It is important to realize that the value of σ depends on the properties of both the membrane and the solute. The data of Anderson and Ussing[29], Dainty and Ginzburg[30], Ginzburg and Katchalsky[31] and Goldstein and Soloman[32] clearly demonstrate this.

In order to clarify the concept of membrane selectivity let us write from equation (31) and (32)

$$\left(\frac{J_D}{J_v}\right)_{\Delta\pi=0} = \frac{L_{PD}}{L_P} = -\sigma \qquad (40)$$

Recognising that

$$J_D \cong v_s - v_w \qquad (41)$$

and $$J_v \cong v_w \qquad (42)$$

where v_s and v_w are respectively the velocities of solute and water the equation (40) can be transferred into

$$\left(\frac{v_s}{v_w}\right)_{\Delta\Pi=0} = 1 - \sigma \qquad (43)$$

Equation (43) shows that for an ideal semipermeable membrane ($\sigma=1$), $v_s=0$ and no solute can cross the membrane. With decreasing selectivity or diminishing σ, v_s increases and solute is transferred. When $\sigma = 0$, $v_s = v_w$ so that for a nonselective membrane solute and solvent move at equal velocities and there is no ultrafilteration. There is also the possibility of σ being negative, and in this case $1 - \sigma > 1$. This would mean that the transfer of solute is more rapid than that of solvent or $v_s > v_w$. Such cases are known and are called negative anamalous

osmosis; they are of special interest in transport of electrolytes through charged membranes. This problem has been discussed in detail by Kedem and Katchalsky[33] and by Schlogl.[34]

The introduction of σ into equation (31) gives, for the volume flow J_v,

$$J_v = L_P (\Delta P - \sigma \Delta \pi) \tag{44}$$

It is often advantageous to study the total solute flow J_s, rather than the relative velocity J_D. For this equation (31) is solved for ΔP in terms of J_v and $\Delta\pi$ to yield

$$\Delta P = \frac{J_v - L_{PD} \Delta \pi}{L_P} \tag{45}$$

Using equation (39) and (45) it is possible to write from equation (31) and (32), the relationship

$$J_s = \overline{C}_s (1 - \sigma) J_v + \omega \Delta \pi \tag{46}$$

in which

$$\omega = \frac{\overline{C}_s (L_P L_D - L_{PD}^2)}{L_P} \tag{47}$$

The new coefficient ω is the coefficient of solute permeability at zero volume flow and can be written as

$$\omega = \left(\frac{J_s}{\Delta \pi} \right)_{J_v=0} \tag{48}$$

It is an important characteristic parameter of both synthetic and natural membranes. As expected, for ideally semipermeably membrane, $\omega = 0$, while for non-selective membranes in which the solute diffuses freely and $L_{PD} = 0$, $\omega = \overline{C}_s L_D$. The equation (44) and (46) were first derived by Kedem and Katchalsky[35] and are more appropriate than equation (31) and (32) because of their operational form.

Within the framework of discontinuous theory it is more convenient to describe the behavior of the membrane system as a whole in terms of measurable quantities.

This can be illustrated with the flow equations (44) and (46). Assuming a constancy of σ, L_P and ω (which seems completely plausible for a single experiment where only small changes of concentration are allowed), we expect straight lines, if J_v in plotted versus ΔP in accordance with equation (44). From the slope and intercept L_P and σ may be calculated, provided that $\Delta \pi$ is known. Equation (46) under the condition of J_v equal to zero, is the basis for the determination of ω. The experimental verification of equation (44) involves measurements of pressure and volume flows only, the verification of equation (46) involves measurements of changes of composition. Smit[36] and Smit et al[37] have emphasised

that σ, L_p and ω should be determined in this way rather than σ and L_p in an ultrafilteration experiment and ω separately in an osmotic experiment. It may of course be noted that this method implies the validity of Onsager's reciprocal relations.

I.4 FRICTIONAL INTERPRETATION OF PHENOMENOLOGICAL COEFFICIENTS

The macroscopic theory of transport processes presented in the foregoing lines is quite general and does not make use of any specific kinetic or statistical model. But the price one has to pay for this generality is that not much can be learnt about the mechanism of the transport process inside the membrane. It is for this reason that several mechanistic models have been proposed.[38] Of these Spiegler's frictional model[39] which relates the various phenomenological coefficients with the coefficient of friction between the permeating species and the permeating species and the membrane is the one that has attracted attention in recent years.[36,37,25,26]

Spiegler's frictional model[39] has been extended by Kedem and Katchalsky[40] to correlate the measurable quantities L_p, σ and ω with various frictional coefficients. This is summarized in the following lines.

Consider an isothermal system consisting of two compartments containing pure water and separated by a membrane, the driving force is provided by a difference in pressure. Let there be a point x in the membrane where the force driving the water is

$$X_w = \frac{d \mu_w}{dx} \tag{49}$$

Under steady state condition, the driving force X_w must be balanced by a mechanical frictional force, X_{wm}, between the water and the membrane. The frictional force is given by

$$X_{wm} = f_{wm} (v_w - v_m) \tag{50}$$

where f_{wm} is the coefficient of friction between water and the membrane, v_m is the geometric velocity of the membrane and v_w is the velocity of water. If membrane is the reference for all flows, v_m is taken to be zero and equating X_w and X_{wm} we obtain

$$- \frac{d \mu_w}{dx} = f_{wm} v_w \tag{51}$$

The flow of water at the point x is given by $J_w = C_w (x) v_w$ where C_w is the water concentration in the membrane.

Assuming that the water concentration in the membrane is uniform throughout the distribution coefficient K_w of water between the membrane phase and the adjoining medium can be written as

$$\frac{C_w}{c_w} = K_w \tag{52}$$

where c_w is the water concentration in the adjoining medium. Multiplying the numerator and denominator in equation (52) by $\bar{V}_w$ we can rewrite equation (52) as

$$\frac{C_w \bar{V}_w}{c_w \bar{V}_w} = \frac{\phi_w}{1} = K_w \tag{53}$$

where ϕ_w is the volume fraction of water in the membrane With these relations equation (51) becomes

$$-\frac{d\mu_w}{dx} = \frac{f_{wm} C_w v_\omega}{C_w} = \frac{J_w f_{wm}}{C_w} = \frac{J_w \bar{V}_w f_{wm}}{\phi_w} \tag{54}$$

Integrating equation (54) across the membrane of thickness Δx and writing $J_w \bar{V}_w$ equal to the total volume flow J_v we can write

$$J_v = \frac{\phi_w \bar{V}_w \Delta P}{f_{wm} \Delta x} \tag{55}$$

Comparison of equation (55) with equation (31) under the condition $\Delta\pi = 0$ shows that

$$L_P = \frac{\phi_w \bar{V}_w}{f_{wm} \Delta x} \tag{56}$$

Equation (55) is a very simple case relating thermodynamic coefficients to frictional coefficients.

Let us now consider a simple case of transport of a simple solute and solvent through a membrane.[40] The fundamental assumption underlying this more general treatment is that the frictional forces that counter balance the thermodynamic driving forces are additive. Thus according to Spiegler[39], the force driving the solute, X_s, is balanced by the sum of the force of interaction of solute with the membrane matrix, X_{sm}, and the force of interaction between solute and solvent in the membrane, X_{sw}. The formal hydrodynamic description of these frictional forces is

$$X_{sm} = f_{sm} (v_s - v_m) \tag{57}$$

$$X_{sw} = f_{sw} (v_s - v_w) \tag{58}$$

where f_{sw} is the frictional coefficient of between a mole of solute and infinite amount of water. Since

$v_m = 0$

$$X_s = X_{sm} + X_{sw} = v_s(f_{sw} + f_{sm}) - v_w f_{sw} \tag{59}$$

Similarly

$$X_w = X_{wm} + X_{ws} = v_w(f_{wm} + f_{ws}) - v_s f_{ws} \tag{60}$$

The coefficient f_{ws} is different from f_{sw} since f_{ws} is the friction between a mole of water and an infinite amount of solute. In a loose membrane, the coefficient f_{sw} approaches the value for free solution, f^o_{sw}, which is related to the diffusion coefficient D by the equation

$$D = \frac{RT}{f^o_{sw}} \tag{61}$$

where R is the usual gas constant and T is the absolute temperature. Equation (60) and (59) can be further transformed into

$$X_w = -\frac{d\mu_w}{d\varkappa} = -\frac{f_{ws} J_s}{C_s(\varkappa)} + \frac{(f_{ws} + f_{wm}) J_w}{C_w(\varkappa)} \tag{62}$$

$$X_s = -\frac{d\mu_s}{d\varkappa} = \frac{(f_{sw} + f_{sm})}{C_s(\varkappa)} J_s - \frac{f_{sw} J_w}{C_w(\varkappa)} \tag{63}$$

where $C_s(\varkappa)$ and $C_w(\varkappa)$ are the concentrations of solute and water respectively at the point $\varkappa$ in the membrane. The equations (62) and (63) have the form of inverted phenomenological equation,

$$X_w = R_{11} J_w + R_{12} J_s \tag{64}$$

$$X_s = R_{21} J_w + R_{22} J_s \tag{65}$$

Now comparing equation (62) with (64) and equation (63) with (65) we can write

$$R_{11} = \frac{f_{ws} + f_{wm}}{C_w(\varkappa)} \; ; \quad R_{21} = -\frac{f_{sw}}{C_w(\varkappa)} \tag{66}$$

$$R_{12} = -\frac{f_{ws}}{C_s(\varkappa)} \; ; \quad R_{22} = \frac{f_{sw} + f_{sm}}{C_s(\varkappa)} \tag{67}$$

Thre requirement $R_{12} = R_{21}$ gives us the relation between the frictional coefficients f_{sw} and f_{ws} :

$$f_{ws} = \frac{C_s(\varkappa)\, f_{sw}}{C_w(\varkappa)} \tag{68}$$

The concentration $C_s(\varkappa)$ and $C_w(\varkappa)$ at the point $\varkappa$ in the membrane can be expressed in terms of the external concentration. The concentration $C_w(\varkappa)$ can be approximated by the equation (52). For evaluation of $C_s(\varkappa)$ one has to use a more complex method. Imagine that at the point $\varkappa$ a small hole is created in the membrane and filled with pure water. Under conditions of steady flow, the hole will fill up, in a short while, with solute of

concentration $C_s'(x)$. As shown above, the chemical potential of the solute in the hole should be equal to that in the membrane so that in the case of a homogeneous membrane the ratio of the concentration at the point x in the membrane to the concentration in the equivalent aqueous phase $C_s'(x)$ should be given by a distribution coefficient K_s,

$$\frac{C_s(x)}{C_s'(x)} = K_s \qquad (69)$$

The value of K_s is assumed to be constant throughout the membrane. The advantage of this device is that, instead of the chemical potential in the membrane, we may use the equivalent potential in the aqueous phase of the small hole, and instead of the unknown concentration $C_s(x)$ we may use $K_s \; C_s'(x)$, which can be determined experimentally by independent measurement on solute distribution between the membrane and the external solution.

For simplifying the integration process let us take into consideration the fact that the permeability coefficient ω and the reflection coefficient σ may be determined at zero volume flow. Since $J_v=0$ is, in most cases, very nearly equivalent to $J_w=0$, we may use the latter condition. Thus equation (63) then becomes

$$-\left(\frac{d\mu_s}{dx}\right)_{J_w=0} = \frac{J_s}{K_s C_s'(x)}(f_{sw} + f_{sm}) \qquad (70)$$

considering the value of $d\mu_s$ as that of the chemical potential in the equivalent aqueous solution, the equation (70) can be rewritten as

$$-\frac{d\pi}{dx} = \frac{J_s(f_{sw} + f_{sm})}{K_s} \qquad (71)$$

Integrating equation (71) across the membrane of thickness Δx, we get

$$(\Delta\pi)_{J_w=0} = \frac{(f_{sw} + f_{sm})\,\Delta x}{K_s} \cdot J_s \qquad (72)$$

The expression in terms of frictional coefficients for the permeability coefficient ω follows from equation (72) i.e.

$$\omega = \left(\frac{J_s}{\Delta\pi}\right)_{J_v=0} \cong \left(\frac{J_s}{\Delta\pi}\right)_{J_w=0} = \frac{K_s}{\Delta x(f_{sw}+f_{sm})} \qquad \ldots (73)$$

The reflection coefficient σ in terms of frictional coefficient can be evaluated by imposing the condition $J_w=0$ and transcribing equation (62) and (63) using equation (68) and the relationship $C_w(x)\,\bar{V}_w = \phi_w$.

Thus

$$-\frac{d\mu_w}{d\varkappa} = -\frac{\bar{V}_w f_{sw}}{\phi_w} J_s \qquad (74)$$

$$-\frac{d\mu_s}{d\varkappa} = \frac{f_{sw} + f_{sm}}{K_s C_s'(\varkappa)} J_s \qquad (75)$$

Eliminating J_s from the above two equations we get

$$-C_s'(\varkappa)\frac{d\mu_s}{d\varkappa} = -\frac{f_{sw}+ f_{sm}}{K_s f_{sw} \bar{V}_w}\phi_w \left(-\frac{d\mu_w}{d\varkappa}\right) \qquad (76)$$

As $C_s'(\varkappa)$ and $d\mu_s$ are regarded as the properties of the equivalent aqueous solutions, we may put $C_s'(\varkappa)(d\mu_s/d\varkappa) = d\pi/d\varkappa$ and integrate the equation (76) to get

$$\left(\frac{\Delta P}{\Delta \pi}\right)_{J_w=0} = \sigma = 1 - \frac{K_s f_{sw}}{(f_{sw}+ f_{sm})\phi_w} \qquad (77)$$

In arriving at equation (77) the relationship (9) has also been made use of. The equation (77) is based on the assumption that $J_w \cong J_v$. In case this assumption is no longer valid a correction in equation (77) is called for because

$$\left(\frac{\Delta P}{\Delta \pi}\right)_{J_w=0} = \left(\frac{\Delta P}{\Delta \pi}\right)_{J_v=0} - \frac{\omega \bar{V}_s}{L_p} \qquad (78)$$

The corrected version of equation (77) can thus be written as

$$\sigma = 1 - \frac{\omega \bar{V}s}{L_P} - \frac{K_s \; f_{sw}}{\phi_w \; (f_{sw} + f_{sm})} \qquad (79)$$

The above equation (79) shows that, when the membrane is impermeable to the solute and $\omega = 0$, the coefficient $\sigma = 1$, as expected for an ideal semipermeable membrane. When ω increases σ decreases and for sufficiently large values of ω, may assume negative values. The negative value of σ means that in an osmotic experiment, at zero volume flow when $\Delta P = \sigma \Delta\pi$ we have to apply negative pressure to the solution for a steady state.

Values of frictional coefficients for several systems (both natural and artificial membranes) have been evaluated[41,42] from the experimentally determined values of L_p, σ and ω. Study of frictional coefficients can be very helpful in understanding the mechanism of transport process through biological membranes. An excellent account of this is available in Stein's celebrated monograph.[43] Study of frictional coefficients can also be helpful in deciding how efficient a membrane would be in a hyperfilteration operation.[44-47] In fact Spiegler and Kedem[44] have developed criteria, in terms

of frictional coefficients, for efficient hyperfilteration membranes.

I.5 NETWORK THERMODYNAMICS

Meixner [48-50] was the first to recognise the connexion between network theory and irreverisble thermodynamics. This has recently been revived by Oster, Perelson and Katchalsky.[51,52] The most recent monograph and probably the only one so far that has appeared on the subject is by Schnakenberg.[53]

Network approach to irreversible processes has several advantages. Not only does it provide an alternative formalism, but it brings thermodynamics of irreversible processes within the framework of modern dynamical system theory.[54]

Thermodynamics is a phenomenological theory and, as such, is a purely formal structure. It offers no explanation of physical events, but serves only to organize knowledge and establish relationships between quantities. Similarly, the principal purpose of Network thermodynamics which also is a phenomenological theory is to provide an organizational framework for treating complex thermodynamic processes. The techniques developed

are especially well suited to the description of biological system, where analysis is complicated by the nonlinearity of the individual dynamic process, the organizational complexity of the system as a whole and the mathematical intractability of the resulting equations.

These problems are similar to those encountered in dynamical systems and control theory, where one particular application of non-equilibrium thermodynamics - electrical network theory - has been extremely successful.

The network approach also makes it possible to construct a graphical representation for thermodynamic systems analogous to circuit diagrams in electrical network theory. Such network graphs are far more than pictorial representations of particular physical systems. Because the dynamical equations may be read algorithmically from the network graph, the diagrams are actually another notation for the equations themselves in much the same way as the operators of vector analysis are a more lucid notation for the component representation. It also reveals system topology.

Underlying the network approach is the duality of the mathematical structures available for the description of dynamical system : Point set topology and algebraic

or combinatorial topology. In the network approach we pull apart the continuum, revealing the implicit topological relations. For example, if we wish to describe the current and potential distribution or a conducting sheet, instead of trying to specify the entire distribution by continuous functions we could overlap the sheet with a network or mesh of a finite number of nodes and branches and tabulate the meter readings giving the current flow through each branch and the potential differences between each node pair. It seems reasonable that, as the mesh is made finer and finer, we can approach the actual continuum distribution to any desired degree of accuracy.

State Variables and Constitutive Relations :-

Most systems that can be analysed with the network approach share one common property : the rate of energy transmission, dissipation or storage is finite and may be expressed as a product of an effort or force variable, e and a flow variable f; that is, energy rate (power) = e.f. In electrical networks these variables are, of course, voltage difference and current; in mechanics : force and velocity; in diffusional processes : chemical potential and mass flow; in chemical reaction : affinity and rate mechanism; and so on.

By integrating e and f we can define two additional state variables: the generalized displacement,

$$q(t) \equiv q(o) + \int_o^t f(t)\, dt \qquad (80)$$

and a generalized momentum,

$$P(t) \equiv P(o) + \int_o^t e(t)\, dt \qquad (81)$$

For example, ξ, the displacement of a chemical reaction, is a generalized displacement variable, defined here by equation (80) as

$$\xi(t) = \xi(o) + \int_o^t J_v\, dt \qquad (82)$$

where J_v the reaction rate is the flow variable.

As in electrical network theory, we associate two dynamical variables with each energy bond: a variable (f or q) which obeys a local conservation law (Kirchhoff's current law, KCL), and a variable (e or p) which is a continuous function (Kirchhoff's voltage law, KVL). The latter property is related to the local equilibrium postulate.[55]

In order to make predictions based on any phenomenological theory, information must be supplied about the system in the form of constitutive relations (equation of state, branch relations). These are obtained either

experimentally or from a more detailed theory, such as statistical mechanics.

There are three kinds of energetic transactions possible that is, three ways of integrating the equation

$$P = e.f. = \sum_{\text{Ports}} e_i \, f_i$$

$$E_c(t) = \int_o^t e.f.dt = \int_{q(o)}^{q(t)} e. \, dq \qquad (83)$$

to give capacitative or displacement energy storage,

$$E_L(t) = \int_o^t f.e.dt = \int_{P(o)}^{P(t)} f.dP \qquad (84)$$

to give inductive, or kinetic energy storage, and

$$E_R(t) = \int_o^t e.f.dt \qquad (85)$$

to give energy dissipation.

To perform the first integration we require capacitive constitutive relations between the displacement and charge variables of the form

$$q = \phi_c(e) \qquad (86)$$

An ideal multiport element, which stores energy by virtue

of a generalized displacement, will be called a capacitor, and denoted generally by C. (In instances of biological interest such a device may be a volume element which stores chemical energy due to a thermodynamic displacement). From the constitutive relation (86) we obtain

$$\frac{dq}{dt} = \frac{d\psi_c}{de} \cdot \frac{de}{dt} \tag{87}$$

Defining the reversible flow on the capacitor :

$$f_{rev} \equiv \frac{dq}{dt} \tag{88}$$

and the incremental capacitance

$$C \equiv \frac{d\psi_c}{de} \tag{89}$$

we obtain :

$$f_{rev} = C \frac{de}{dt} \tag{90}$$

where e is the unique potential characterizing the capacitor. To illustrate this generalized notion of a capacitor we can consider the case of an ideal mixture for which the chemical potential of the ith component is $\bar{\mu}_i = \mu_i^\circ + RT \ln X_i$, where X_i is the mole fraction, μ_i

is the chemical potential and μ_i° the reference potential of the ith component. By equation (89) the incremental capacitance is

$$C_i = \left(\frac{\partial N_i}{d\mu_i}\right)_{P,T,nj} = \frac{N_i}{RT(1-X_i)} \approx \frac{N_i}{RT} \text{ for } X_i \ll 1 \qquad (91)$$

where N_i the number of moles of species i, is the displacement variable q and the effort, e, is $\mu_i - \mu_i^\circ$. Energy may also be stored as a result of the relative motion of mass or charge (that is, kinetic or electromagnetic energy). In such cases, the second integration can be performed, given the constitutive relation $P = \psi_L(f)$. This type of energy storage device will be denoted by L, a generalized inductance. In mechanical networks the constitutive relation between momentum and velocity is merely the mass.[56-58]

Finally, for the dissipative element, denoted by R, we require the constitutive relation between e and f in order to compute the energy dissipation. For example, in a chemical reaction the effort, conjugate to the reaction flow, J_r, is the chemical affinity, A, which is related to J_r, by the constitutive relation

$$A = \psi_R(J_r) \qquad (92)$$

The incremental resistance R of a chemical process is

$$R \equiv \frac{\partial A}{\partial J_r} = \frac{\partial \psi_R}{\partial J_r} \qquad (93)$$

It is worth noting that as a chemical reaction proceeds, the free energy dissipated by the reaction is the difference between the free energy supplied by the reversible discharging of the local capacitors of the reactants and the free energy stored by the charging of the product capacitors.

Bond Graph Notation

A more satisfactory graphical procedure, which is due to Paynter[59], is called Bond Graphs. This notation is particularly well suited for irreversible thermodynamics and does not become unwieldy unlike linear graphs (which is what conventional network notation is). The Skeleton features, are given below. A more detailed account can be found in the texts by Karnopp and Rosenberg[60] or by Paynter.[59]

(1) Bond graphs treat all energy flows on an equal footing and hence provide an easily visualised notation for energy conversion (e.g. chemical potential to affinity in a reaction system).

(2) A set of junctions are introduced which will generalise the notion of series and parallel connections. These are ideal in the sense that they neither store nore dissipate power.

(a) Parallel or 0-junction

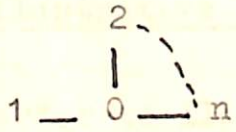

defined by $e_1 = e_2 = \ldots\ldots = e_n$ or since $\Sigma e_i f_i = 0$

$$\Sigma f_i = 0 \qquad (94)$$

This is a statement of KCL and hence an 0-junction may be regarded as a distribution point for flows.

(b) Series or 1-junction

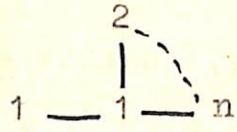

defined by $f_1 = f_2 = \ldots\ldots = f_n$ or since $\Sigma e_i f_i = 0$

$$\Sigma e_i = 0 \qquad (95)$$

This is a statement of KVL and hence the 1-junction is a distribution point for efforts.

(3) The arrows connecting elements to junctions indicate energy flow directions. Hence

$\xrightarrow[f_i]{e_i}$ R indicates energy flowing into element

while $\xleftarrow[f_i]{e_i}$ C indicates energy flowing out of element.

A Simple illustrative example

In order to illustrate the network representations and their corresponding bond graphs, let us consider a dissipative two flux - two force irreversible processes given by the phenomenological equations

$$\begin{pmatrix} J_1 \\ J_2 \end{pmatrix} = \begin{pmatrix} L_{11} & L_{12} \\ L_{21} & L_{22} \end{pmatrix} \begin{pmatrix} X_1 \\ X_2 \end{pmatrix} \qquad (96)$$

between the fluxes J_1, J_2 and the conjugate thermodynamic forces X_1, X_2. This can be represented by π or a Y network shown in Fig. I.1, where y's are conductances. The phenomenological coefficients L_{ik} in equation (96) can be defined as follows

$$L_{11} = \left(\frac{J_1}{X_1}\right)_{X_2=0} \quad ; \quad L_{12} = \left(\frac{J_1}{X_2}\right)_{X_1=0} \qquad (97)$$

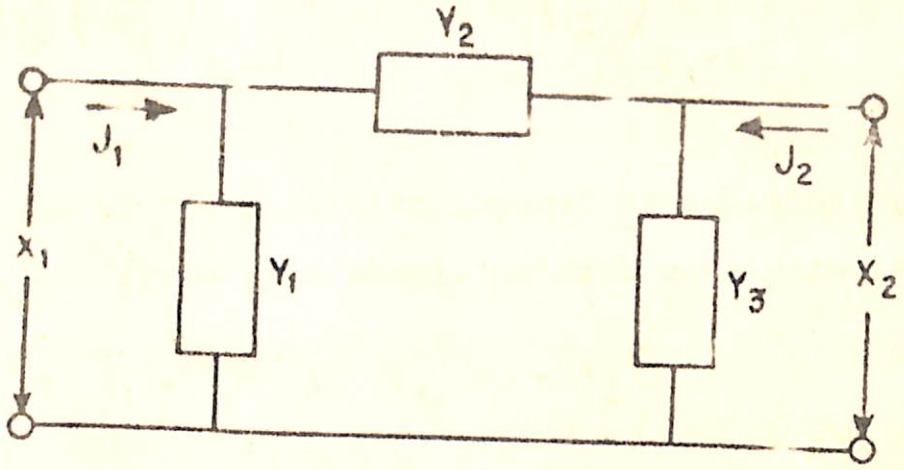

FIG. I.1

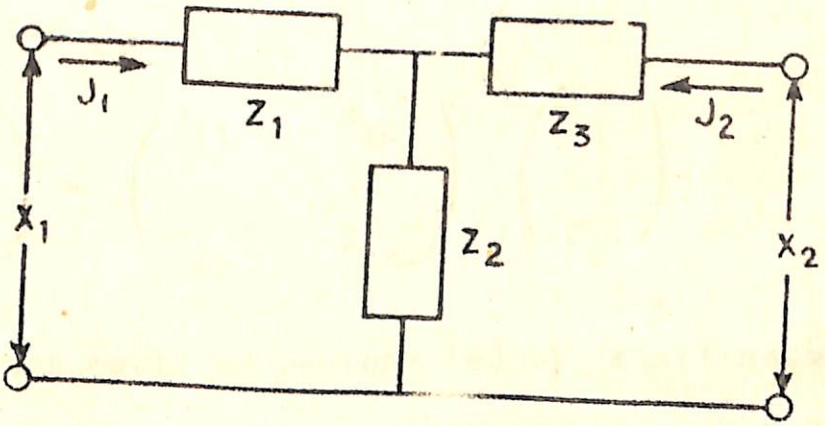

FIG. I.2

Fig. I.1 Delta Network representation for a two flux two force irreversible system. J_1, J_2 fluxes; X_1, X_2 forces, Y_1, Y_2, Y_3 are conductances.

Fig. I.2 Star Network representation for a two flux two force irreversible system. J_1, J_2 fluxes, X_1, X_2 forces, Z_1, Z_2, Z_3 resistances.

$$L_{21} = \left(\frac{J_2}{X_1}\right)_{X_2=0} \quad ; \quad L_{22} = \left(\frac{J_2}{X_2}\right)_{X_1=0} \tag{98}$$

Making use of the condition imposed by equations (97) and (98) we can write from simple network consideration

$$L_{11} = Y_1 + Y_2 \quad ; \quad L_{12} = -Y_2 \tag{99}$$

$$L_{21} = -Y_2 \quad ; \quad L_{22} = Y_2 + Y_3 \tag{100}$$

If however the phenomenological relation (96) are written in the form

$$\begin{pmatrix} X_1 \\ X_2 \end{pmatrix} = \begin{pmatrix} R_{11} & R_{12} \\ R_{21} & R_{22} \end{pmatrix} \begin{pmatrix} J_1 \\ J_2 \end{pmatrix} \tag{101}$$

the system would be represented by 'star' network shown in Fig. I.2, where Z's are resistances. The coefficients R_{ik} in equation (101) can be defined as

$$R_{11} = \left(\frac{X_1}{J_1}\right)_{J_2=0} \quad ; \quad R_{12} = \left(\frac{X_1}{J_2}\right)_{J_1=0} \tag{102}$$

$$R_{21} = \left(\frac{X_2}{J_1}\right)_{J_2=0} \quad ; \quad R_{22} = \left(\frac{X_2}{J_2}\right)_{J_1=0} \tag{103}$$

From consideration of the star network (Fig. I.2) and conditions in equations (102) and (103) we have

$$R_{11} = Z_1 + Z_2 \quad ; \quad R_{12} = Z_2 \tag{104}$$

$$R_{21} = Z_2 \quad ; \quad R_{22} = Z_2 + Z_3 \tag{105}$$

The bond graph representations for the network (Fig.1) has been shown in Fig. I.3, where (1— 0 —n) represents a parallel or a zero junction defined by $e_1=e_2=....= e_n$ or since $\Sigma e_i f_i=0$; $\Sigma f_i=0$ and (1 — 0 — n) represents a series or one-junction defined by $f_1=f_2=f_3= .... f_n$ or since $\Sigma e_i f_i=0$; $\Sigma e_i=0$.

Similarly for a three flux three force dissipative irreversible process the bond graph representation of the network would be as shown in Fig. I.4. The phenomenological coefficients L_{ik} in this case also can be evaluated in terms of conductances from network considerations. Thus the phenomenological equations for the three flux three forces irreversible process would read as

$$\begin{pmatrix} J_1 \\ J_2 \\ J_3 \end{pmatrix} = \begin{pmatrix} Y_1+Y_2+Y_4 & -Y_2 & -Y_4 \\ -Y_2 & Y_2+Y_3+Y_5 & -Y_5 \\ -Y_4 & -Y_5 & Y_4+Y_5+Y_6 \end{pmatrix} \begin{pmatrix} X_1 \\ X_2 \\ X_3 \end{pmatrix} \tag{106}$$

We can go on like this to generalise these considerations for a n flux n force system.

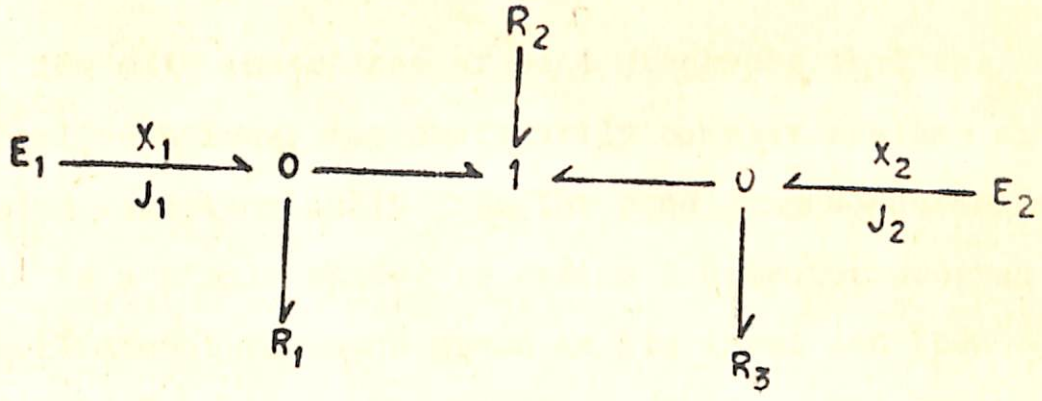

FIG.I.3

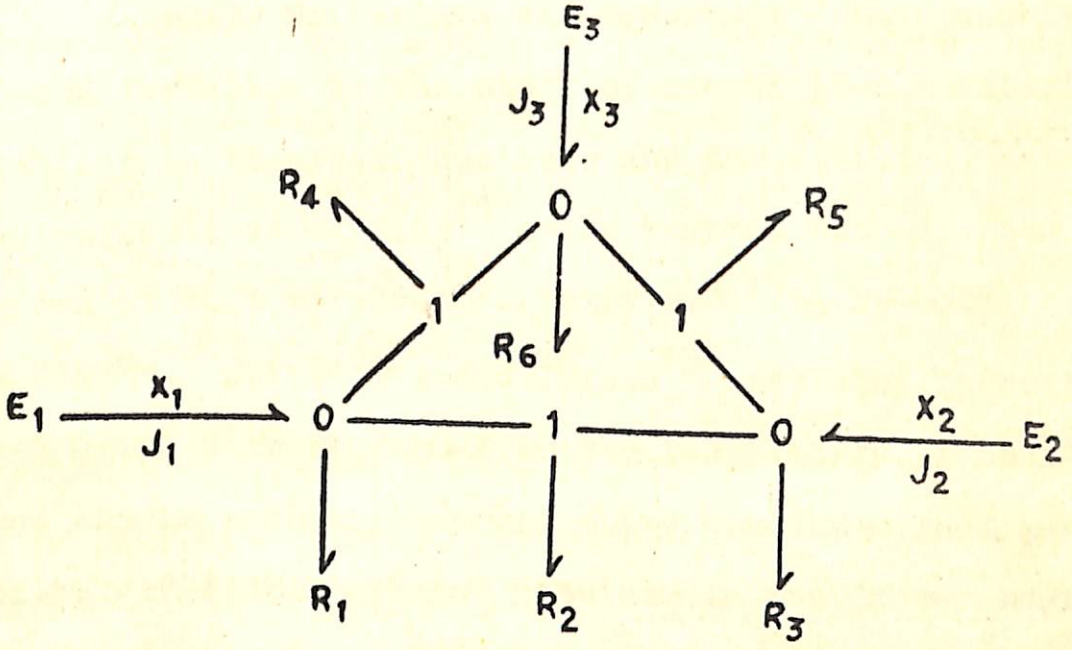

FIG.I.4

Fig. I.3 Bond graph representation of Fig I.1. E_1, E_2 are effort sources, corresponding to the forces X_1, X_2. $Y_i = 1/R_i$

Fig. I.4 Bond graph representation for 3 flux - 3 force irreversible system, E_1, E_2, E_3 are effort sources, corresponding to the forces X_1, X_2, X_3.

The main importance of bond graphs is that the dynamical equations, for arbitrarily complex systems are generated algorithmically from the bond graphs and therefore it is a simple matter to design a computer program that will accept the bond graph as its input and then compute the dynamical behavior directly from the graph.

Recently Srivastava and coworkers[61] have applied network formalism to the study of linear phenomenological relations in chemical reactions and demonstrated that the results obtained earlier[62] using kinetic methods, can be arrived at much more conveniently by using Network formalisms. Srivastava and Chacko[63] have also investigated using network formalism the feasibility of oscillatory phenomena in membrane transport and concluded that oscillatory fluxes are not possible in the linear region. This result is in keeping with the deduction arrived from the discussion of the stability of steady state.[64]

I.6 REFERENCES

1. O.Kedem and A. Katchalsky, Trans. Faraday Soc. 59 1918 (1963).

2. A. Katchalsky and P.F. Curran, Non-equilibrium thermodynamics in Biophysics, Harvard University Press Mass. Cambridge (1965).

3. I. Michaeli and O.Kedem, Trans. Faraday Soc. 57, 1185 (1961).

4. H. Helmholtz, Wied. Ann. 7, 337 (1879).

5. M.V. Smoluchowski in Graetz, ed., Handbuch der Elektrizitat und des Magnetismus (Barth, Leipzig,1914) Vol. 2, p. 366.

6. A. Gouy, J. Physique 9, 457 (1910).

7. J. Perrin, J. Chem. Phys. 2, 601 (1904).

8. U.Saxen, Ann. Physik. Chem. N.F. 47, 46 (1892).

9. P. Mazur and J. Th. G. Overbeek, Rec. trav. chim. 70, 83 (1951).

10. S.R. DeGroot and P. Mazur, Non-equilibrium thermodynamics, North-Holland Publishing Company, Amsterdam (1962).

11. I. Prigogine, Introduction of thermodynamics of Irreversible processes, C.C. Thomas, Springfield, Illinois (1955).

12. R.C.Srivastava and Raj Pal, Non-equilibrium thermodynamics in soil physics, Oxford and IBH (1973).

13. R. Haase, Thermodynamics of irreversible Processes, Addison-Wesley, New York (1969).

14. D.D. Fitts, Non-Equilibrium Thermodynamics, McGraw-Hill New York (1962).

15. L.Onsager, Phys. Rev., 37, 405 (1931); 38, 2265 (1931).

16. R.P.Rastogi and K.M.Jha, J. Phys.Chem. 70, 1017 (1966).

17. R.P.Rastogi and K.M.Jha, Trans. Faraday Soc. 62, 585 (1966).

18. R.P.Rastogi, Kehar Singh, S.N.Singh, J. Phys. Chem. 73, 1593 (1969).

19. R.P.Rastogi and M.L.Srivastava, J. Phys. Chem. 73, 46 (1969).

20. R.P.Rastogi, M.L.Srivastava and S.N.Singh, J. Phys. Chem. 74, 2960 (1970).

21. R.P.Rastogi and B.P.Misra, J. Phys. Chem. 74, 112 (1970).

22. R.P.Rastogi, J. Sci. Ind. Res. 98, 284 (1969).

23. R.P.Rastogi, Kehar Singh and Jhulan Singh, J.Phys. Chem., 79, 2574 (1975).

24. R.P.Rastogi and Ram Shabad, J. Phys. Chem., 20, 1953 (1977).

25. R.C.Srivastava, M.G.Abraham and A.K.Jain, J. Phys.Chem. 81, 906 (1977).

26. R.C.Srivastava and M.G.Abraham, J. Colloid Interface Sci., 57, 58 (1976).

27. R.C.Srivastava and M.G.Abraham, J.C.S. Faraday I, 72, 2631 (1976).

28. A.J.Staverman, Rec. trav.chim, 70, 344 (1961).

29. B.Anderson and H.H.Ussing, Acta Physiol. Scand., 39, 228 (1957).

30. J.Dainty and B.Z.Ginzburg, Biochim Biophys. Acta, 79, 102,112 122, 129 (1964).

31. D.G.Goldstein and A.K.Solomon, J.Gen.Physiol. 44, 1 (1960).

32. B.Z.Ginzburg and A.Katchalsky, J. Gen. Physiol. 47, 403 (1963).

33. O.Kedem and A. Katchalsky, J. Gen. Physiol., 45, 143 (1961).

34. R. Schlogl, Stofftransport durch Membranen (Steinkopff, Darmstadt, 1964).

35. O. Kedem and A. Katchalsky, Biochim. Biophys. Acta 27, 229 (1958).

36. J.A.M. Smit, Partition and friction in membranes, Ph.D. Thesis, University of Leiden (1970).

37. J.A.M. Smit, J.C. Eijsermans and A.J. Staverman, J. Phys. Chem. 79, 2168 (1975).

38. P. Meares (ed.) Membrane Separation processes. Elsevier Scientific Publishing Co., Amsterdam (1976).

39. K.S.Spiegler, Trans. Faraday Soc. 54, 1409 (1958).

40. See Reference 33.

41. B.Z. Ginzburg and A. Katchalsky, J. Gen. Physiol. 47, 403 (1963).

42. G. Eisenman (ed), Membranes, Vol.1 Macroscopic Systems and models, Marcel Dekker, INC, New York (1972).

43. W.D. Stein, The movement of molecules across cell membranes, Academic Press, New York (1967).

44. K.S. Spiegler and O.Kedem, Desalination 1, 311 (1966).

45. E. Hoffer and O.Kedem, Desalination 2, 25 (1967).

46. E. Hoffer and O.Kedem, J. Phys. Chem. 76, 3638 (1972).

47. J.S. Johnson, L. Dresner and K.A. Kraus, Chapter 8 in K.S. Spiegler (Editor), Principles of Desalination, Academic Press, New York (1966).

48. J. Meixner, J. Math. Phys., 41, 154 (1963).

49. J. Meixner, Acta Physica Polonica, 28, 113 (1965).

50. J. Meixner, in Symposium on Generalized Network, 16 (Polytechnic Press of the Polytechnic Institute of Brooklyn, Brooklyn, New York, 1966).

51. G.Oster, A.Perelson and A.Katchalsky, Nature 234, 393 (1971).

52. G.Oster, A.Perelson and A.Katchalsky, Quart. Rev. Biophys. 6, 1 (1973).

53. J.Schnakenberg, Thermodynamic Network Analysis of Biological System, Springer-Verlag, Berlin Heidelberg, New York (1977).

54. E.C.G.Sudarshan, The Structure of Dynamical Theories, Brandeis Lectures, 1962, 2 (W.A.Benjamin Inc. New York 1963).

55. R.Rohrer Circuit Theory: The State space Approach (McGraw-Hill, New York, 1970).

56. J.Shearer, A.T.Murphy and H.H.Richardson, Introduction to System Dynamics (Addison-Wesley,Reading Mass 1967).

57. H.Koening, Y.Tokad and H.K.Kesavan, Analysis of Discrete Physical Systems (McGraw-Hill, New York, 1969).

58. H.Martins and D.Allen, Introduction to Systems Theory (Merrill, Columbus, Ohio, 1969).

59. H.Paynter, Analysis and Design of Engineering Systems (MIT, Cambridge, Mass., 1961).

60. D.Karnopp and R.Rosenberg, Analysis and Simulation of Multiport Systems (MIT, Cambridge Mass., 1968).

61. P.V.Chacko, S.Srivastava and R.C.Srivastava, Indian J. Chem., 16A, 179 (1978).

62. R.P.Rastogi, R.C.Srivastava and K.Singh, Trans. Faraday Soc., 61, 854 (1965).

63. R.C.Srivastava and P.V.Chacko, Curr. Sci. 47, 267 (1978).

64. G.Nicolis in Adv. in Chem. Phys. (ed. I. Prigogine and S.A. Rice) 19, 209, (Wiley Inter Science, New York, 1971).

STUDIES RELEVANT TO WATER DESALTING

CHAPTER II

SALT SIEVING BY COMPACTED CLAYS*

---

* A paper based on the work contained in this chapter has been published in the INDIAN JOURNAL OF CHEMISTRY, 16A 920-924 (1978).

SALT SIEVING BY COMPACTED CLAYS

II.1 INTRODUCTION

Water desalination especially the desalination of sea water is a problem which has attracted the attention of the workers world over for very obvious reasons. The need for converting brackish water into the fresh water worthy of irrigation and also human consumption is felt in many parts of the country especially in the arid and semi-arid zones. In view of increased fertilizer usage in coming years water which is presently potable might also become brackish in due course. These are some of the reasons why the problem of water desalting has been identified as a priority problem in the science and Technology Plans[1-3] of Government of India.

Reverse osmosis has by now been accepted to be one of the most important methods for water desalination.[4-9] Consequently quite a bit of effort has been invested in search for suitable membranes for reverse osmosis operation.[10,11] Since clays are known[12] to possess salt rejecting properties when aqueous solution of salts are forced through them, it is worth while to assess the performance and efficiency of clay membranes in an hyper-filteration operation. With

this object in view the data on simultaneous transport of salt and water through kaolinite and bentonite clay membranes have been analysed in this chapter in the light of the formalism developed by Johnson, Dresner and Kraus[4] and the criteria developed by Spiegler and Kedem[5] for efficient hyper-filteration membranes. The treatment of Johnson, Dresner and Kraus[4] and of Spiegler and Kedem[5] assumes reflection coefficient and salt permeability to be independent of salt concentrations. In order to conform to these assumptions the experiments on the simultaneous transport of salt and water described in this chapter were confined to low salt concentrations and concentration differences.

Although data on osmosis of electrolytic solutions through both kaolinite and bentonite clays are available in literature[13,14] fresh experiments have been performed on the osmosis of sodium chloride solution through kaolinite clay membrane to estimate the values of the parameters relevant to salt rejection behaviour. This became necessary because the data of Abdel-Aziz and Taylor[13] on osmosis of electrolytic solutions through kaolinite clay is not in a form convenient for the analysis presented in this chapter. In case of bentonite clay, however, the data obtained by Letey and Kemper[14] for the osmosis of sodium sulphate solution have been utilised.

II.2 THE PHENOMENOLOGICAL RELATIONS

Consider a system consisting of two compartments containing the same binary aqueous solutions of unequal concentrations and separated by a membrane of a porous plug of thickness Δx. The phenomenological relations for the simultaneous transport of solute and solvent for such a situation have been described in chapter I. But in writing these equations the system has been considered to be a discontinuous one and therefore differences of potentials across the porous barrier have been considered as thermodynamic driving forces. Since in the experiments described in this chapter the gradients of potentials have to be taken as driving forces the phenomenological relations between fluxes and forces have to be rewritten in the appropriate forms.

Rewriting the linear phenomenological relations for the present case between fluxes and forces we get[14,15]

$$J_v = L_P \nabla P + L_{PD} \nabla \pi \qquad (1)$$

$$J_D = L_{DP} \nabla P + L_D \nabla \pi \qquad (2)$$

with

$$L_{PD} = L_{DP} \qquad (3)$$

on account of Onsager's theorem. In equations (1) to (3) J_v represents the volume flux, J_D represents the velocity of the solute relative to that of the solvent, P and π stand for the pressure and osmotic pressure respectively and L_P, L_{DP}, L_{PD} and L_D are phenomenological coefficients. Following the procedure adopted by Kedem and Katchalsky[15,16] and described in the chapter I the linear phenomenological equations can be further transformed into

$$J_v = L_P (\nabla P - \sigma \nabla \pi) \qquad (4)$$

and

$$J_s = \omega \nabla \pi + \bar{C}_s (1 - \sigma) J_v \qquad (5)$$

where J_s stands for the solute flux. The quantities σ and ω in equations (4) and (5) are called reflection coefficient and solute permeability respectively and are defined as

$$\sigma = - \frac{L_{PD}}{L_P} \qquad (6)$$

and

$$\omega = \left(\frac{J_s}{\nabla \pi} \right)_{J_v=0} = \frac{\bar{C}_s (L_P L_D - L_{PD}^2)}{L_P} \qquad (7)$$

where $\bar{C}_s$ is the average of the solute concentration in the two compartments. The value of the reflection coefficient σ lies between zero and unity. When $\sigma = 1$ the membrane is said to be an ideal semipermeable membrane.

The equation (4) and (5) which were first deduced by Kedem and Katchalsky[15,16], because of their operational form, are more appropriate than the equations (1) and (2) for the evaluation of L_p, σ and ω - the three parameters which adequately describe the salt rejection properties of a membrane system. This fact has already been emphasised in chapter I. It should be borne in mind that in the deduction of equation (4) and (5) validity of the linear phenomenological relations and Onsager's reciprocal relation has been supposed.

II.3 EXPERIMENTAL

Materials

Kaolinite clay obtained from M/s Impex Chemical Corporation (Bombay), sodium chloride (BDH Analar) and distilled water distilled once over alkaline potassium permanganate in an all glass still were used in the present experiments.

The Osmosis Cell

The osmosis cell used for the measurement of fluxes has been depicted in Fig. II.1 and has been well labelled to make it self-explainatory. The kaolinite clay plug was compacted on the sintered glass disc (S) Porosity G-4

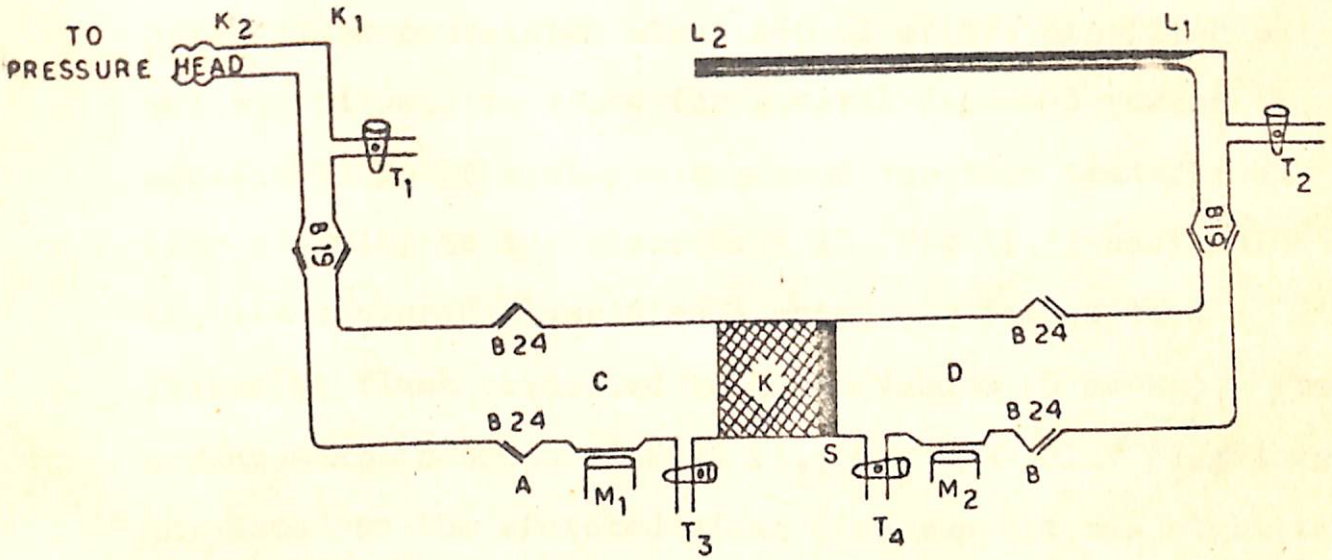

FIG. II.1

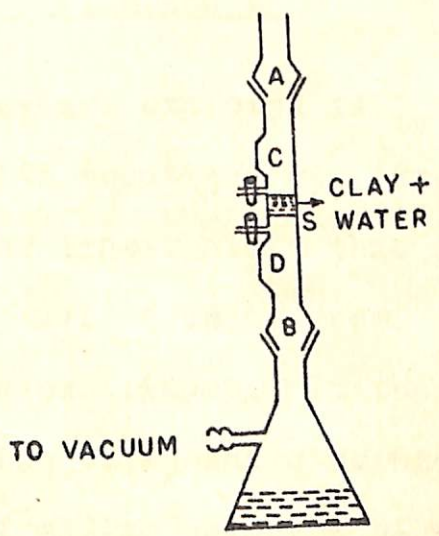

FIG. II.1(a)

Fig.II.1 The osmosis cell - T_1, T_2, T_3 and T_4 are stop cocks. M_1 and M_2 are magnetic stirrers. K - kaolinite plug - thickness 1 cm and area 10.9 cm^2. S - sintered glass disc of porosity G-4. L_1 L_2 - capillary tube of length 19 cms and diameter 0.0138 cms. Volumes of the compartments C and D 288 and 372 ml respectively.

Fig.II.1(a) Arrangement for compaction of the clay on the sintered glass support.

(Fig. II.1) using the following procedure. A known amount (about 10 gms) of the sodium saturated clay was put in a pyrex flask containing about 250 ml of the distilled water and was allowed to stand for several days and shaken occasionally. The clay suspension was then transferred with stirring to the glass tube AB (Fig II.1) containing the G-4 sintered glass disc S which was joined to a filtering flask connected to known vacuum (5 mm Hg). The arrangement is shown in Fig. II.1(a). The clay plug thus compacted on the sintered glass disc support was stabilised further by making use of rubber gasket on one side.

II.4 EVALUATION OF L_p, σ and ω

Linear curves are expected if J_v is plotted against ∇p in accordance with equation (4). From the slope and the intercept of the linear plots thus obtained, L_p, σ can be calculated provided $\nabla\pi$ is known and is more or less constant during the experiment. In the actual experiments for the determination of L_p and σ using equation (4), an aqueous solution of sodium chloride of known strength (say .00022 M) was filled in the compartment C on the left hand side of the clay plug and distilled water was filled in the compartment D (Fig. II.1) on the right hand

side of the clay plug. The system was allowed to stand till recession in the capillary L_1L_2 due to osmosis was noticed. As soon as recession in the capillary L_1L_2 was noticed known pressure was applied on the solution compartment by adjusting the pressure head and the rate of advancement of liquid miniscus in the capillary was noted with time, using a cathetometer reading upto 0.001 cms and a stop watch reading upto 0.1 sec. Since the back flow of water in the solution compartment due to osmosis is expected to be quite small the value of $\nabla\pi$ can be taken to be more or less constant during a particular run of the experiment. In order to maintain the condition $\nabla\pi$ = constant in all such runs the electrolyte solution in the osmosis cell was replaced by the fresh stock solution before the volume flux measurement corresponding to the next value of ∇P was made. The data obtained in this manner have been given in Table II.1&2 and plotted in Fig. II.2 for the two different values of $\nabla\pi$.

The equation (5) under the condition J_v equal to zero was the basis for the determination of ω. In the actual experiments for the determination of ω a solution of sodium chloride of known concentration (say .00022 M) was filled in the compartment C (Fig. II.1) on the left hand

The volume flux data for the determination of L_p and σ using equation (4).

Table II.1

(For $\nabla\pi$ = 11.79 cm cm^{-1})

S.No.	∇P cm cm^{-1}	$J_v \times 10^5$ cm sec^{-1}
1.	14	1.57
2.	16	1.9
3.	18	2.32
4.	20	2.7
5.	22	3.2
6.	24	3.6

Table II.2

(For $\nabla\pi$ = 15.15 cm cm^{-1})

S.No.	∇P cm cm^{-1}	$J_v \times 10^5$ cm sec^{-1}
1.	16	1.4
2.	18	1.9
3.	20	2.3
4.	22	2.65
5.	24	3.2

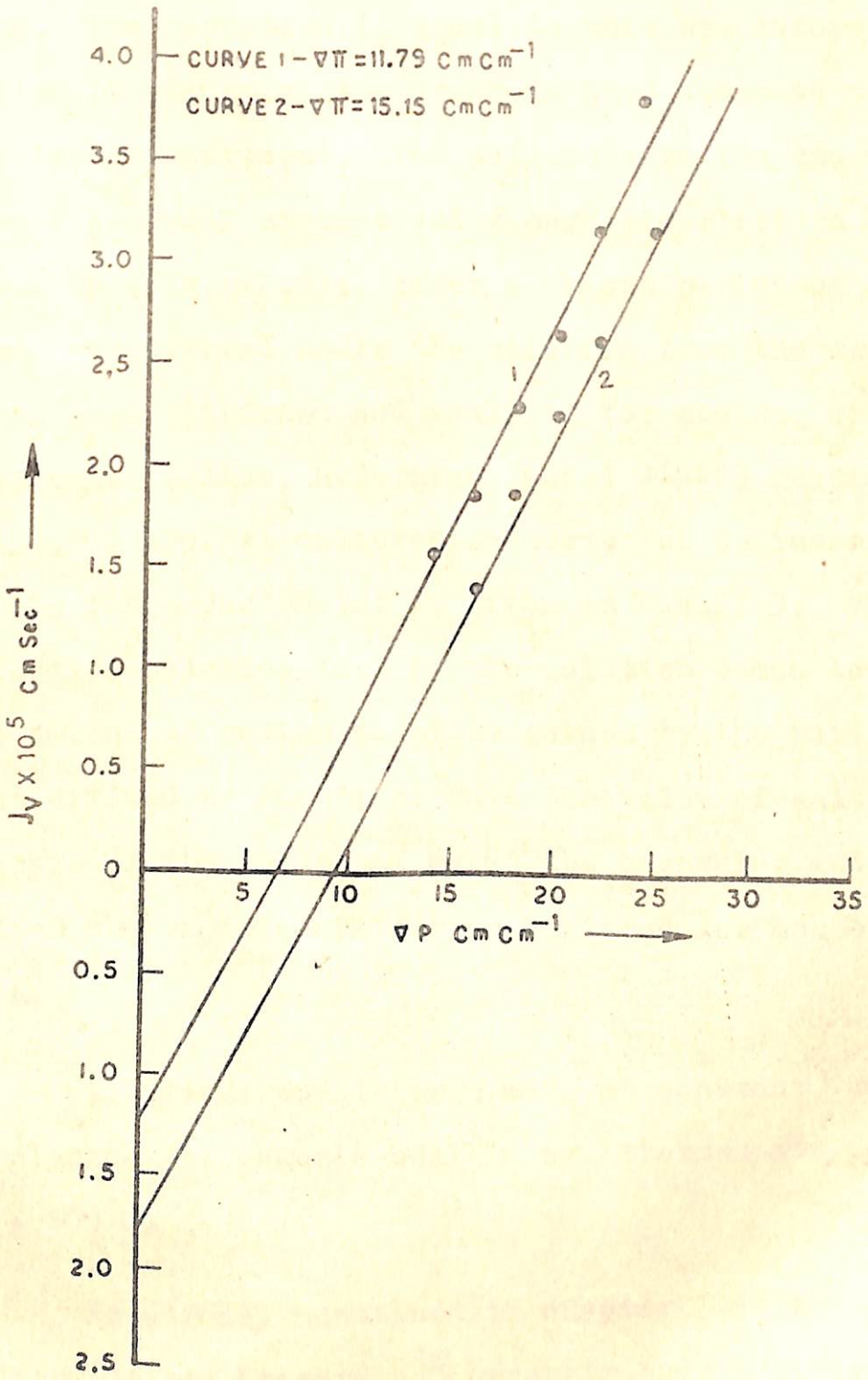

Fig.II.2 Determination of L_p and σ using equation (4)

side of the clay plug and distilled water was filled in the other compartment D on the right hand side of the clay plug. The condition J_v equal to zero was enforced on the system by adjusting the pressure head attached to the solution compartment. The solutions in the two compartments were vigorously stirred using magnetic stirrers M_1 and M_2 shown in (Fig. II.1). After a known period of time (t) which was several hours the solution from the two compartments were withdrawn and analysed for sodium, using a flame photometer (Elico, Hyderabad, Model CL-22) reading upto 2 ppm. A typical calibration curve for sodium estimation by the flame photometer is given in Fig.II.3. The amount of sodium chloride lost by the solution compartment or the amount of sodium chloride gained by the water compartment divided by the time, gave the value of salt flux. Average of the values of v_n at the beginning and at the end of the experiments were considered for the estimation of ω.

All measurements were made at constant temperature by placing the osmosis cell in a thermostate set at $40 \pm 0.1^{\circ}C$.

As already mentioned in chapter I Smit[17] and Smit, Eijsermans and Staverman[18] have stressed that it is

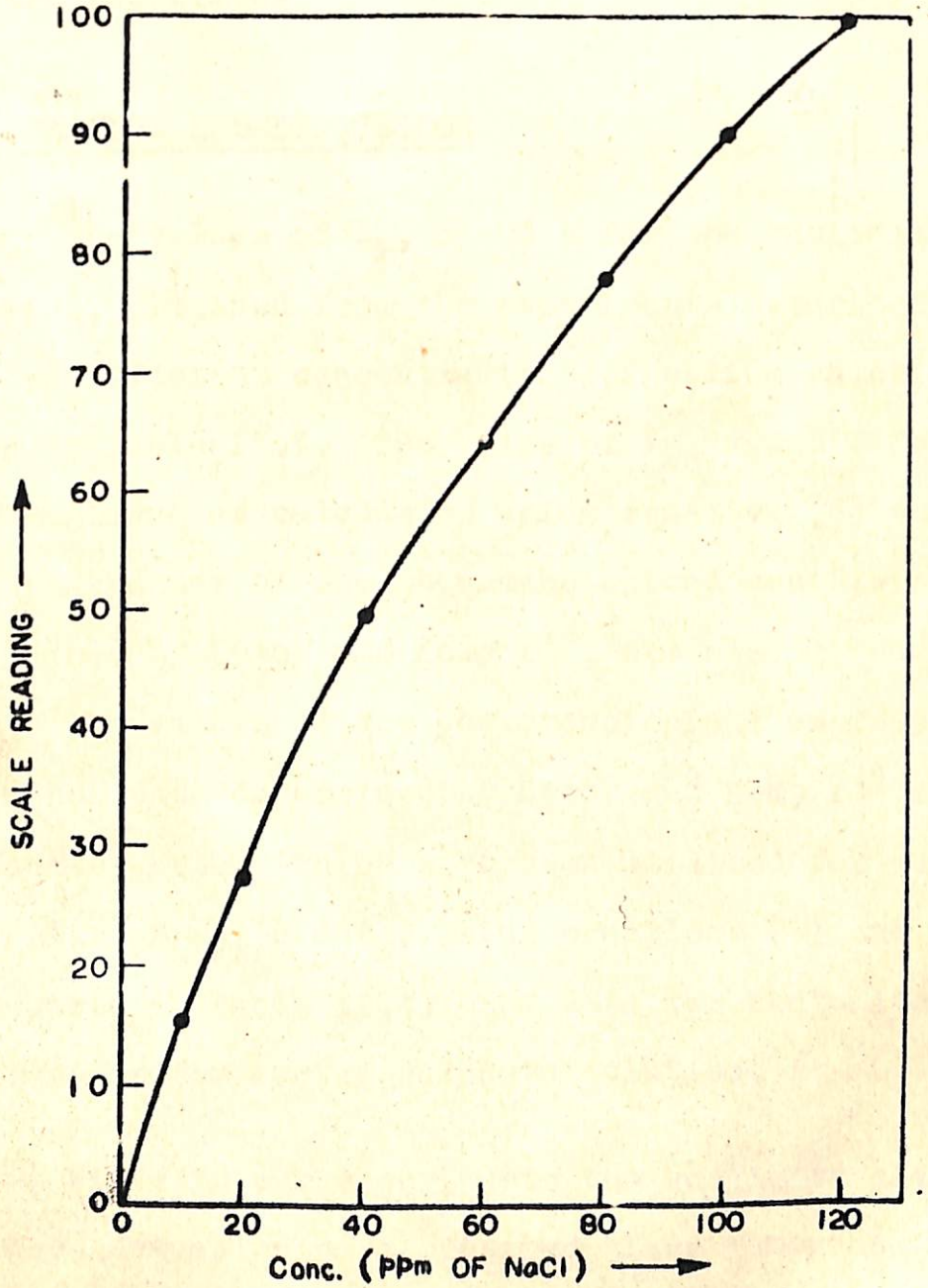

Fig II 3 Calibration curve for sodium estimation using flame photometer.

recommendable to determine σ, L_p and ω in this way i.e. using equation (4) and (5) rather than σ and L_p in an ultra filteration experiment and ω separately in an osmotic experiment.

II.5 RESULTS AND DISCUSSION

The values of L_p, σ and ω for the kaolinite clay membrane, obtained from the experiments described above for two different concentrations of sodium chloride are given in Table II.3. The value of L_p, σ and ω for bentonite clay membrane as calculated using equation (6) and (7), from the values of the phenomenological coefficients determined by Letey and Kemper[14], are also given in Table II.3. The values of the phenomenological coefficients and other data determined by Letey and Kemper[14] for the bentonite system which have been utilised for estimating the value of L_p, σ and ω using equations (6) and (7) are reproduced in Table II.4. The data for bentonite clay membrane is for sodium sulphate solution.

Since in our experiments the kaolinite clay membrane has been compacted on a sintered glass membrane (porosity G-4) it may appear at first sight that the values of the permeability coefficients evaluated in the present studies

Table II.3

Values of L_p, σ, ω, and various frictional coefficients for Kaolinite/Sodium chloride solution and Bentonite/Sodium sulphate solution system.

Sl No	System	σ	ω mole cm^{-2} sec^{-1} $\times 10^{15}$	L_p $Cm\ sec^{-1}$ $\times 10^{7}$	f_{sm} Cm^2 mole^{-1} sec $\times 10^{-11}$	f_{sw} Cm^2 mole^{-1} sec $\times 10^{-11}$	f_{wm} Cm^2 mole^{-1} sec $\times 10^{-7}$
1.	Kaolinite/Sodium chloride solution	0.53†	5825.00*	20.00	0.1682	1.2696	0.9035
2.	Kaolinite/Sodium chloride solution	0.59‡	5774.00**	20.00	0.0545	1.3961	0.9035
3.	Bentonite/Sodium sulphate solution	0.824	4.291	0.00233	996.00	1394.00	7754.93

† $\nabla\pi$ = 11.79 cm cm^{-1}

‡ $\nabla\pi$ = 15.15 cm cm^{-1}

* Average $\nabla\pi$ = 11.50 cm cm^{-1}

** Average $\nabla\pi$ = 11.60 cm cm^{-1}

The values for the Bentonite/Sodium sulphate solution system have been calculated from the data of Letey and Kemper (ref. 14).

Table II.4

The values of the various phenomenological coefficients (obtained by Letey and Kemper[14]) utilised for the evaluation of σ and ω for bentonite/sodium sulphate solution system, using equation (6) and (7).

Run No.	$\bar{C}_s$ gm cm^{-3} $\times 10^3$	L_P cm hr^{-1} $\times 10^7$	L_D cm hr^{-1} $\times 10^6$	L_{PD} cm $hr^{-1} \times 10^7$
1	1.42	-	1.45	6.87
2	1.42	-	1.51	6.86
3	1.42	8.4	1.48	7.11

Table II.5

The Hydraulic permeability data for the pyrex-sinter membrane (porosity G-4).

∇P cm cm^{-1}	$J_v \times 10^3$ cm sec^{-1}
5	0.5
10	0.825
15	1.4
20	1.925
25	2.4
30	2.9

are for the total membrane consisting of sintered glass membrane and the kaolinite clay membrane in a series array and not for the kaolinite clay membrane alone. But following the arguments given by Srivastava, Jain and Upadhya[19] for a similar situation, it can be shown that it is not so. The values of the permeability coefficient evaluated from the present experimental data are more or less equal to the values for the kaolinite clay membrane. As an example let us take the hydraulic permeability coefficient L_p.

Kedem and Katchalsky[20] have demonstrated, from the consideration of stationarity of flows and Kirkwoods'[21] hypothesis of continuity of potentials of driving forces across the boundaries, that the constants L_p for the total series membrane and its constituent membrane elements (clay membrane and glass sinter in the present case) are related in the following manner:

$$\frac{1}{L_p} = \frac{1}{L_p^C} + \frac{1}{L_p^G} \qquad (8)$$

The superscripts C and G in equation (8) represent clay membrane and the glass sinter, respectively. Rearranging equation (8) we can write:

$$L_P^c = \frac{L_P}{1 - (L_P / L_P^G)} \qquad (9)$$

In order to evaluate the value of L_P^G, water flow measurements through pyrex-glass sinter (G-4) were made. These are plotted in Fig II.4. The value of L_P^G evaluated from the slope of the straight line in Fig II.4 (Table II.5), comes out to be equal to 0.979×10^{-4} cm sec^{-1} which is much larger than the value of L_P. This makes the quantity (L_P / L_P^G) quite small in comparison to unity. The equation (9) therefore approximates to:

$$L_P \cong L_P^c \qquad (10)$$

With the data of L_P, σ and ω at hand (Table II.3) the salt rejection performance of both kaolinite and bentonite clay membranes, in a hyper-filteration process can be assessed using the formalism developed by Johnson, Dresner and Kraus[4]. Defining salt rejection parameter r as

$$r \equiv 1 - \frac{C_s''}{C_s'} \qquad (11)$$

where C_s'' is the salt concentration in the hyper filterate and C_s' is the concentration of the feed solution,

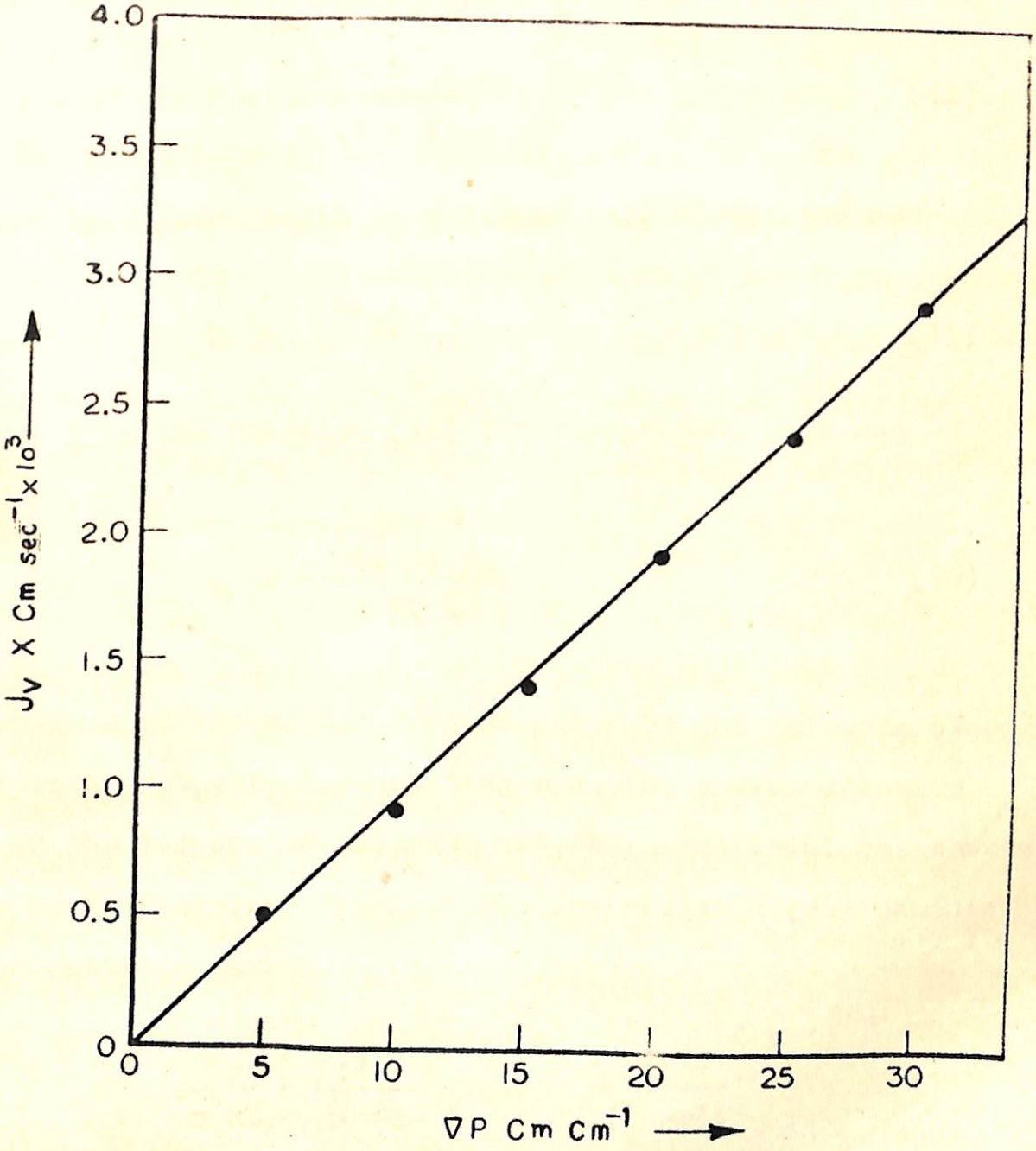

Fig.II.4 The Hydraulic permeability data for the pyrex sintered membrane (porosity G-4).

Johnson et al[4] have obtained the following equation describing the salt rejection, r, at different flow rates:

$$F = \frac{\sigma - r}{\sigma (1 - r)} \qquad (12)$$

The flow parameter F in equation (12) is defined as

$$F \equiv e^{-J_v A} \qquad (13)$$

and A in the relation (13) for the present case can be written as

$$A = \frac{(1- \sigma)\ \Delta\pi}{n\ RT\ \omega} \qquad (14)$$

where n is the number of ions given by one molecule electrolyte on complete dissociation e.g. for sodium chloride n=2 and for sodium sulphate n=3, R is the usual gas constant T is the absolute temperature. The equation (12) can now be rewritten as

$$\frac{J_v}{n\ RT} = \frac{2.303\ \omega}{\Delta\pi\ (1-\sigma)} \log \frac{\sigma\ (1-r)}{(\sigma - r)} \qquad (15)$$

At high flow rate $F \to 0$ and hence the reflection coefficient is the limiting value of r when filteration flow overtakes diffusion:

$$J_v \rightarrow \infty ; \qquad r \rightarrow \sigma \qquad (16)$$

By mea ns of equation (15) it is possible to predict the expected salt rejection curve using the value of σ and ω determined from suitable experiments. The r versus J_v, data for the kaolinite membrane/sodium chloride solution and bentonite membrane/sodium sulphate solution, calculated from equation (15) using the values of σ and ω given in Table II.3, have been given in Table II.6,7 and plotted in Figures II.5. The curves in Fig. II.5 predicts the salt rejection performance of the compacted clay membranes in a reverse osmosis operation.

The data on L_P, σ and ω (Table II.3) can be further utilised to assess how efficient these clay membranes would be for salt rejection, in a reverse osmosis operation, by using the criteria for efficient hyper-filteration membranes, developed by Spiegler and Kedem[5] from the consideration of thermodynamics of hyperfilteration. The criteria developed by Spiegler and Kedem[5] can be stated as follows

$$f_{sm} \gg f_{wm} \qquad (17)$$

$$f_{sm} \gg f_{sw} \qquad (18)$$

where f represents the coefficient of friction between the

Values of the salt rejection parameter r at various values of volume flux, as predicted by equation (15)

Table II.6

(For Kaolinite/Sodium Chloride solution system, $\sigma = 0.56$).

S.No.	r	$\frac{J_v}{2\ RT} \times 10^{11}$ mole sec^{-1} cm^{-3}
1.	6.1	0.1149
2	0.2	0.2757
3.	0.3	0.5175
4.	0.4	0.9352
5.	0.5	1.90

Table II.7

(For Bentonite/Sodium Sulphate solution system, $\sigma = 0.824$).

S.No.	r	$\frac{J_v}{3\ RT} \times 10^{15}$ mole sec^{-1} cm^{-3}
1.	0.1	0.567
2.	0.2	1.33
3.	0.3	2.30
4.	0.4	3.72
5.	0.5	5.86
6.	0.6	9.37
7.	0.7	16.80

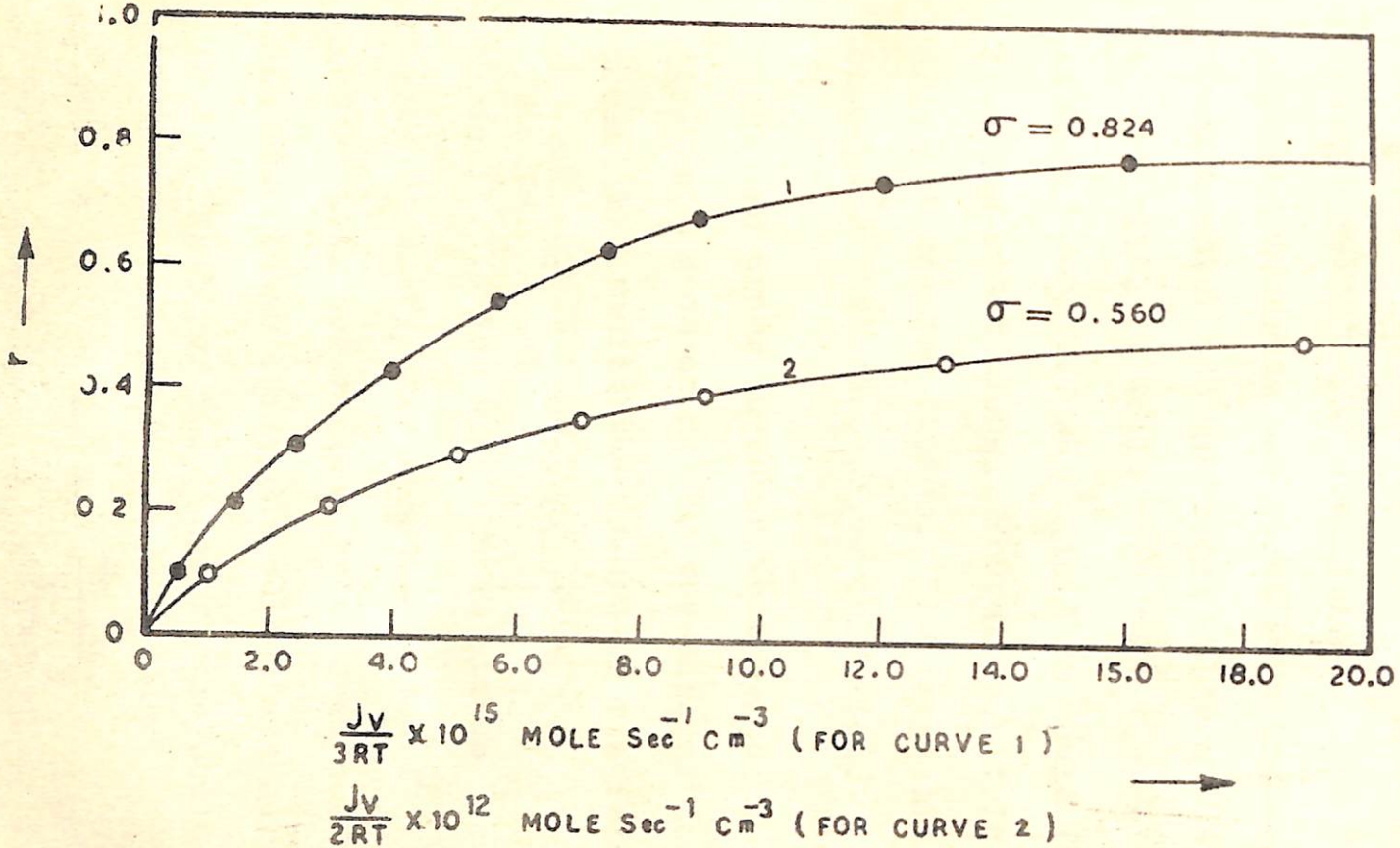

Fig. II.5 Variation of salt rejection parameter with volume flux, as predicted by equation (15) (Curve 2 is for kaolinite membrane/sodium chloride solution system. For this average of the values of σ and ω given in Table II.3 have been considered. Curve 1 is for bentonite membrane/sodium sulphate solution system).

species indicated by the subscripts. The subscripts s, m, w in the present case stand for the salt, the membrane and water respectively. The inequality (17) expresses a kinetic selectivity coefficient. The friction between the salt and membrane has to be much higher than the friction between water and membrane. This alone is not enough. If f_{sw} is high, it would mean that the salt and water are strongly coupled, which in turn would imply that one will drag the other along. Therefore, it is necessary to decouple the two fluxes. The inequality (18) in fact expresses this decoupling condition.

In order to check whether the inequalities (17) and (18) hold good or not in the case of the clay membranes presently studied the values of the frictional coefficient, f_{sm}, f_{sw} and f_{wm} were calculated from the data given in Table II.3. For this the equations obtained[15,22] on the basis of Spiegler's frictional model[23] connecting L_p, σ and ω with the various frictional coefficients were made use of. These equations which have already been discussed in chapter I for the present case would read as follows:

$$L_p = \frac{\varphi_w \bar{V}_w}{f_{wm}} \qquad (19)$$

$$\sigma = 1 - \frac{K_s f_{sw}}{(f_{sw} + f_{sm}) \varphi_w} \qquad (20)$$

$$\omega = \frac{K_s}{(f_{sw} + f_{sm})} \qquad (21)$$

In equations (19) and (20) φ_w and $\bar{V}_w$ represent the volume fraction and the partial molar volume of water respectively and K_s represents the distribution coefficient of the electrolyte between the membrane phase and the aqueous phase. For determination of the value of K_s, known amount of the clay was taken in a pyrex flask and known volume of the electrolyte solution of known concentration was added to it and was well stirred for several days using magnetic stirrer. The supernant liquid was analysed for sodium using a flame photometer. The concentrations of the electrolyte chosen were within the range of concentration used in the osmosis experiments. The electrolytes chosen were sodium chloride for kaolinite and sodium sulphate for bentonite. The value of K_s for kaolinite and bentonite were found to be 0.8376 and 0.9778 respectively. Using the value of K_s thus obtained and the values of L_p, σ and ω given in Table II.3, the frictional coefficients f_{sm}, f_{sw} and f_{wm} were calculated using equation (19) to (21) and are given in Table II.3.

Looking at the values of the frictional coefficients in Table II.3 it is obvious that for both the systems namely kaolinite membrane/sodium chloride solution and bentonite membrane/sodium sulphate solution the inequality (17) is satisfied while the inequality (18) is not which is an indication of the coupling between salt and water. Thus both kaolinite and bentonite membranes only partially satisfy the criteria, for efficient hyperfilteration membranes for reverse osmosis, evolved by Spiegler and Kedem[5] from kinetic consideration of the membrane process.

Although the inequality (18) is not satisfied but the difference in the order of magnitudes of f_{sm} and f_{sw} (Table II.3) is not very large. This encourages us to suggest that the idea of using compacted clays as membranes in hyper-filteration operation is worth giving a trial in spite of the fact that these membranes only partially satisfy the criterion for efficient membranes developed by Spiegler and Kedem[5]. The indigeneous availability of clays and the ease with which they can be compacted into membranes further adds to our suggestion.

II.6 REFERENCES

1. Science and Technology Plan 1974-79 vol. II page 274 National Committee on Science and Technology, 1973.

2. Report on Science and Technology Plan for Chemical Industry vol. I submitted to N.C.S.T. 1973, page 139.

3. Report on Science and Technology Plan for Chemical Industry. Vol. II submitted to N.C.S.T. 1973, pages 179, 181, 182.

4. J.S.Johnson, L.Dresner and K.A.Kraus, cited in Principles of desalination (Academic Press, New York) 1966, page 345-439.

5. K.S.Spiegler and O.Kedem, Desalination, 1, 311 (1966).

6. E.Hoffer and O.Kedem, Desalination, 2, 25 (1967).

7. E.Hoffer and O.Kedem, Desalination, 5, 167 (1968).

8. E.Hoffer and O.Kedem, J. Phys. Chem. 76, 3638 (1972).

9. G.R.Garbarini, R.F.Eaton, T.K.Kwei and A.V.Tobolsky, J. Chem Ed. 48, 226 (1971).

10. Saline Water Conversion Report, 1968, Office of Saline Water, U.S. Deptt. of Interior.

11. Saline Water Conversion Report, 1969-70, Office of Saline Water, U.S. Deptt. of Interior.

12. G.H.Bolt and P.H.Groenevelt, Bull. Intern., Assoc. Sci. Hydrol. XIV, 2, 17 (1969).

13. M.H. Abd-el-Aziz and S.A.Taylor, Soil Sci. Soc. Am. Proc. 29, 141 (1965).

14. J.Letey and W.D.Kemper, Soil Sci. Soc. Am. Proc. 33, 25 (1969).

15. A.Katchalsky and P.F.Curran, Non-equilibrium thermodynamics in biophysics (Harvard University Press) 1967 pp. 113-132.

16. O.Kedem and A.Katchalsky, Biochem. Biophys. Acta, 27, 229 (1958).

17. A.M.Smit, Partition and Friction in Membranes, Ph.D. Thesis, University of Leidon, 1970.

18. J.A.M.Smit, J.C.Eijsermans and A.J.Staverman, J. Phys. Chem., 79, 2168 (1975).

19. R.C.Srivastava, A.K.Jain and S.K.Upadhyay, J.Hydrol. 26, 295 (1975).

20. O.Kedem and A.Katchalsky, Trans. Faraday Soc., 59, 1941 (1963).

21. J.G.Kirkwood, In H.T.Clarke (Editor) Ion Transport Across Membranes. Academic Press, New York (1954).

22. O.Kedem and A.Katchalsky, J. gen. Physiol., 45 143 (1961).

23. K.S.Spiegler, Trans. Faraday Soc., 54, 1408 (1958).

CHAPTER III

TRANSPORT THROUGH LIQUID MEMBRANES*

---

* Two papers based on the work contained in the chapter have been accepted for publication - one is in press with the JOURNAL OF COLLOID AND INTERFACE SCIENCE (U.S.A.) and the other one is to appear in the INDIAN JOURNAL OF CHEMISTRY.

TRANSPORT THROUGH LIQUID MEMBRANES

III.1 INTRODUCTION

It has been well known[1] that the addition of soluble surfactants influences material transport across phase interfaces. This gave rise to the speculation[1,2] of the formation of surfactant films at the interface which might act as liquid membranes affecting mass transfer. But the use of liquid membranes in the science and technology of separation processes is of very recent origin.[2-5]

The application of liquid membrane to water desalination technology owes its origin to Martin's[6] discovery that the addition of a small amount of surfactants like poly vinyl methyl ether (PVME) to saline feed in reverse osmosis effected a large increase in the salt retention capacity of cellulose acetate membranes with but a small decrease in the flux of product water. Michaels, Bixler, and Hodges[7] subsequently ascribed this effect to the physical blockage of larger pores by feed additive molecules. The explanation of the increased permselectivity as given by Kesting et al[8-10] was, however, based on the hypothesis of the existence of a surfactant layer liquid membrane at the interface between the cellulose acetate membrane and

the saline solution. Bixler and Cross[11] have favoured the liquid membrane hypothesis proposed by Kesting et al.[8-10]

According to the liquid membrane hypothesis,[8-10] the surfactant layer which forms spontaneously at the cellulose acetate membrane/saline solution interface acts as a liquid membrane in series with the solid membrane gel. The experiments of Kesting et al[10] also demonstrated that as concentration of the surfactant is increased, the cellulose acetate membrane gets progressively covered with the surfactant layer liquid membrane and at the critical micelle concentration (CMC) the coverage of the cellulose acetate membrane with the surfactant layer is complete.

The experiments on hydraulic permeability, electro-osmotic velocity, streaming potential and current reported in this chapter lend further support to Kesting's liquid membrane hypothesis.[8-10] The transport data have been utilised to estimate the fraction of total area of the supporting membrane covered with the liquid membrane when concentration of surfactant is lower than its CMC value and it has been concluded that when concentration of the surfactant is half its CMC value the area covered by the liquid membrane is half the area covered at the critical micelle concentration. The data also indicate the

the saline solution. Bixler and Cross[11] have favoured the liquid membrane hypothesis proposed by Kesting et al.[8-10]

According to the liquid membrane hypothesis,[8-10] the surfactant layer which forms spontaneously at the cellulose acetate membrane/saline solution interface acts as a liquid membrane in series with the solid membrane gel. The experiments of Kesting et al[10] also demonstrated that as concentration of the surfactant is increased, the cellulose acetate membrane gets progressively covered with the surfactant layer liquid membrane and at the critical micelle concentration (CMC) the coverage of the cellulose acetate membrane with the surfactant layer is complete.

The experiments on hydraulic permeability, electro-osmotic velocity, streaming potential and current reported in this chapter lend further support to Kesting's liquid membrane hypothesis.[8-10] The transport data have been utilised to estimate the fraction of total area of the supporting membrane covered with the liquid membrane when concentration of surfactant is lower than its CMC value and it has been concluded that when concentration of the surfactant is half its CMC value the area covered by the liquid membrane is half the area covered at the critical micelle concentration. The data also indicate the

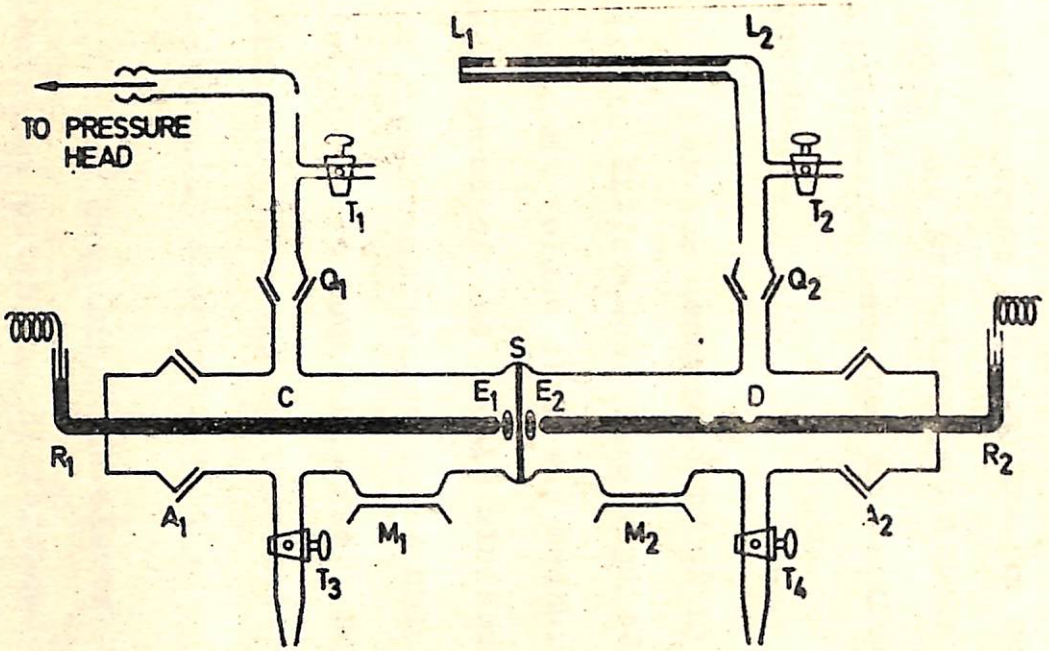

FIG. III.1 The Transport cell. T_1, T_2, T_3 and T_4 are stop cocks M_1 and M_2 are magnetic stirrers. S . . . Cellulose acetate millipore filter with pore size 0.2 μ. L_1L_2 . . . capillary tube of length 18 cms and diameter with 0.38×10^{-4} m. The volume of the compartments C and D are 96 ml and 86 ml respectively. A_1 and A_2 are B-19 Glass joints. Q_1 and Q_2 are B-14 glass joints. E_1, E_2 . . . Bright Platinum Electrodes; R_1 R_2 . . . glass tubes containing mercury

filled in the compartment C on the right hand side of the millipore filter S (Fig. III.1) and distilled water was filled in the compartment D. Since value of the critical micelle concentration (CMC) for the aqueous solutions of PVME is 6 ppm[10] the concentration ranges from zero to twelve ppm were purposely chosen so that we get data on both the lower and the higher side of the CMC, at which the supporting membrane is expected to be completely covered with the liquid membrane. The hydraulic permeability, electro-osmotic velocity and streaming potentials were measured following the procedure described in earlier studies[12-14] from this laboratory.

For the measurements of hydraulic permeability known pressure differences were applied across the membrane. The consequent volume flux was measured by noting the rate of advancement of the liquid miniscus in the capillary L_1L_2 with a cathetometer of least count 0.001 cm and a stop watch of least count 0.1 sec. During the measurements of hydraulic permeability the electrodes E_1 and E_2 were electrically short-circuited.

For measuring the electro-osmotic velocity known electrical potential differences were applied across the membrane by connecting the respective electrodes E_1 and

E_2 to the terminals of an electronically operated D.C. power supply (Beltronix Model ED-101) and the volume flow induced by various potential differences was observed by noting the rate of advancement of the liquid miniscus in the capillary L_1L_2. The uncertainty in the applied potential was $\pm$ 0.05v. In all the measurements of the electro-osmotic velocity the condition $\Delta P=0$ was enforced on the system.

The streaming potentials across the membrane were measured using a V.T.V.M (Philips GM 6020/90) of least count 0.1 mV. Known pressure differences were applied across the membrane and when the flow in the capillary L_1L_2 became steady, the streaming potential was measured by connecting the electrodes to the terminals of the V.T.V.M. The assymetry potential of the electrodes were taken into account in these measurements. The electrical resistance of the system was measured with a leitfahig Kettz-messer conductivity meter. The values of streaming current were calculated from the streaming potential and resistance of the system using ohm's law.

All measurements were made at constant temperature by placing the apparatus (Fig.III.1) in a thermostat set at 40 $\pm$ 0.1^{o}C. During the volume flux measurements the solutions in the two compartments (Fig.III.1) were well stirred using magnetic stirrers M_1 and M_2.

III.3 RESULTS AND DISCUSSION

The data on hydraulic permeability, electro-osmotic velocity, streaming potential and streaming current for different concentrations of PVME is given in Tables III.1 to 4 and plotted in Figures III.2 to 5. The usual linear phenomenological equations described in chapter I i.e.

$$J_v = L_{11} \Delta P + L_{12} \Delta \phi \qquad (1)$$

$$I = L_{21} \Delta P + L_{22} \Delta \phi \qquad (2)$$

obtained using the non-equilibrium thermodynamics treatment[15] for the simultaneous transport of water and electricity predict the following linear relationships. For hydraulic permeability

$$(J_v)_{\Delta\phi=0} = L_{11} \Delta P \qquad (3)$$

For electro-osmotic velocity

$$(J_v)_{\Delta P=0} = L_{12} \Delta\phi \qquad (4)$$

For streaming potential

$$(\Delta\phi/\Delta P)_{I=0} = -\frac{L_{21}}{L_{22}} \qquad (5)$$

Table III.1

Hydraulic Permeability data for various concentrations of PVME, using cellulose acetate millipore filter as a supporting membrane.

$\Delta P \times 10^{-2}$ N m^{-2}	Concentration of PVME (ppm)			
	0	3	6	12
	$J_v \times 10^4$ m sec^{-1}	$J_v \times 10^4$ m sec^{-1}	$J_v \times 10^4$ m sec^{-1}	$J_v \times 10^4$ m sec^{-1}
2.5	0.009	0.05	0.009	0.009
4	0.19	0.055	0.02	0.01
4.9	0.23	0.06	0.03	0.02
9.8	0.45	0.20	0.12	0.11
14.7	0.72	0.35	0.25	0.24
19.6	0.95	0.55	0.37	0.34
24.5	1.3	0.75	0.51	0.41
29.4	1.6	0.91	0.60	0.51

Table III.2

The Electro-osmotic velocity data for various concentration of PVME, using cellulose acetate millipore filter as a supporting membrane.

$\Delta \phi$ Volts	Concentration of PVME (ppm)			
	0	3	6	12
	$J_v \times 10^4$ m sec^{-1}	$J_v \times 10^4$ m sec^{-1}	$J_v \times 10^4$ m sec^{-1}	$J_v \times 10^4$ m sec^{-1}
10	.099	.08	.05	.025
15	.139	.10	.062	.055
20	.20	.122	.085	.08
25	.24	.155	.112	.089
30	.285	.20	.13	.11
35	.320	.22	.15	.13

Table III.3

The streaming potential data for various concentration of PVME, using cellulose acetate millipore filter as a supporting membrane.

$\Delta P \times 10^{-2}$ Nm^{-2}	Concentration of PVME (ppm)			
	0	3	6	12
	$\Delta \phi \times 10^2$ volts	$\Delta \phi \times 10^2$ volts	$\Delta \phi \times 10^2$ volts	$\Delta \phi \times 10^2$ volts
4.9	2	1.5	1.1	0.90
9.8	4	3.1	2.3	1.5
14.7	6	4.9	3.5	2.9
19.6	8.2	6.3	4.7	3.9
24.5	10.5	8.1	5.6	4.7
29.4	12.5	9.9	7.0	5.4

Table III.4

The streaming current data for the various concentration of PVME, using cellulose acelate millipore filter as a supporting membrane.

$\Delta P \times 10^{-2}$ N m^{-2}	Concentration of PVME (ppm)			
	0	3	6	12
	$I \times 10^{8}$ Amp.	$I \times 10^{8}$ Amp.	$I \times 10^{8}$ Amp.	$I \times 10^{8}$ Amp.
4.9	4.5	3.0	2.5	2.0
9.8	9.5	7.0	5.0	3.5
14.7	13.7	11.0	7.5	6.0
19.6	18.7	14.0	10.0	8.0
24.5	23.5	18.0	12.0	9.5
29.4	28.5	22.0	15.0	11.0

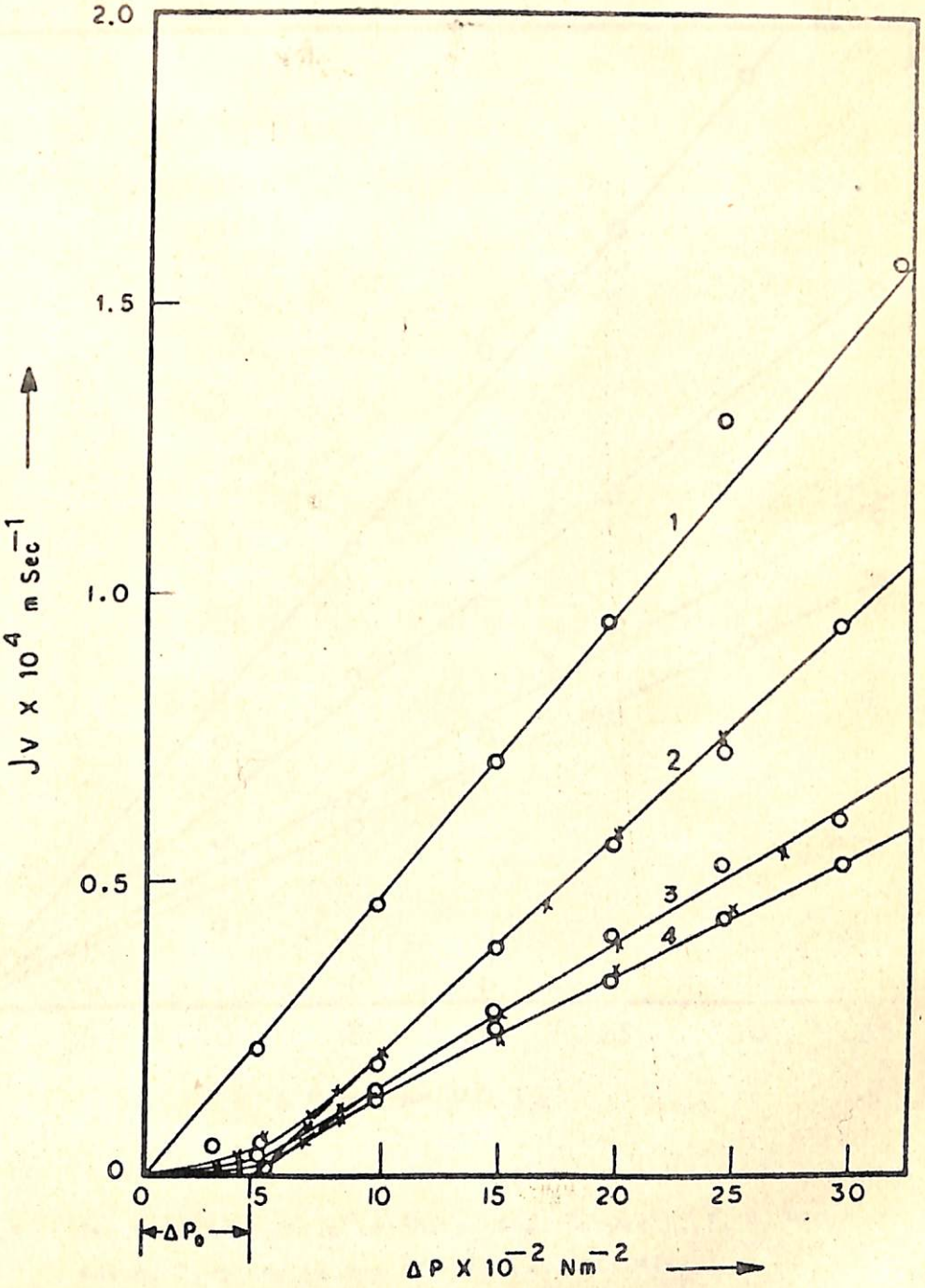

Fig. III.2 The Hydraulic permeability data, Curves 1, 2, 3, 4 are for 0, 3, 6 and 12 ppm PVME respectively. -O- experimental points, -X - theoretical points as predicted by the equation 8.

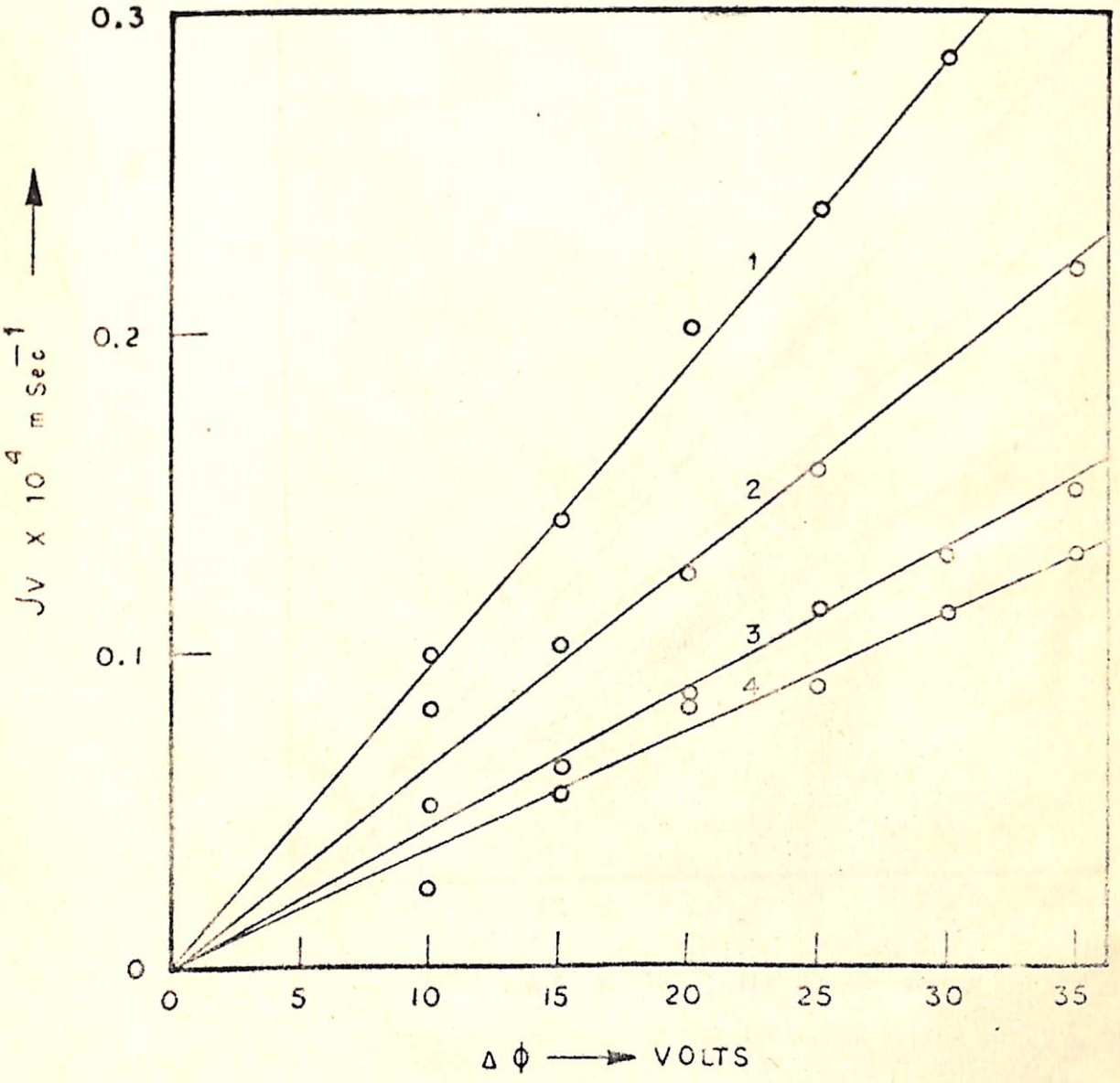

Fig. III.3 The Electro-osmotic velocity data. Curves 1, 2, 3, 4 are for 0, 3, 6 and 12 ppm of PVME respectively.

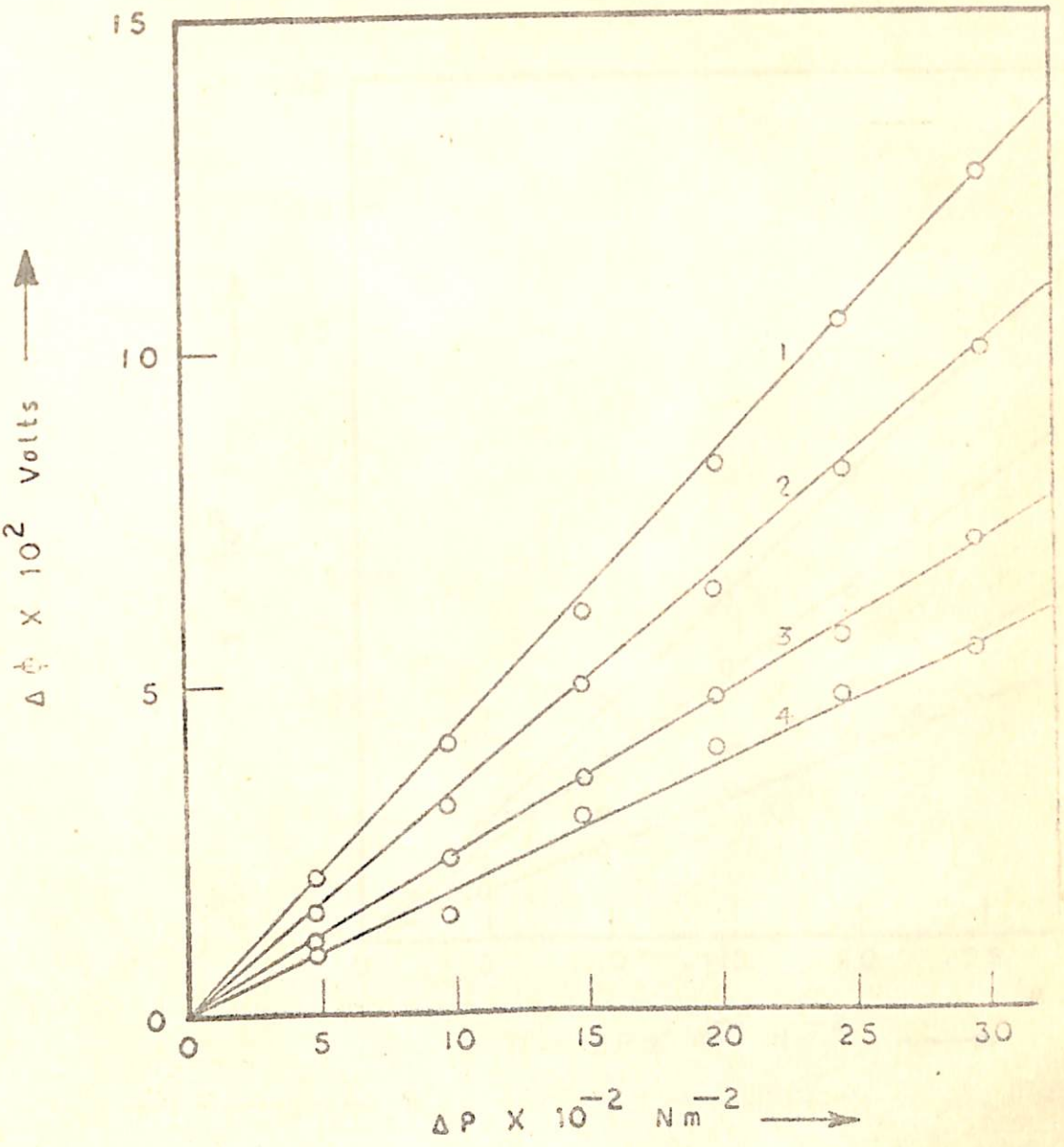

Fig. III.4 The streaming potential data. Curves 1, 2, 3, 4 are for 0, 3, 6 and 12 ppm of PVME respectively.

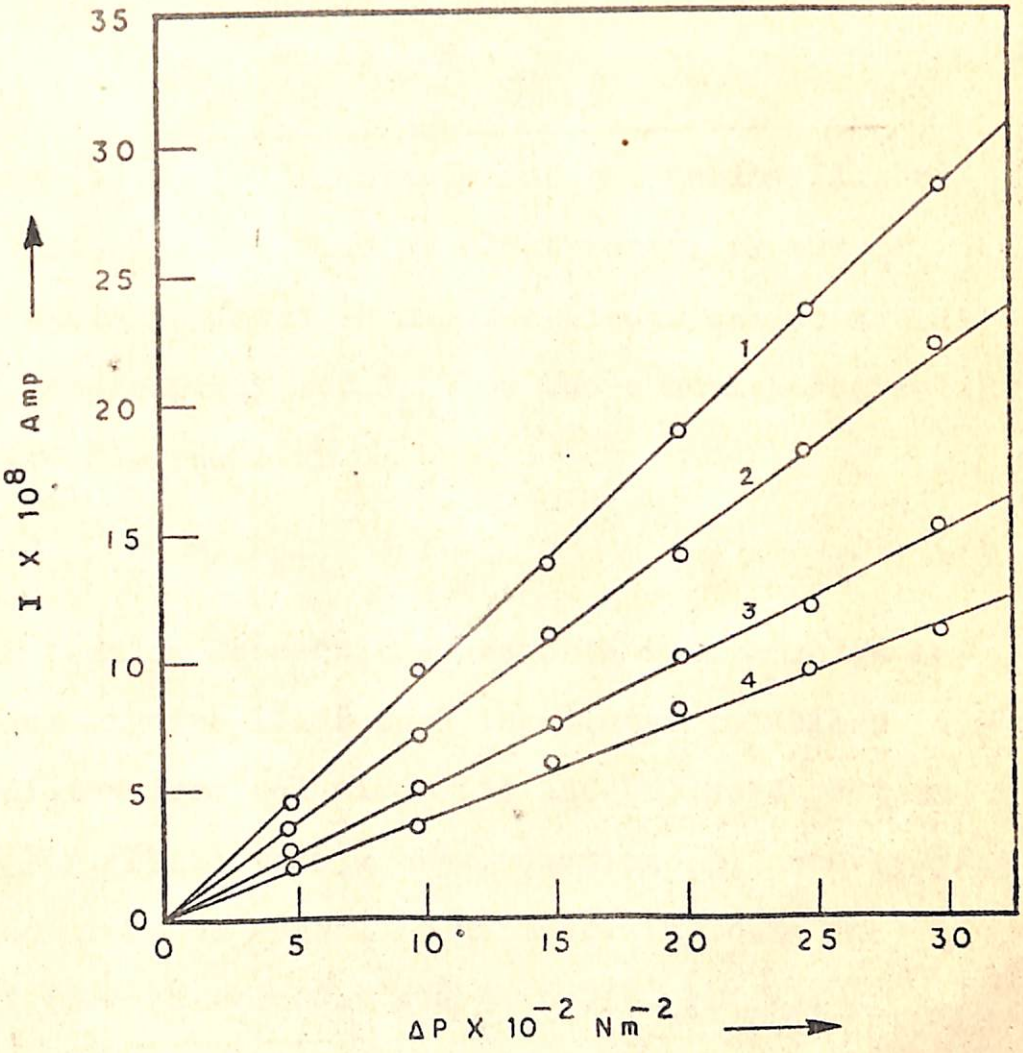

Fig. III.5 The streaming current data. Curves 1, 2, 3, 4 are for 0, 3, 6 and 12 ppm of PVME respectively.

and for streaming current

$$(I)_{\Delta\phi=0} = L_{21} \Delta P \qquad (6)$$

In equations (1) to (6) J_v stands for the volume flux of water, I stands for the flow of electricity, ΔP and $\Delta\phi$ are the pressure differences and the electrical potential difference respectively and L_{ik} are the phenomenological coefficient. The equality

$$L_{12} = L_{21} \qquad (7)$$

holds among them on account of Onsager's theorem. As in apparent from figures III.2 to 5 the linear relations (4) to (6) predicted from equations (1) and (2) hold good in all cases (Fig. III.3 to 5). The equation (3) however does not hold good for the hydraulic permeability data in presence of PVME (curves 2,3 and 4 in Fig. III.2).

The water flux (J_v) versus pressure difference (ΔP) curves in all cases where PVME concentration is greater than zero (curves 2,3,4 in Fig. III.2) start from the origin bend upward, then approach straight lines which extrapolate to intercept ΔP_0 on the ΔP-axis. The following equation was formed to fit in the hydraulic flow data in all such cases.

$$J = L_{11} [\Delta P - \Delta P_o \{1 - \exp(-\frac{\Delta P}{\Delta P_o})\}] \quad (8)$$

When ΔP assumes such high values that the term $\exp(-\frac{\Delta P}{\Delta P_o})$ becomes much smaller than unity the equation (8) simplifies to

$$J = L_{11} [\Delta P - \Delta P_o] \quad (9)$$

which represents the straight line parts of the curves 2 to 4 in Fig.III.2. Since water flow through the cellulose acetate millipore filter obeys the linear relationship (3) (Fig. III.2 curve 1) this kind of non-ideal behaviour (equation (8)) appears to be on account of the flow through the PVME liquid membrane formed in series with the cellulose acetate millipore filter as hypothesised by Kesting et al.[8-10] A more definite indication of the formation of the liquid membrane can be had from the gradation in the values of the coefficient L_{11} as concentration of PVME is increased from zero to 12 ppm. Values of the coefficients L_{11} for various concentrations of PVME as estimated from the slopes of the straight line positions of the curves in Fig. III.2 have been given in Table III.5. Values of the coefficient L_{12}, L_{21} and L_{22} estimated from the slopes of the straight lines in Fig III.3 to 5, for various concentrations of PVME are also given in Table III.5. Values of the coefficients L_{11} which measure conductivity

Table III.5

Values of the various phenomenological coefficients, electrical resistance and the solute permeability (ω) at various concentrations of PVME.

Concentration of PVME (ppm)	0	3	6	12
$L_{11} \times 10^{7}$ $m^3 N^{-1} sec^{-1}$	0.486	0.38	0.246	0.212
$L_{12} \times 10^{6}$ $m\ AJ^{-1}$	0.936	0.63	0.44	0.37
$L_{21} \times 10^{6}$ $m\ AJ^{-1}$	0.925	0.62	0.45	0.36
$L_{22} \times 10^{2}$ $ohm^{-1}\ m^{-2}$	2.36	2.33	2.23	2.14
Resistance $\times 10^{-6}$ ohm	0.445	0.45	0.47	0.49
$\omega \times 10^{11}$ mole $sec^{-1}\ N^{-1}$	0.991	-	0.244	0.12

to volume flow of water, show a progressive decrease as the concentration of PVME is increased from zero to 6 ppm (the CMC value). When the concentration of PVME is increased further the value of L_{11} also decreases but this decrease is less pronounced than the decrease which is observed upto 6 ppm - the CMC value for aqueous PVME. Similar trend can be seen in the values of L_{12} and L_{21}. This trend is in keeping with the liquid membrane hypothesis of Kesting et al[8-10] according to which as concentration of the surfactant (PVME in the present case) is increased the supporting membrane (the cellulose acetate millipore filter in the present case) gets progressively covered with the surfactant layer liquid membrane, and at CMC the coverage is complete. The decrease in the values of L_{11} beyond the CMC was ascribed by Kesting et al,[10] to densing of the liquid membrane which at CMC is fully developed and completely covers the supporting membrane. There is, however, another possibility which must be looked into e.g. the possibility of formalion of multilayers of the liquid membrane. We will discuss the investigation of this possibility a little later.

Before we take up the discussion of our investigation on the possibility of the formation of multilayer of the

liquid membrane let us try to estimate the fraction of the total area of the supporting membrane covered with the liquid membrane at concentrations lower than the CMC value of the surfactant. This can be conveniently done by utilising the analysis[16-18] for mosaic membranes. Since at critical micelle concentration of the surfactant (PVME in the present case) the supporting membrane (the cellulose acetate millipore filter in the present case) is supposed to be fully covered with the liquid membrane, one can logically expect that at concentrations lower than the CMC value of the surfactant the supporting membrane would be only partially covered with the liquid membrane. The situation has been pictorially depicted in the Fig. III.6. For such a situation the total volume flow per unit area (J_v) through the mosaic membrane (depicted in Fig. III.6) would be given by

$$J_v (A^s + A^c) = J_v^s A^s + J_v^c A^c \qquad (10)$$

where the superscripts s and c stand for the supporting membrane and the composite membrane consisting of the liquid membrane and the supporting membrane in series with each other (Fig III.6) and A represents the area of the membrane denoted by the superscripts. If we focus our attention only on the linear region of the curves in

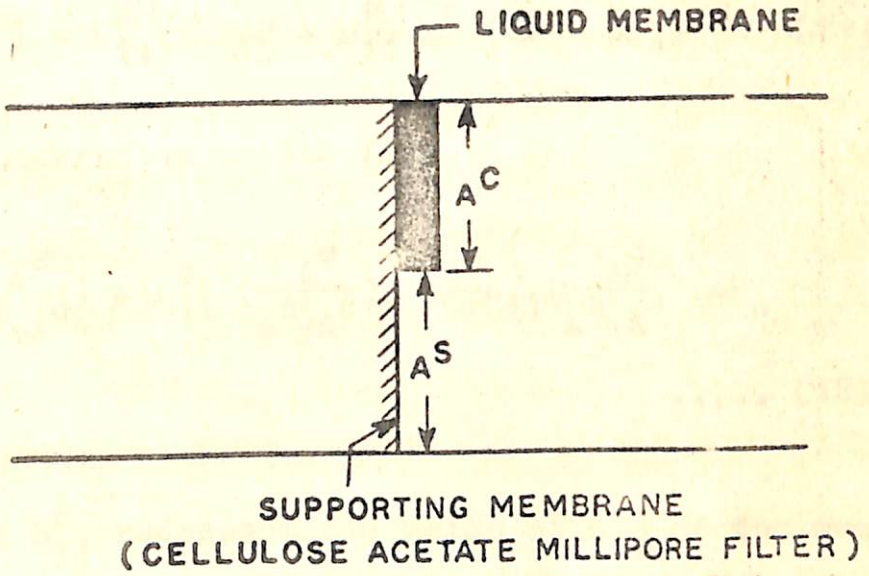

Fig.III.6 The mosaic membrane formed when concentration of the surfactant is lower than the critical micelle concentration value.

Fig III.2 the equation (10) with the help of equation (3) and equation (9) can be transformed into

$$J_v (A^s + A^c) = L_{11}^s A^s \Delta P + L_{11}^c A^c (\Delta P - \Delta P_o) \qquad (11)$$

which can be rewritten in the form

$$J = \left[L_{11}^s \left(\frac{A^s}{A^s+A^c}\right) + L_{11}^c \left(\frac{A^c}{A^s+A^c}\right)\right] \Delta P - L_{11}^c \left(\frac{A^c}{A^s+A^c}\right) \Delta P_o \qquad \ldots\ldots (12)$$

where L_{11}^s and L_{11}^c represent the value of L_{11} of the membrane denoted by the superscripts. For the present discussion let us focus our attention on the hydraulic permeability data corresponding to PVME concentration equal to 0, 3 and 6 ppm. Since at 6 ppm (the CMC value) concentration of PVME the supporting membrane is fully covered with the liquid membrane it is logical to expect that at 3 ppm concentration the fraction of the total area covered with the liquid membrane will be equal to half. Thus the slope of the straight line part of the J_v versus ΔP curve for 3 ppm concentration of PVME (Fig III.2) should be equal to $\frac{L_{11}^s + L_{11}^c}{2}$ where L_{11}^s and L_{11}^c respectively are values of the slopes corresponding to 0 and 6 ppm concentrations of

PVME. Value of the slope thus computed comes out to be equal to 0.366×10^{-7} m^3 N^{-1} sec^{-1} which matches well with the experimental value of L_{11} for 3 ppm concentration of PVME (Table III.5). Similar conclusions can be arrived at from the analysis of the electro-osmotic velocity and streaming current data (Table III.2 and III.4).

Our further experiments on the hydraulic permeability gave sufficient indication of the formation of the surfactant (PVME) layer liquid membrane even at a sintered glass disc support. For this the hydraulic flow experiments were repeated using a sintered glass membrane (porosity G-4) in place of the cellulose acetate millipore filter membrane in the electro-osmotic cell. The transport cell used for these measurements was similar to the one shown in FigIII.1. The only difference was that the cellulose acetate millipore filter was replaced by a sintered glass membrane (porosity G-4, area 0.1 m^2). The hydraulic flow data for various concentrations of PVME for such a case where the sintered glass membrane was used as a support have been given in Table III.6 and plotted in Fig. III.7. The trend of the curves in Fig III.7 is similar to the trend of the curves in Fig. III.2 where cellulose acetate millipore filter membrane was used as a support for the liquid membrane.

Table III.6

Hydraulic permeability data for various concentrations of PVME using sintered glass membrane (porosity G-4) supporting membrane.

$\Delta P \times 10^{-4}$ N m^{-2}	Concentration of PVME (ppm)				
	0	3	6	9	12
	$J_v \times 10^5$ m sec^{-1}	$J_v \times 10^5$ m sec^{-1}	$J_v \times 10^5$ m sec^{-1}	$J_v \times 10^6$ m sec^{-1}	$J_v \times 10^6$ m sec^{-1}
4.0	0.75	0.40	0.10	0.75	0.25
4.9	-	0.45	0.20	0.80	0.30
9.6	1.6	1.0	0.49	1.95	0.75
14.7	2.5	1.75	0.80	3.0	1.5
19.6	3.4	2.6	1.35	4.75	2.40
24.5	4.2	3.0	1.80	6.30	3.5
29.4	4.75	3.5	2.45	8.30	4.5

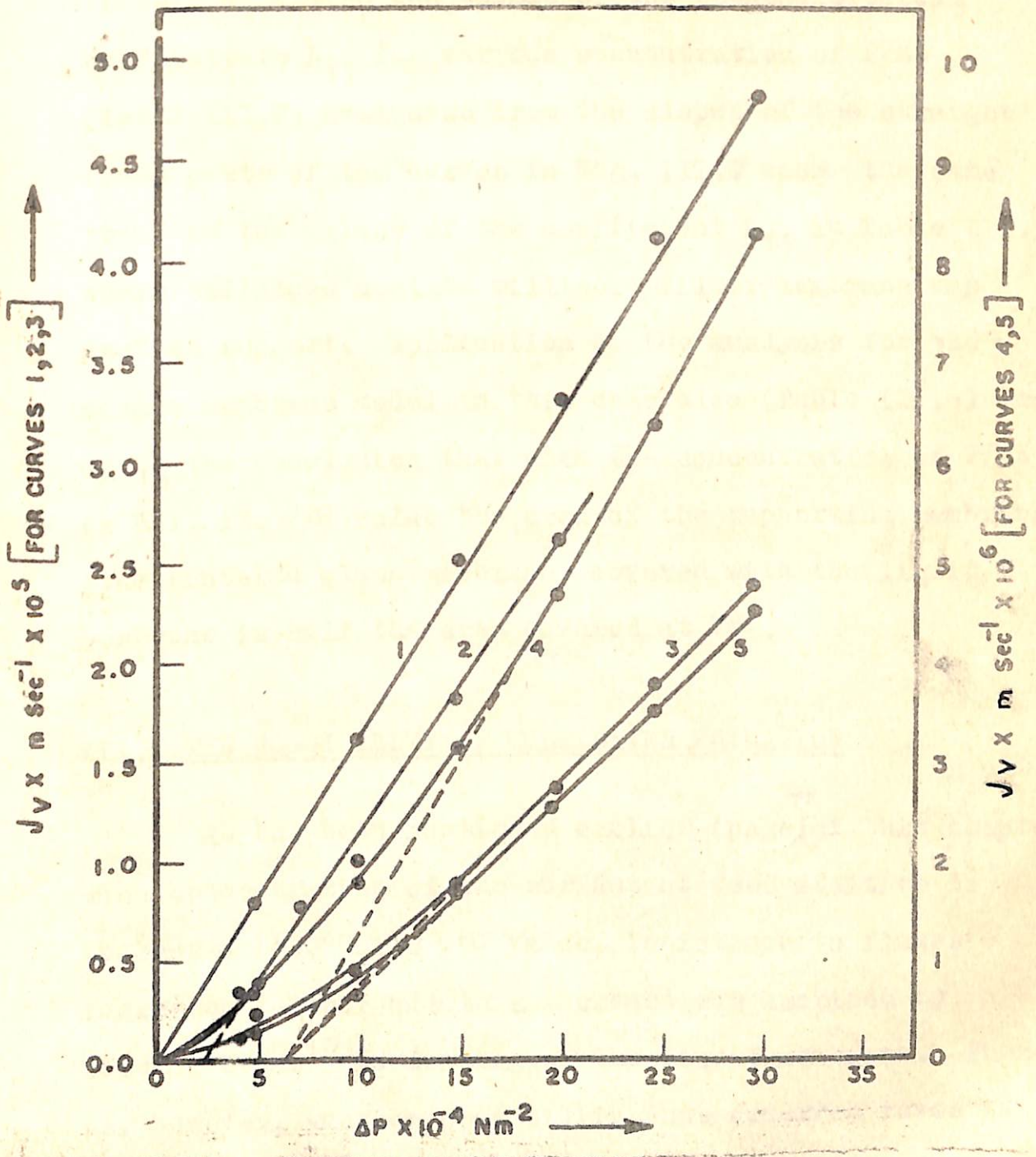

Fig.III.7 The hydraulic permeability data, using sintered glass disc as a supporting membrane. Curves 1, 2, 3, 4 and 5 are for 0, 3, 6, 9 and 12 ppm of PVME respectively.

In this case also the values of the phenomenological coefficients L_{11} for various concentration of PVME (Table III.7) evaluated from the slopes of the straight lines parts of the curves in Fig. III.7 show the same trend as the values of the coefficient L_{11} in Table III.5 where cellulose acetate millipore filter membrane was used as support. Application of the analysis for the mosaic membrane model in this case also (Table III.6) leads us to the conclusion that when the concentration of PVME is half its CMC value the area of the supporting membrane (the sintered glass membrane) covered with the liquid membrane is half the area covered at CMC.

III.4 THE POSSIBILITY OF MULTILAYER FORMATION

As has been mentioned earlier (page 77 of this chapter) when concentration of the surfactant feed additive is increased beyond its CMC value, resistance to fluxes increases further but this increase was ascribed by Kesting et al[10] to densing of the liquid membrane. There is, however, another possibility that deserves investigation - the possibility of formation of multilayers of the liquid membrane when concentration of the surfactant is increased beyond its CMC value. The data on electrical resistances of the system (Table III.5) can be utilised to

Table III.7

Values of L_{11} and ΔP_0 at various concentrations of PVME, using the sintered glass membrane (porosity G-4) as the supporting membrane

	Concentration of PVME in ppm				
	0	3	6	9	12
$L_{11} \times 10^{10}$ m^3 N^{-1} sec^{-1}	1.64	1.5	1.11	0.47	0.197
$\Delta P_0 \times 10^{-4}$ $N\ m^{-2}$	0	2.2	6.13	6.13	6.13

check this possibility. Since at CMC (6 ppm) the liquid membrane completely covers the supporting membrane, the total membrane at 6 ppm can be viewed as the cellulose acetate millipore filter membrane plus the PVME liquid membrane in a series arrangement. Therefore the electrical resistance at 6 ppm can be written as

$$R_6 = R_o + R_1 \qquad (13)$$

where R_o and R_6 represent the values of the resistances at 0 ppm and 6 ppm of PVME and R_1 stands for the resistance of the liquid membrane. If at 12 ppm concentration which is twice the CMC value for PVME, another layer of the liquid membrane is formed in series, the electrical resistance at 12 ppm concentration would be given by

$$R_{12} = R_0 + 2 R_1 \qquad (14)$$

where R_{12} stands for the value of R at 12 ppm concentration of PVME. From equations (13) and (14) we can write

$$R_{12} = 2 R_6 - R_0 \qquad (15)$$

The value of R_{12} computed from equation (15) using the experimentally determined values of R_0 and R_6 (Table III.5), comes out to be equal to 0.495×10^6 ohms which matches

well with the experimentally determined value (Table III.5). This clearly indicates the formation of multilayers of the liquid membrane at the surfactant concentrations higher than the CM C.

The data on salt permeability (ω) can also be utilised to confirm the possibility of multilayer formation. If the supporting membrane is completely covered with the liquid membrane at 6 ppm concentration of PVME the total membrane at 6 ppm concentration of PVME, as stated earlier, can be viewed as series composite membrane consisting of the supporting membrane and the liquid membrane. For such a situation the salt permeability would be given by the relationship

$$\frac{1}{\omega_6} = \frac{1}{\omega_o} + \frac{1}{\omega_1} \qquad (16)$$

deduced by Kedem and Katchalsky[19,20] on the basis of their theory for the permeability of series composite membranes. In equation (16) ω_o and ω_6 respectively represent the values of ω for zero and 6 ppm, concentration of PVME and ω_1 represents the value of ω for the liquid membrane. At 12 ppm concentration which is twice the CMC value for PVME, another layer of liquid membrane would be formed in series. Hence ω for such a case would

be given by the equation

$$\frac{1}{\omega_{12}} = \frac{1}{\omega_o} + \frac{2}{\omega_1} \qquad (17)$$

where ω_{12} stands for the value of ω at 12 ppm concentration PVME. From equation (16) and (17) we can write:

$$\frac{1}{\omega_{12}} = \frac{2}{\omega_6} - \frac{1}{\omega_o} \qquad (18)$$

The value of ω_{12} for sodium chloride, computed from equation (18) using the experimentally determined values of ω_o and ω_6 (Table III.5) comes out to be equall to 0.13×10^{-11} mole sec^{-1} N^{-1} which is in good agreement with the experimentally determined value (Table III.5). This can be taken to be another evidence in favour of formation of multilayers of the liquid membrane when concentration of the surfactant is increased beyond its CMC value.

The values of salt permeability ω were determined using the method outlined in chapter II and utilising the all glass cell diagrammed in Fig III.1. Solutions of sodium chloride (BDH and AR grade) of known strength prepared in aqueous PVME solutions of concentration 0, 6 and 12 ppm were filled in the compartment C of the cell (Fig. III.1)

and distilled water was filled in the compartment D. The condition of no net flux i.e. $J_v=0$ was imposed on the system by adjusting the pressure head attached to the compartment C such that the liquid miniscus in the capillary L_1L_2(Fig III.1) remained stationary. After a known period of time which was of the order of 20 hours or so solutions from the two compartments were withdrawn through the stopcocks T_3 and T_4 (Fig. III.1) and analysed for sodium using a flame photometer reading upto 2 ppm. The amount of sodium chloride lost by the solution compartment or the amount of sodium chloride gained by the water compartment divided by the time gave the value of salt flux (J_s). Knowing the value of J_s the value of ω was estimated using the definition[15,19,20]

$$\omega = \left(\frac{J_s}{\Delta\pi}\right)_{J_v=0} \qquad (19)$$

where $\Delta\pi$ is the osmotic pressure difference. The value of $\Delta\pi$ used in the calculations of ω was the average of the values of $\Delta\pi$ at the beginning of the experiment (t=0) and at the end of the experiment. All experiments for the measurement of ω were made at constant temperature by placing the osmotic cell (Fig. III.1) in a thermostat set at $40 \pm 0.1^{\circ}C$.

III.5 REFERENCES

1. A.Schwartz, J. Perry and J. Berch., Surface Active agents and detergents, vol. 2, p. 418, Interscience New York 1958.

2. S.T. Hwang and K.Kammermeyer, Membranes in Separations, Vol. VII, A Wiley-Interscience publication. John Wiley and Sons, New York 1975.

3. N.N.Li, A I Ch E Journal, 17, 459 (1971).

4. N.N.Li, Ind. Eng. Chem. Process Des. Develop, 10, 215 (1971).

5. P.Meares, Membrane Separation processes. Elsevier Scientific Publishing Company, Amsterdam, New York 1976.

6. F. Martin, Aerojet-General Corp., Private Communication to R.E.Kesting, March, 1963, as quoted in ref. 10

7. A.Michaels, H.Bixler and R.Hodges Jr., J. Colloid. Sci. 20, 1034 (1965).

8. R.E.Kesting, A. Vincent and J. Eberlin, OSW R and D Report, 117, August 1964.

9. R.E.Kesting, Reverse Osmosis Process Using Surfactant feed additives. OSW Patent Application SAL-830, Nov. 3 (1965).

10. R.E.Kesting, W.J. Subcasky and J.D. Paton, J. Colloid Interface Sci. 28, 156 (1968)

11. H.Bixler and R. Cross, Paper presented at the Research Conference on Reverse Osmosis at San Diego sponsored by OSW (U.S. Dept. of Interior) Feb. 14, 1967.

12. R.C.Srivastava and M.G.Abraham; J. Colloid and Interface Sci., 57, 58 (1976).

13. R.C.Srivastava and P.K.Avasthi; Kolloid Z.Z. Polym. 250, 253 (1972)

14. R.C.Srivastava and P.K.Avasthi; J. Hydrol., 20, 37 (1973).

15. A. Katchalsky and P.F. Curran; 'Non-Equilibrium Thermodynamics in Biophysics', P. 244, Harvard University Press, Massachusetts, 1965.

16. K.S. Spiegler and O.Kedem, Desalination, 1, 311 (1966).

17. T.K. Sherwood, P.L.T. Brian and R.E. Fischer, Ind. Eng. Chem. Fundam. 6, 2 (1967).

18. F.L. Harris, G.B. Humphreys and K.S. Spiegler, Chapter 4 in Membrane Separation Processes, ed. P. Meares, Elsevier, 1976.

19. A. Katchalsky and O.Kedem, Biophys. J., 2, 53 (1962).

20. O.Kedem and A.Katchalsky, Trans. Faraday Soc., 59, 1941 (1963).

CHAPTER IV

ELECTRO-OSMOSIS OF SALINE WATER THROUGH A CELLULOSE-NITRATE MILLIPORE FILTER MEMBRANE - STUDIES ON ELECTROKINETIC ENERGY CONVERSION

ELECTRO-OSMOSIS OF SALINE WATER THROUGH A CELLULOSE-NITRATE MILLIPORE FILTER MEMBRANE - STUDIES ON ELECTRO-KINETIC ENERGY CONVERSION.

IV.1 INTRODUCTION

In this chapter we report our experiments on electro-osmosis of saline water through a cellulose nitrate millipore filter membrane with the prime objective of studying the efficiency of electro-kinetic energy conversion. These studies in addition to being relevant to water desalting problem have their intrinsic value because they throw light on the non-equilibrium thermodynamics theory of electro-kinetic energy conversion.

The phenomena of electro-osmotic flow and streaming potential can be taken advantage of in the design of energy conversion devices. In the former the electrical energy is converted into mechanical work, while in the latter case reverse conversion of mechanical work into electrical energy takes place. A unified thermodynamic theory of steady state energy conversion under the restriction that deviation from equilibrium are small enough to permit the use of linear phenomenological equations was first presented by Osterle[1]. Shortly after Osterle, the degree of coupling and its

relations to the efficiency of energy conversion has been deduced and discussed by Kedem and Caplan.[2] The phenomenological description of two coupled flows leads to the definition of their 'degree of coupling.' Kedem and Caplan[2] have considered a variety of coupled flow processes to describe the degree of coupling and its relation to the efficiency of energy conversion. Osterle and co-workers[1,3-5] have discussed at length the efficiency of electro-kinetic energy conversion on the basis of non-equilibrium thermodynamics.

IV.2 THE NON-EQUILIBRIUM THERMODYNAMIC THEORY OF ENERGY CONVERSION

The condition for energy conversion to take place is contained in the entropy production function. For a two flux - two force system the entropy production function $\frac{d_i S}{dt}$ can be written as

$$d_i S/dt = J_1 X_1 + J_2 X_2 \qquad (1)$$

where J_1, J_2 are the two fluxes and X_1 and X_2 are the corresponding conjugate forces. Suppose the term $J_1 X_1$ is negative. Process 1 then consumes entropy at the expense of process 2, and accordingly part of the free energy expended by - and characteristic of -

process 2 is converted into the form characteristic of process 1. The entropy withdrawn from the system in this manner may or may not make its appearance in the outside world simultaneously. If it does, the system is in a stationary state and the converted energy is being dissipated externally. If it does not, the system is storing energy (e.g. by charging a condensor, increasing the affinity of a reaction or developing a concentration gradient across a membrane). The efficiency of energy conversion is a function of state, and thus time dependent in non-stationary systems. In such systems the instantaneous value may still be useful if the rate of change is slow.

In general, the efficiency function η of the system is defined as[1,6]

$$\eta = \frac{J_o X_o}{J_i X_i} \qquad (2)$$

which follows from the following dissipation equation

$$d_i S/dt = J_i X_i - J_o X_o \qquad (3)$$

where subscript i and o represent the input and output powers respectively. In equation (3) negative sign ($- J_o X_o$) indicates that output forces and output fluxes are in opposite direction to that of input fluxes and forces.

Since in electro-osmosis the input force is the applied electrical potential difference $\Delta\emptyset$ and the output force is the consequent pressure difference ΔP, the equation (2) would read as

$$\eta_e = \frac{J\Delta P}{I\Delta\emptyset} = \frac{J\Delta P}{(\Delta\emptyset)^2/R} \qquad (4)$$

where J represents the volume flux, I represents the current flow and R is the resistance of the system. Similarly for streaming potential where the input force is the applied pressure difference ΔP, one can write

$$\eta_s = \frac{I\Delta\emptyset}{J\Delta P} = \frac{(\Delta\emptyset)^2/R}{J\Delta P} \qquad (5)$$

The subscript e and s in equations (4) and (5) represent the penomena of electro-osmosis and streaming potential respe ctively.

In an electro-osmosis experiment the applied potential difference $\Delta\emptyset$ across the membrane is used to derive the liquid uphill. This liquid when allowed to accumulate exerts a hydraulic pressure difference across the membrane causing a back flow of liquid. When ΔP equals the electro-osmotic pressure the net volume flux J becomes zero. Thus from equation (4) it is obvious that η_e would be zero either

when $\Delta P=0$ or when ΔP equals the electro-osmotic pressure which corresponds to the condition $J=0$. It, therefore, appears that the graph between η_e and ΔP for a fixed value of input force $\Delta \emptyset$ would pass through a maximum as ΔP varied from zero to the electro-osmotic pressure. Naturally the optimum value of η_e would occur when ΔP is less than the electro-osmotic pressure. Similar considerations would apply to η_s represented by equation (5)

If the linear phenomenological relations

$$J_i = L_{ii} X_i + L_{io} (- X_o) \tag{6}$$

$$J_o = L_{oi} X_i + L_{oo} (- X_o) \tag{7}$$

between fluxes J and forces X are obeyed, Osterle et al[3,4] have shown that maximum value of conversion efficiency η is related to the figure of merit β in the following manner[1]

$$(\eta)_{max} = \frac{(1 + \beta_{io})^{\frac{1}{2}} - 1}{(1 + \beta_{io})^{\frac{1}{2}} + 1} \tag{8}$$

where β_{io} is given by the relationship

$$\beta_{io} = \left(\frac{L_{ii} L_{oo}}{L_{io}^2} - 1 \right)^{-1} \tag{9}$$

Since the validity of linear phenomenological relations (6) and (7) is assumed, the phenomenological coefficients L_{ik} are not supposed to vary with thermodynamic forces. This makes β in equation (9) and consequently $(\eta)_{max}$ in equation (8) independent of the input forces.

On account of the Onsager's relation $L_{io} = L_{oi}$ it is obvious from equation (9) that

$$\beta_{io} = \beta_{oi} \qquad (10)$$

which implies that the value of $(\eta)_{max}$ given by equation (8) would remain the same for either direction of conversion. This for electro-osmosis and streaming potential would mean

$$(\eta_e)_{max} = (\eta_s)_{max} \qquad (11)$$

IV.3 EXPERIMENTAL

Materials: Sodium chloride (BDH Analar) and distilled water distilled once over potassium permanganate were used in the present experiments.

Apparatus and Procedure: An all glass electro-osmotic cell similar to the one described earlier by Srivastava and Abraham[7] was used. The apparatus is diagrammed in Fig. IV.1 for a ready reference. The electro-osmotic cell was

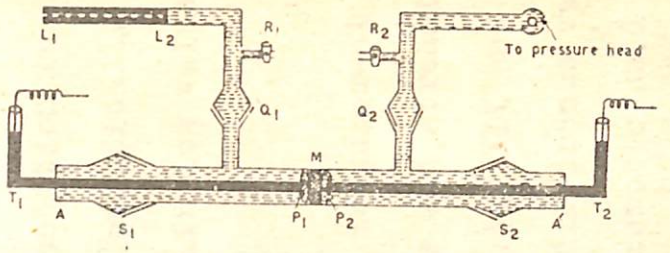

FIG. IV.1 Electro-osmotic cell (AA' = Glass tube of length 35 cm, diam. 2.5 cm, M = cellulose nitrate millipore filter; S_1 and S_2 = standard joints (B-24); P_1 and P_2 = Platinum electrodes fused to tubes T_1 and T_2 filled with mercury; Q_1 and Q_2 = standard joints (B-14); R_1 and R_2 = Stop cocks; L_1 L_2 = capillary tube of length 25 cm and diam = 0.2084 cm).

separated into two compartments by a saratorius cellulose nitrate filter membrane (Cat. No. SM 11307) of thickness 1×10^{-4}m and area 0.951×10^{-4}m^2. The silver-silver chloride electrodes E_1 and E_2 (Fig. IV.1) were prepared using the method of Carmody.[8] The electrodes when not in use were kept under short-circuited condition in dark and immersed in distilled water which was periodically changed. This procedure is necessary to maintain low value of asymmetry potential.

The procedure followed for the measurement of ordinary permeability, electro-osmotic velocity and streaming potentials has already been described in the chapter III and also in earlier publications.[7,9,10] The only difference was that in the present measurements the electro-osmotic cell was filled with various concentrations of aqueous sodium chloride solution. The streaming potentials were measured using a V.T.V.M (philips GM 6009/90) reading upto 0.01 mV. During the measurements of streaming potentials the asymmetry potential of the electrodes E_1 and E_2 (Fig. IV.1) was cared for. Resistances of the system were measured with a leitfahigkeitmesser conductivity meter. Values of streaming current were calculated using Ohm's law, from the values of the streaming potentials and resistances thus obtained.

The volume flux was measured by noting the rate of advancement of liquid meniscus in the capillary L_1L_2 with a cathetometer reading upto 0.001 cm and a stop watch of least count 0.1 seconds. Electrical potential differences needed for the measurement of electro-osmotic velocity were tapped from an electronically operated stabilised power supply (Beltronix, Electrophoresis Power supply). During the measurement of ordinary permeability the electrodes E_1 and E_2 were electrically short circuited. The sodium chloride solution in the electro-osmotic cell was changed with fresh stock solution after each reading of ordinary permeability, electro-osmotic velocity and streaming potential.

All measurements were made at constant temperature by placing the electro-osmotic cell in a thermostat maintained at $40 \pm 0.1^{\circ}C$.

IV.4 RESULTS AND DISCUSSION

The data on ordinary permeability, electro-osmotic velocity, streaming potentials and current for various concentrations of sodium chloride solution have been given in Tables IV.1 to IV.4 and plotted in Figs. IV.2 to IV.5. The straight line plots in Figs. IV.2 to IV.5 amply demonstrate the validity of the linear phenomenological

Table IV.1

The ordinary permeability data for various concentration of Sodium chloride

$\Delta P \times 10^{-2}$ N m^{-2}	Concentration of Sodium Chloride (M)					
	0	2.5×10^{-4}	3×10^{-4}	5×10^{-4}	1×10^{-3}	1×10^{-2}
	$J_v \times 10^4$ m sec^{-1}	$J_v \times 10^4$ m sec^{-1}	$J_v \times 10^4$ m sec^{-1}	$J_v \times 10^4$ m sec^{-1}	$J_v \times 10^4$ m sec^{-1}	$J_v \times 10^4$ m sec^{-1}
4.9	0.08	0.11	0.12	0.13	0.15	0.25
9.8	0.15	0.23	0.24	0.27	0.34	0.45
14.7	0.235	0.35	0.35	0.40	0.48	0.7
19.6	0.315	0.465	0.465	0.53	0.65	0.925
24.5	0.39	0.56	0.585	0.64	0.8	1.30
29.4	0.475	0.69	0.71	0.74	1.00	1.52

Table IV.2

The electro-osmotic velocity data for various concentrations of Sodium Chloride

$\Delta\varphi$ volts	Concentration of sodium chloride (M)					
	0	2.5×10^{-4}	3×10^{-4}	5×10^{-4}	1×10^{-3}	1×10^{-2}
	$J_v\times10^4$ m sec^{-1}	$J_v\times10^4$ m sec^{-1}	$J_v\times10^4$ m sec^{-1}	$J_v\times10^4$ m sec^{-1}	$J_v\times10^4$ m sec^{-1}	$J_v\times10^4$ m sec^{-1}
5	0.03	0.035	0.05	0.07	0.09	0.14
10	0.06	0.08	0.102	0.135	0.17	0.26
15	0.085	0.13	0.169	0.20	0.26	0.38
20	0.119	0.16	0.209	0.26	0.32	0.48
25	0.142	0.22	0.27	0.32	0.48	0.54
30	0.175	0.25	0.30	0.39	0.62	0.66

Table IV.3

The streaming potential data for various concentration of Sodium Chloride

$\Delta P \times 10^{-2}$ N m^{-2}	Concentration of Sodium Chloride (M)					
	0	2.5×10^{-4}	3×10^{-4}	5×10^{-4}	1×10^{-3}	1×10^{-2}
	$\Delta\phi \times 10^{3}$ volts	$\Delta\phi \times 10^{3}$ volts	$\Delta\phi \times 10^{3}$ volts	$\Delta\phi \times 10^{3}$ volts	$\Delta\phi \times 10^{3}$ volts	$\Delta\phi \times 10^{3}$ volts
4.9	1.2	1.4	1.5	1.6	1.7	2.0
9.8	2.6	3.0	3.2	3.25	3.4	4.1
14.7	4.2	4.55	4.75	5.0	5.1	6.25
19.6	5.7	6.2	6.5	6.6	6.9	8.25
24.5	7.2	7.6	8.0	8.3	8.5	13.5
29.4	8.8	9.4	9.6	10.0	11.4	14.0

Table IV.4

The streaming current data for various concentrations of Sodium chloride

$\Delta P \times 10^{-2}$ N m^{-2}	Concentration of Sodium chloride (M)					
	0	2.5×10^{-4}	3×10^{-4}	5×10^{-4}	1×10^{-3}	1×10^{-2}
	$I \times 10^{4}$ amp m^{-2}	$I \times 10^{+4}$ amp m^{-2}	$I \times 10^{4}$ amp m^{-2}	$I \times 10^{4}$ amp m^{-2}	$I \times 10^{4}$ amp m^{-2}	$I \times 10^{4}$ amp m^{-2}
4.9	2	3.5	5	6.5	8.0	10.0
9.8	5	7.5	10	13	15.5	22.0
14.7	7.5	11.5	15	19.5	23.5	33
19.6	11	15.5	20	21.5	31	43
24.5	13	19.5	25	33	39	54
29.4	16	23.5	30	40	47	65

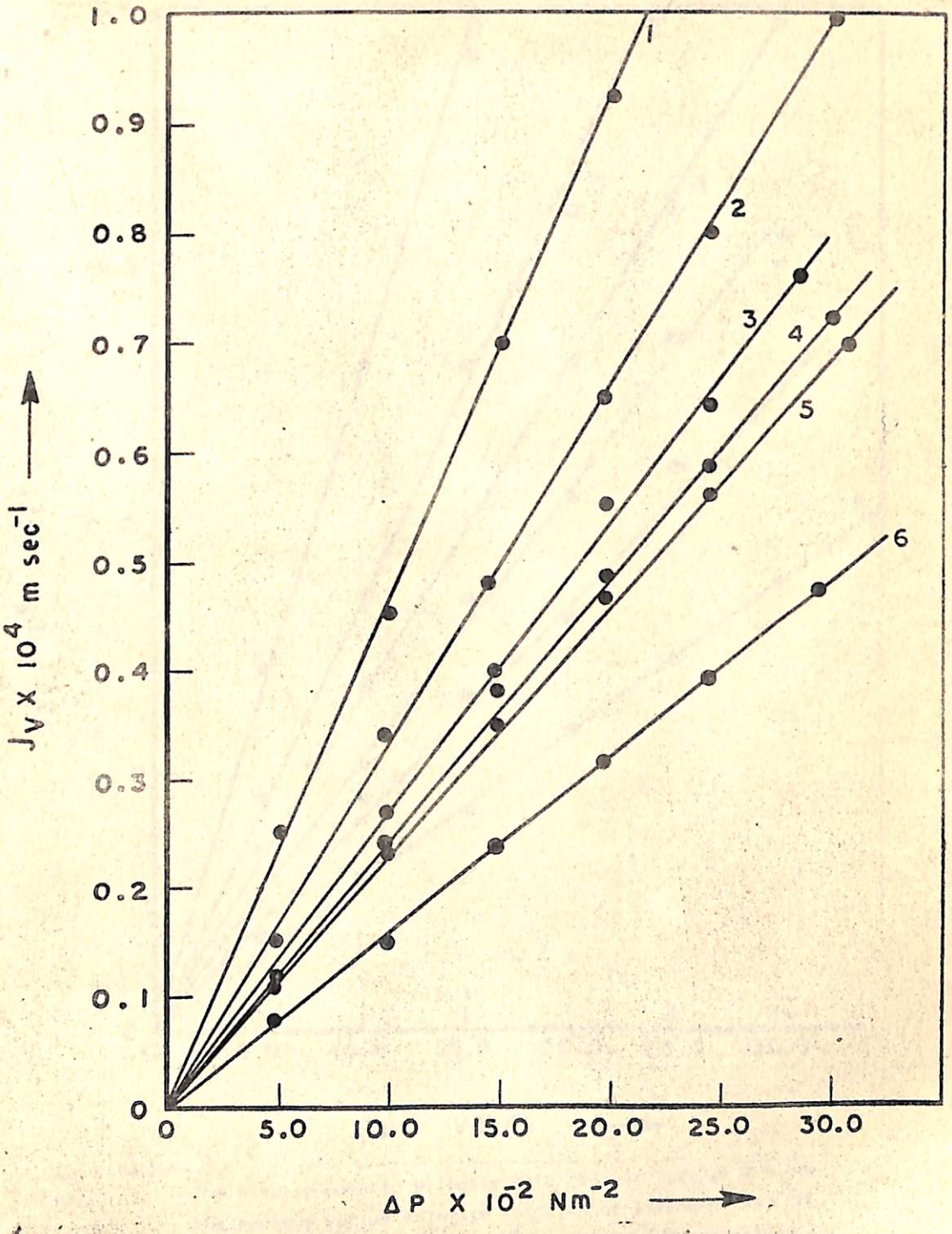

Fig. IV.2 The Hydraulic permeability data (curves 1,2,3,4 & 5 are for aqueous sodium chloride solution of strength 1×10^{-2} M, 1×10^{-3} M, 5×10^{-4} M, 3×10^{-4} M, 2.5×10^{-4} M respectively. The curve 6 is for distilled water)

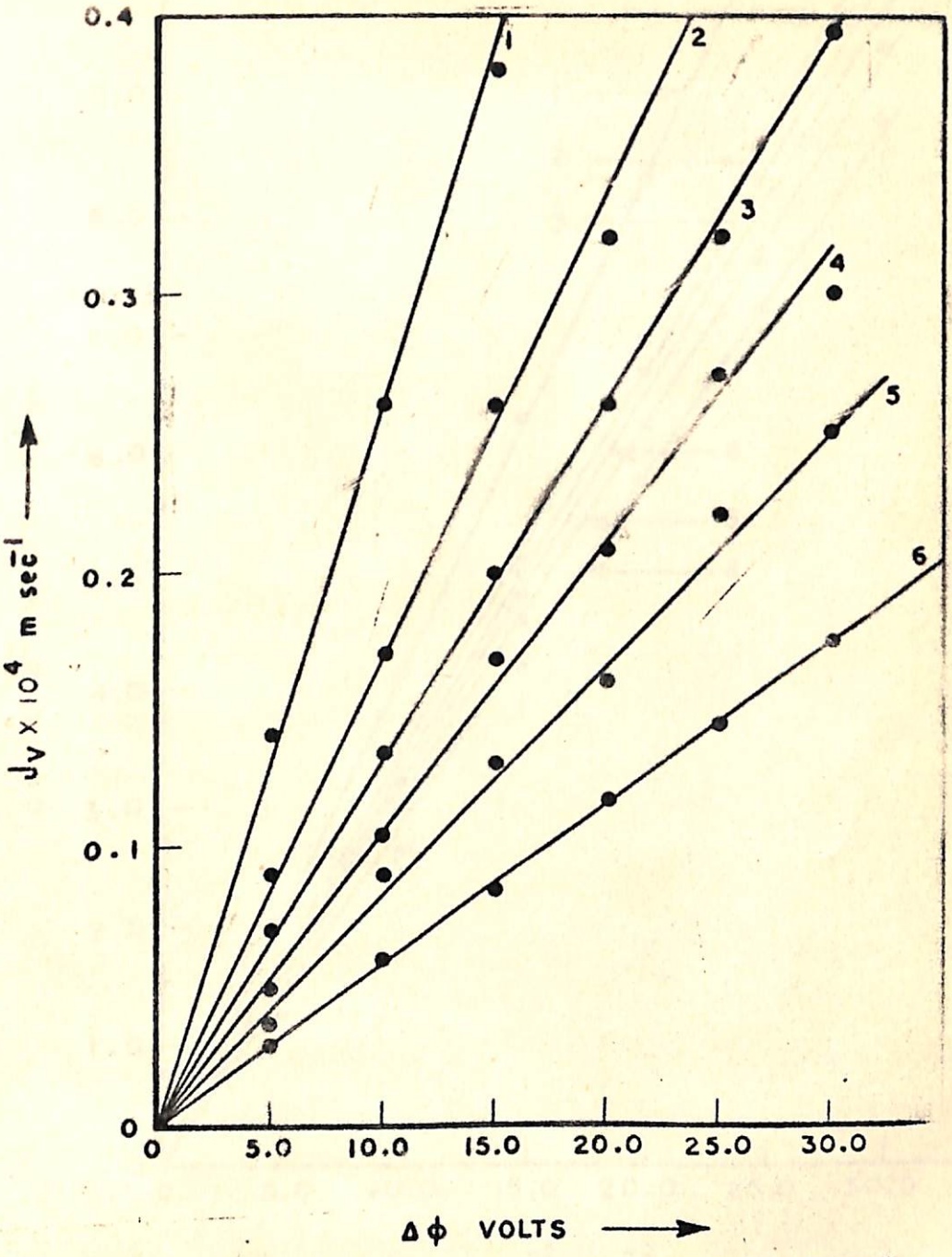

Fig. V.3 The electro-osmotic velocity data (curves 1,2,3,4 & 5 are for aqueous sodium chloride solution of strength 1×10^{-2} M, 1×10^{-3} M, 5×10^{-4} M, 3×10^{-4} M, 2.5×10^{-4} M respectively. The curve 6 is for distilled water.

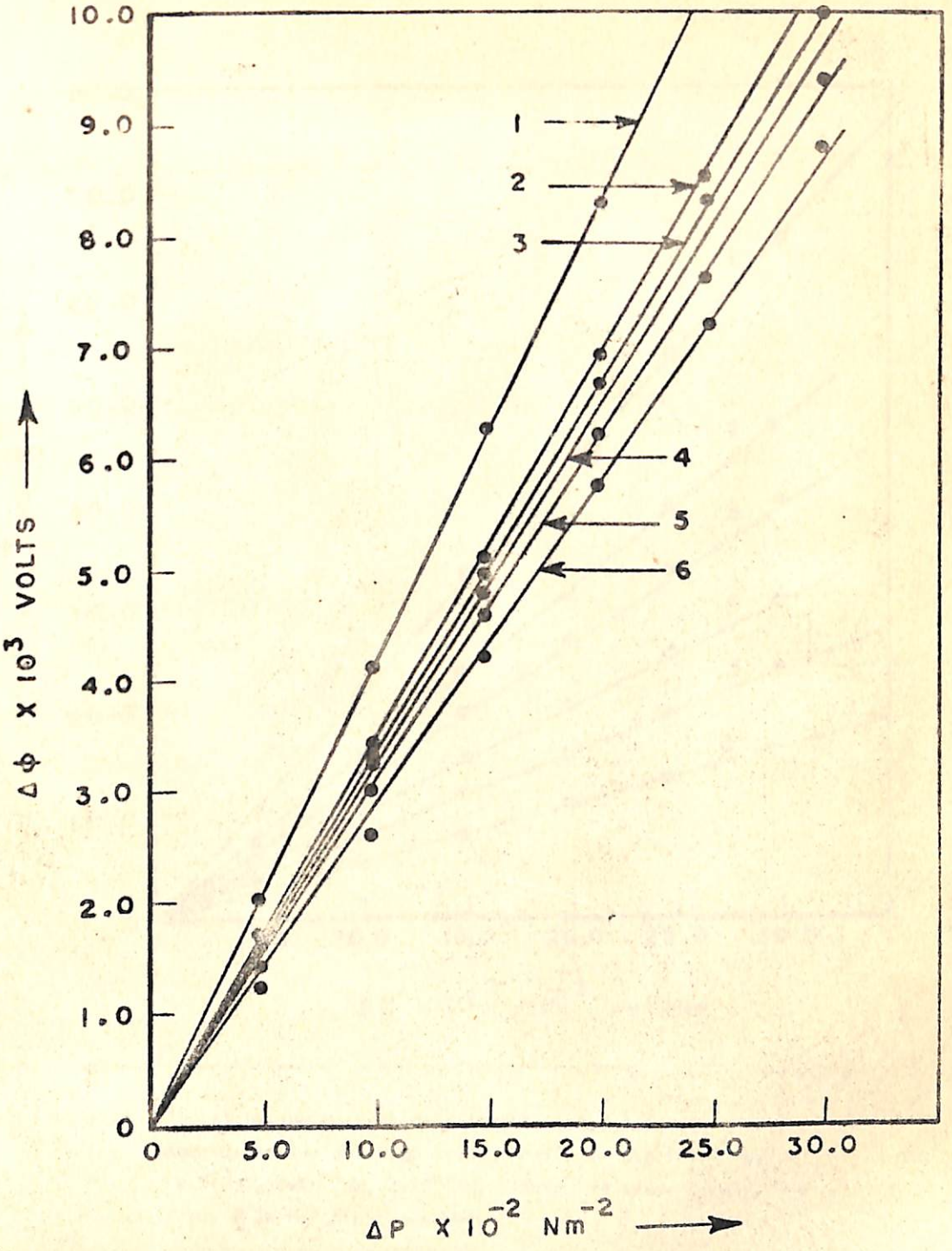

Fig. IV.4 The streaming potential data. (Curves 1,2,3,4 & 5 are for aqueous sodium chloride solution of strength 1×10^{-2} M.

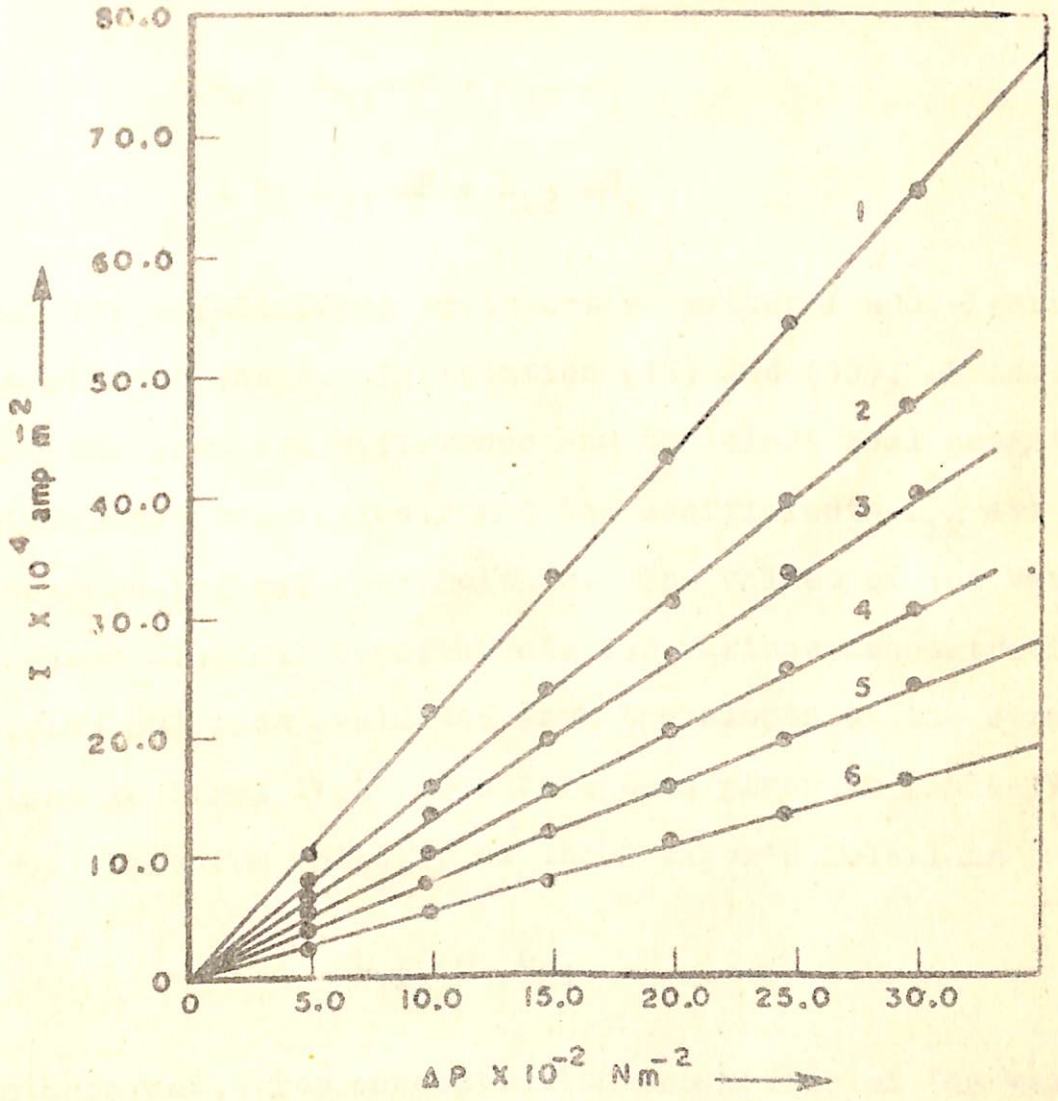

Fig. IV.5 The streaming current data (curves 1,2,3,4 & 5 are for aqueous sodium chloride solution of strength 1×10^{-2} M, 1×10^{-3} M, 5×10^{-4} M, 3×10^{-4} M, 2.5×10^{-4} M respectively. The curve 6 is for distilled water.

equations[11] described in chapter III i.e.

$$J_v = L_{11} \Delta P + L_{12} \Delta \phi \qquad (12)$$

$$I = L_{21} \Delta P + L_{22} \Delta \phi \qquad (13)$$

for the simultaneous transport of matter J and electricity I, in all the cases. In equation (12) and (13), ΔP and $\Delta \phi$ are the pressure difference and the electrical potential difference respectively and the coefficients L_{ik} are the phenomenological coefficients. The values of the various phenomenological coefficients for various concentrations of sodium chloride evaluated from the slopes of the straight lines in Figs. IV.2 to 5 have been given in Table IV.5 from which the validity of the Onsager's relations

$$L_{12} = L_{21} \qquad (14)$$

is apparent. The concentration dependence of the various phenomenological coefficients have been plotted in Figs. IV.6-8.

IV.5 THE ENERGY CONVERSION EFFICIENCY

The values of η_e and η_s for various concentrations of sodium chloride solutions, corresponding to two fixed values of input forces, utilising the transport data in

Table IV.5

Values of the various Phenomenological coefficients and $(\eta)_{max}$ at various concentration of sodium chloride solution

Concentration of Sodium chloride solution (M)	$L_{11} \times 10^7$ $m^3 N^{-1} sec^{-1}$	$L_{12} \times 10^5$ $m\ AJ^{-1}$	$L_{21} \times 10^5$ $m\ AJ^{-1}$	L_{22} $ohm^{-1}\ m^{-2}$	Values of $(\eta_e)_{max} \times 10^5$ (from the plot η_e vs ΔP)	Values of $(\eta_s)_{max} \times 10^5$ (from the plot η_s vs $\Delta\phi$)	Computed values of $(\eta_e)_{max} \times 10^5$ (from eqn. 8)	Computed values of $(\eta_s)_{max} \times 10^5$ (from eqn. 8)
0	0.162	0.059	0.059	0.190	2.40	2.42	2.85	2.82
1×10^{-2}	0.455	0.23	0.225	0.525	4.92	4.91	5.52	5.29
1×10^{-3}	0.322	0.16	0.162	0.477	4.35	4.30	4.35	4.26
5×10^{-4}	0.260	0.135	0.131	0.403	3.93	3.94	4.15	4.08
3×10^{-4}	0.243	0.102	0.097	0.309	3.37	3.36	3.49	3.16
2.5×10^{-4}	0.225	0.083	0.082	0.258	2.99	2.99	2.98	2.90

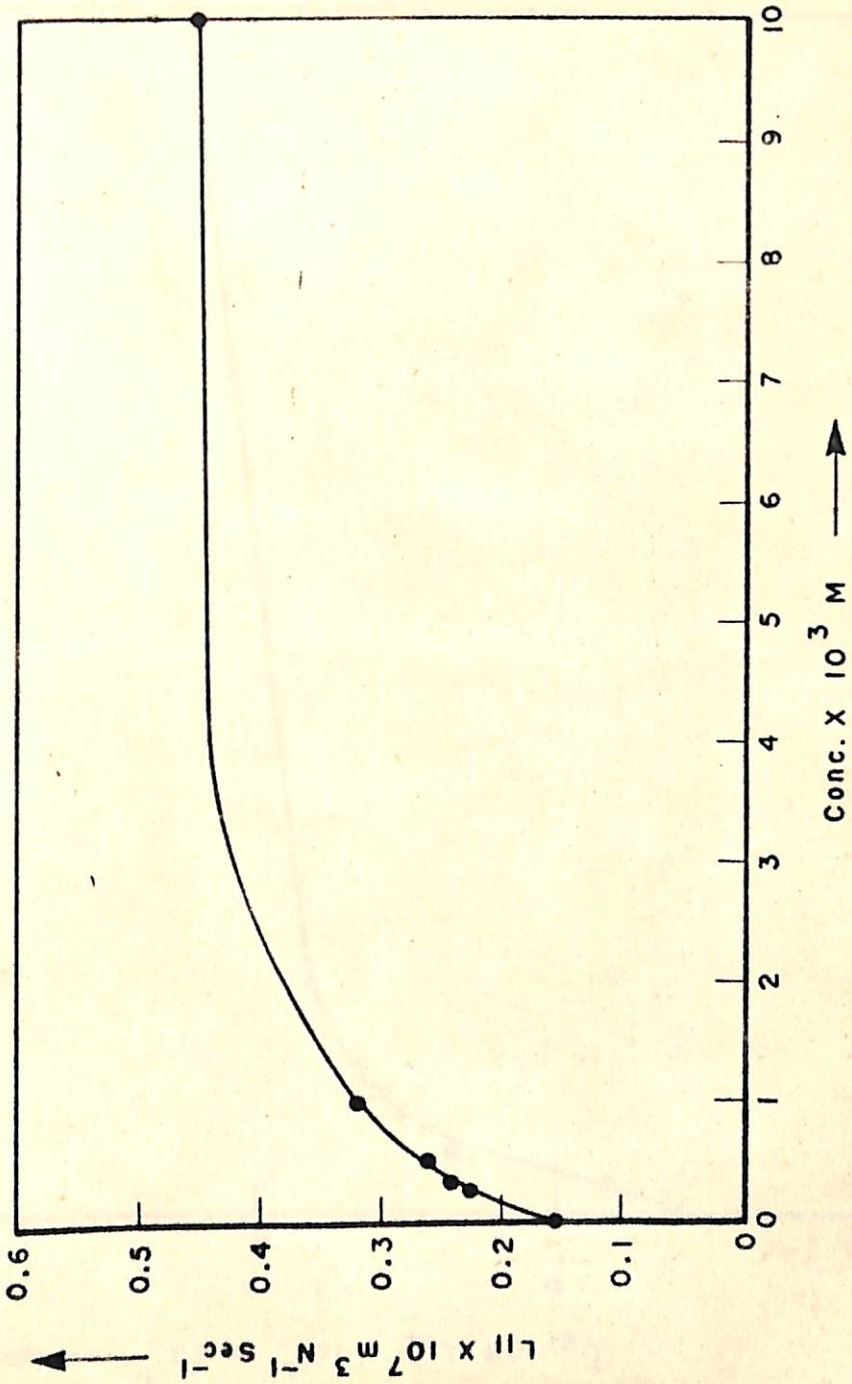

Fig. IV.6 Dependence of L_{11} with sodium chloride concentration.

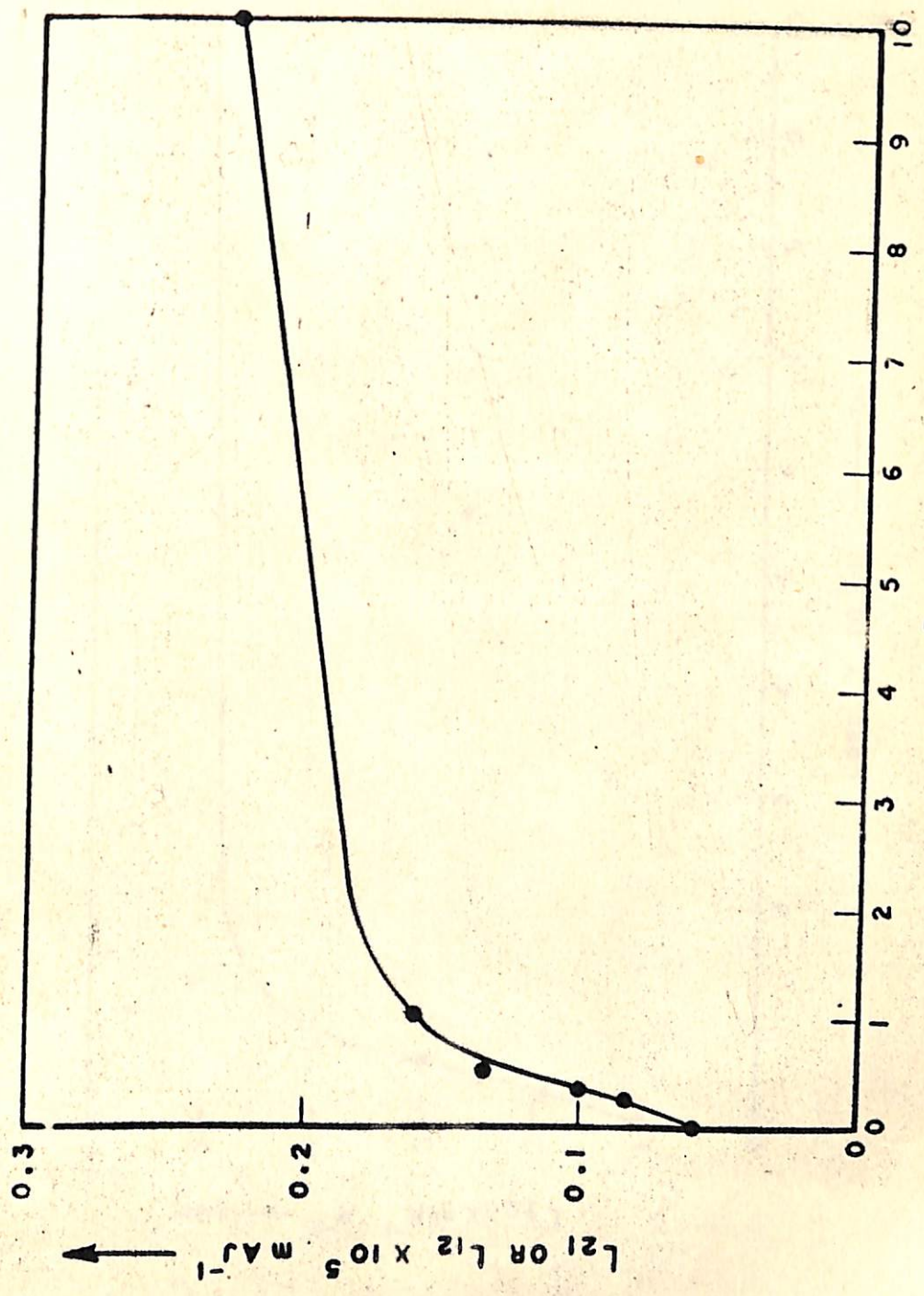

Fig. IV.7 Dependence of L_{12} or L_{21} with sodium chloride concentration.

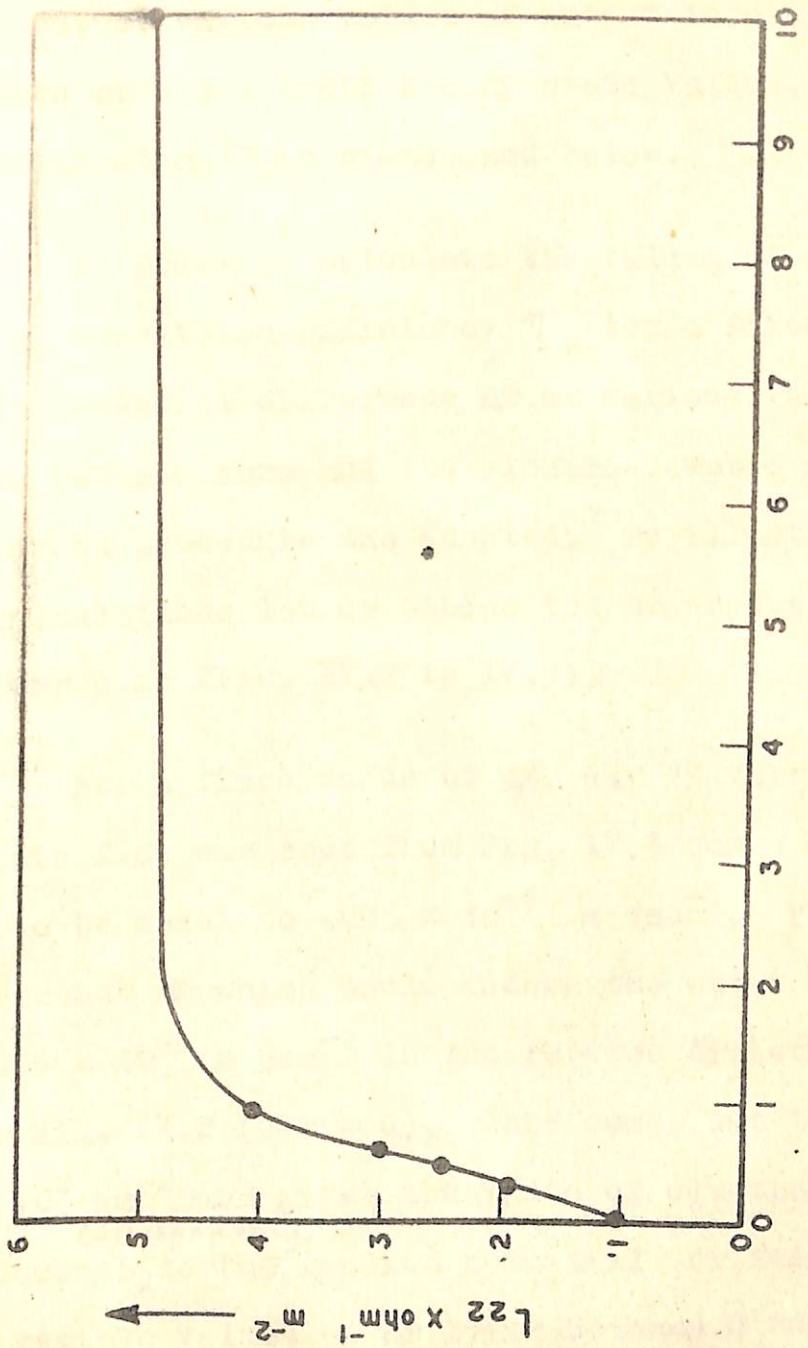

Fig. IV.8 Dependence of L_{22} with sodium chloride concentration.

Tables IV.1 to IV.4 and Figs. IV.2 to IV.5 have been calculated, at various values of output forces ranging between zero and their steady state values. The method of calculation[12] is summarised below.

In order to calculate the values of electro-osmotic energy conversion efficiency η_e for a fixed value of input potential difference $\Delta\phi$ at various values of ΔP, lying between zero and the electro-osmotic pressure, the following procedure was adopted. To illustrate the method of calculations let us choose the transport data for water (curves 6 in Figs. IV.2 to IV.5).

For a fixed value of $\Delta\phi$, say 15 volts, the electro-osmotic flow was read from Fig. IV.3 curve 6 and this comes out to be equal to $.085 \times 10^{-4}$ m sec^{-1}. The pressure difference ΔP which would induce the water flux of magnitude 0.085×10^{-4} m sec^{-1} in the reverse direction was read from Fig. IV.2 (curve 6). This comes out to be equal to 6×10^2 Nm^{-2} and gives the value of electro-osmotic pressure difference corresponding to the applied potential difference, 15 volts. Now various values of ΔP lying between 0 and 6×10^2 Nm^{-2} were chosen and the water fluxes corresponding to them were read from Fig. IV.2 (curve 6). These values of water flux were substracted from the value of electro-osmotic

water flux corresponding to 15 volts. This gave the values of net water flux J corresponding to various values of pressure difference ΔP lying between 0 and 6×10^2 Nm^{-2}. With this data at hand it was easy to calculate using equation (4) the values of η_e at various ΔP corresponding to the fixed value of $\Delta\emptyset$ = 15 volts. Using this procedure the values of η_e at various ΔP's for various concentrations of sodium chloride solutions, corresponding to two fixed values of $\Delta\emptyset$ were calculated from the electro-osmotic transport data (Table IV.1 to IV.4). An identical procedure was adopted to calculate the values of η_s.

The values of η_e and η_s thus calculated at various values of output forces ranging between zero and their steady state values for various concentrations of sodium chloride solutions corresponding to two fixed values of input forces are recorded in Tables IV.6 to IV.17 and plotted in Figures IV.9 to IV.14.

From data on energy conversion efficiency (Figs. IV.9 to IV.14) the following conclusions can be drawn in all the cases.

1. For a particular concentration of sodium chloride solution $(\eta_e)_{max}$ was always equal to the value of $(\eta_s)_{max}$.

Table IV.6

Dependence of conversion efficiency η_e on the output force ΔP at two different values of the input force $\Delta\phi$.

Sodium chloride concentration = 5×10^{-4} (M)

Input force $\Delta\phi$ = 15 volts		Input force $\Delta\phi$ = 20 volts	
$\Delta P \times 10^{-2}$ N m^{-2}	$\eta_e \times 10^5$	$\Delta P \times 10^{-2}$ N m^{-2}	$\eta_e \times 10^5$
0.0	0.0	0.0	0.0
1.0	1.9	1.0	1.44
2.0	3.2	2.0	2.52
3.0	3.9	3.0	3.39
4.0	4.0	5.0	3.93
5.0	3.63	7.0	3.08
6.0	2.68	9.0	1.13
7.0	0.783	10.0*	0.0
8.0*	0.0		

* The values of electro-osmotic pressure.

Table IV.7

Dependence of conversion efficiency η_e on the output force ΔP at two different values of the input force $\Delta\phi$.

Sodium Chloride concentration = 3×10^{-4} M

Input force $\Delta\phi$ = 15 volts		Input force $\Delta\phi$ = 20 volts	
$\Delta P \times 10^{-2}$ N m^{-2}	$\eta_e \times 10^5$	$\Delta P \times 10^{-2}$ N m^{-2}	$\eta_e \times 10^5$
0.0	0.0	0.0	0.0
0.5	1.05	1.0	1.53
1.0	1.96	2.0	2.66
1.5	2.62	3.0	2.8
2.0	3.13	4.0	3.2
3.0	3.37	5.0	3.37
3.5	3.30	6.0	3.31
4.0	3.29	7.0	2.43
5.0	2.91	8.0	1.55
6.0*	0.0	9.0	0.8
		10.0*	0.0

*The values of electro-osmotic pressure

Table IV.8

Dependence of conversion efficiency η_e on the output force ΔP at two different values of the input force $\Delta\phi$

Sodium chloride concentration = 1×10^{-3} M

Input force $\Delta\phi$ = 15 volts		Input force $\Delta\phi$ = 20 volts.	
$\Delta P \times 10^{-2}$ N m^{-2}	$\eta_e \times 10^5$	$\Delta P \times 10^{-2}$ N m^{-2}	$\eta_e \times 10^5$
0.0	0.0	0.0	0.0
1.0	2.04	2.0	2.82
2.0	3.53	3.0	3.76
3.0	4.46	5.0	4.35
4.0	4.35	7.0	3.2
5.0	4.2	9.0	1.6
6.0	3.2	10.0*	0.0
7.0	1.30		
8.0*	0.0		

* The values of electro-osmotic pressure.

Table IV.9

Dependence of conversion efficiency η_e on the output force ΔP at two different values of the input force $\Delta\phi$.

Sodium chloride concentration = 2.5×10^{-4} M

Input force $\Delta\phi$ = 15 volts		Input force $\Delta\phi$ = 20 volts	
$\Delta P \times 10^{-2}$ N m^{-2}	$\eta_e \times 10^5$	$\Delta P \times 10^{-2}$ N m^{-2}	$\eta_e \times 10^5$
0.0	0.0	0.0	0.0
0.5	1.02	0.5	0.782
1.0	1.78	1.0	1.40
1.5	2.55	1.5	2.04
2.0	2.87	2.0	2.42
2.5	2.89	2.5	2.55
3.0	2.95	3.0	2.87
4.0	2.51	4.0	2.94
5.0	1.65	4.5	2.47
6.0*	0.0	8.0	1.81
		8.0*	0.0

* The values of electro-osmotic pressure.

Table IV.10

Dependence of conversion efficiency η_e on the output force ΔP at two different values of the input force $\Delta\phi$.

Sodium chloride concentration = 1×10^{-2} M

Input force $\Delta\phi$ = 15 volts		Input force $\Delta\phi$ = 20 volts	
$\Delta P \times 10^{-2}$ N m^{-2}	$\eta_e \times 10^5$	$\Delta P \times 10^{-2}$ N m^{-2}	$\eta_e \times 10^5$
0.0	0.0	0.0	0.0
0.5	1.4	1.0	2.4
1.0	2.6	2.0	3.3
1.5	3.6	3.0	4.0
2.0	4.0	4.0	4.6
3.0	4.6	5.0	4.92
4.0	4.92	6.0	3.6
5.0	4.6	8.0	3.0
6.0	3.6	9.0	1.6
6.5	2.4	10.0*	0.0
8.0*	0.0		

* The values of electro-osmotic pressure.

Table IV.11

Dependence of conversion efficiency η_e on the output force ΔP at two different values of the input force $\Delta\phi$.

Sodium chloride concentration = 0 M

Input force $\Delta\phi$ = 15 volts		Input force = 20 volts	
$\Delta P \times 10^{-2}$ N m^{-2}	$\eta_e \times 10^5$	$\Delta P \times 10^{-2}$ N m^{-2}	$\eta_e \times 10^5$
0.0	0.0	0.0	0.0
0.5	0.6	1.0	0.9
1.0	1.0	2.0	1.4
2.0	1.7	3.0	1.8
3.0	2.1	4.0	2.1
4.0	2.4	5.0	2.4
5.0	2.2	6.0	2.2
6.0	1.8	7.0	1.8
7.0	1.2	8.0	1.4
8.0*	0.0	9.0	1.0
		10.0*	0.0

*The values of electro-osmotic pressure.

Table IV.12

Dependence of conversion efficiency η_s on the output force $\Delta\phi$ at two different values of the input force ΔP.

Sodium chloride concentration = 5×10^{-4} M

Input force $\Delta P = 10 \times 10^{+2}$ Nm^{-2}		Input force $\Delta P = 15 \times 10^{+2}$ $N\,m^{-2}$	
$\Delta\phi \times 10^{+3}$ volts	$\eta_s \times 10^5$	$\Delta\phi \times 10^{+3}$ volts	$\eta_s \times 10^5$
0.0	0.0	0.0	0.0
0.4	1.69	0.6	1.74
0.8	2.911	1.0	2.2
1.2	3.3	1.2	2.98
1.6	3.94	1.6	3.5
2.0	3.8	2.0	3.75
2.4	3.09	2.45	3.99
2.8	1.95	3.0	3.7
3.2*	0.0	3.6	3.0
		4.9*	0.0

*The value of streaming potential

Table IV.13

Dependence of conversion efficiency η_s on the output force $\Delta\phi$ at two different values of the input force ΔP.

Sodium chloride concentration = 3×10^{-4} M

Input force $\Delta P = 10 \times 10^2$ Nm^{-2}		Input force $\Delta P = 10 \times 10^2$ N m^{-2}	
$\Delta\phi \times 10^{+3}$ volts	$\eta_s \times 10^5$	$\Delta\phi \times 10^{+3}$ volts	$\eta_s \times 10^5$
0.0	0.0	0.0	0.0
0.41	1.52	0.40	0.137
0.50	1.76	0.6	1.46
0.82	2.56	1.0	2.2
1.0	2.85	1.2	2.50
1.55	3.36	2.0	3.2
2.0	3.2	2.4	3.36
2.47	2.42	3.0	3.17
3.0	0.902	4.0	1.5
3.1*	0.0	4.8*	0.0

* The value of streaming potential.

Table IV.14

Dependence of conversion efficiency η_s on the output force $\Delta\emptyset$ at two different values of the input force ΔP.

Sodium chloride concentration = 2.5×10^{-4} M

Input force $\Delta P = 10 \times 10^2$ N m^{-2}		Input force $\Delta P = 15 \times 10^2$ N m^{-2}	
$\Delta\emptyset \times 10^{+3}$ volts	$\eta_s \times 10^5$	$\Delta\emptyset \times 10^3$ volts	$\eta_s \times 10^5$
0.0	0.0	0.0	0.0
0.38	1.16	0.57	1.18
0.76	1.99	1.0	1.8
1.0	2.34	1.15	2.03
1.5	2.97	1.6	2.40
2.2	2.06	2.3	2.91
2.5	1.64	3.45	2.05
3.0*	0.0	4.0	1.26
		4.6*	0.0

* The value of streaming potential.

Table IV.15

Dependence of conversion efficiency η_s on the output force $\Delta\phi$ at two different values of the input force ΔP.

Sodium chloride concentration = 1×10^{-3} M

Input force $\Delta P = 10 \times 10^2$ Nm^{-2}		Input force $\Delta P = 15 \times 10^2$ N m^{-2}	
$\Delta\phi \times 10^3$ volts	$\eta_s \times 10^5$	$\Delta\phi \times 10^3$ volts	$\eta_s \times 10^5$
0.0	0.0	0.0	0.0
0.2	1.0	0.5	1.2
0.5	1.75	1.0	1.9
0.9	2.91	2.0	3.6
1.3	3.4	2.75	4.3
1.8	4.3	3.0	4.2
2.0	4.0	4.0	3.1
2.6	2.8	5.0	1.4
3.0	1.8	5.5*	0.0
3.2	0.8		
3.6*	0.0		

* The values of streaming potential

Table IV.16

Dependence of conversion efficiency η_s on the output force $\Delta\phi$ at two different values of the input force ΔP.

Sodium Chloride concentration = 1×10^{-2} M

Input force $\Delta P = 10 \times 10^2$ N m^{-2}		Input force $\Delta P = 15 \times 10^2$ N m^{-2}	
$\Delta\phi \times 10^3$ volts	$\eta_s \times 10^5$	$\Delta\phi \times 10^3$ volts	$\eta_s \times 10^5$
0.0	0.0	0.0	0.0
0.25	0.6	0.25	0.4
0.5	1.8	0.5	1.4
0.75	2.8	0.15	1.8
1.0	3.6	1.0	2.4
1.5	4.6	1.25	2.8
2.0	4.9	1.5	3.4
2.5	4.6	2.25	4.4
3.0	3.6	3.0	4.9
3.25	3.0	3.5	4.6
3.0	2.0	4.0	4.0
3.75	1.2	4.5	3.4
4.0*	0.0	5.0	2.4
		5.5	1.6
		6.0*	0.0

* The values of streaming potential.

Table IV.17

Dependence of conversion efficiency η_s on the output force $\Delta\phi$ at two difference values of the input force ΔP.

Sodium Chloride concentration = 0 M

Input force $\Delta P = 10 \times 10^2$ N m^{-2}		Input force $\Delta P = 15 \times 10^2$ N m^{-2}	
$\Delta\phi \times 10^3$ volts	$\eta_s \times 10^5$	$\Delta\phi \times 10^3$ volts	$\eta_s \times 10^5$
0.0	0.0	0.0	0.0
0.25	0.4	0.5	1.0
0.5	1.2	1.0	1.4
1.0	1.8	1.75	2.0
1.25	2.2	2.5	2.4
1.5	2.5	3.0	2.2
1.75	2.2	3.75	1.6
2.0	2.0	4.5	1.0
2.5	1.2	5.0*	0.0
2.75	0.8		
3.0*	0.0		

* The values of streaming potential.

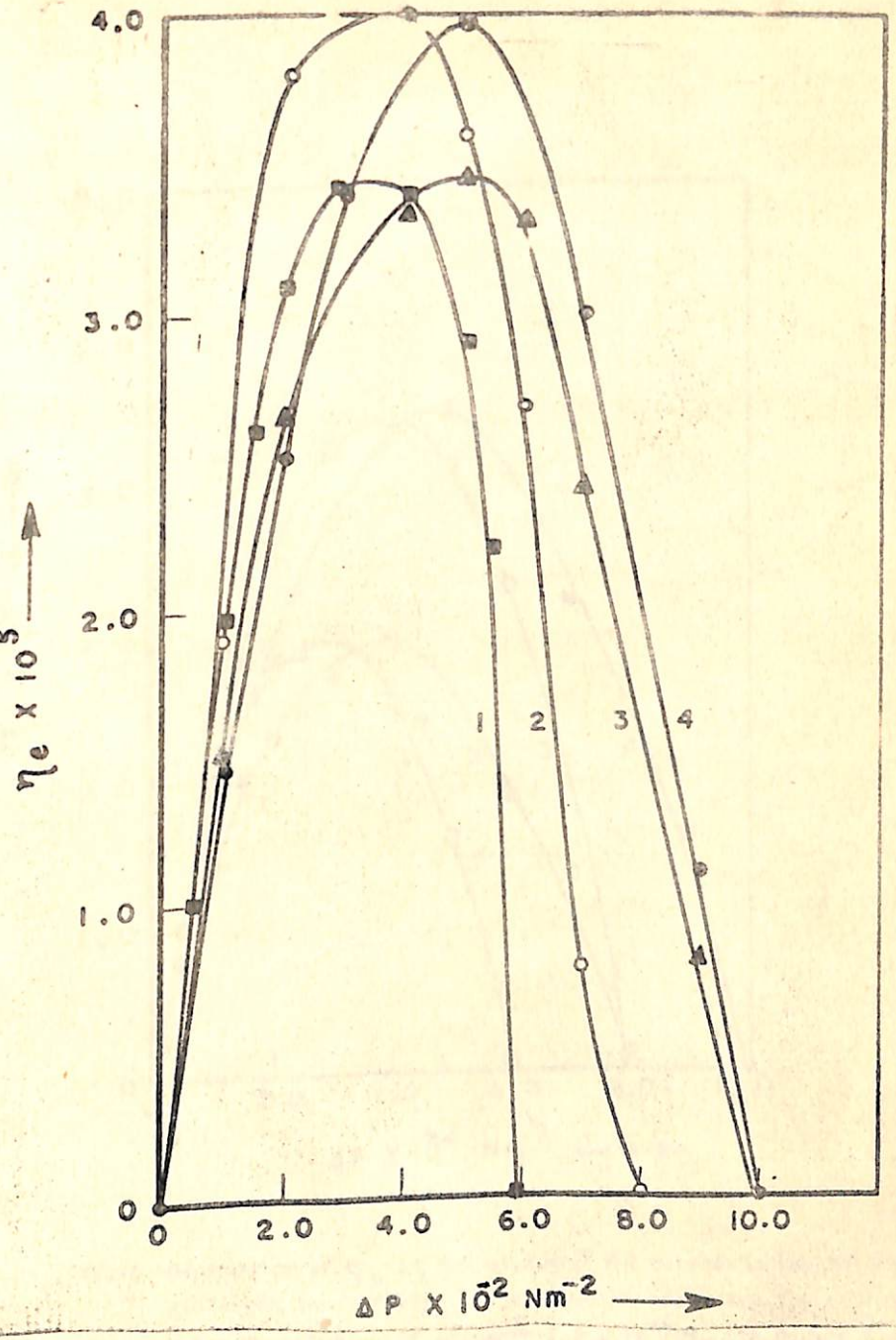

Fig. IV.9 Dependence of η_e an output force ΔP corresponding to two different input forces. The curves 1 and 3 are for sodium chloride solution of strength 3×10^{-4} M. The curves 2 and 4 are for sodium chloride solution of strength 5×10^{-4} M. The input forces of curves 1 and 4 are 15 volts and for curves 2 and 3 are 20 volts.

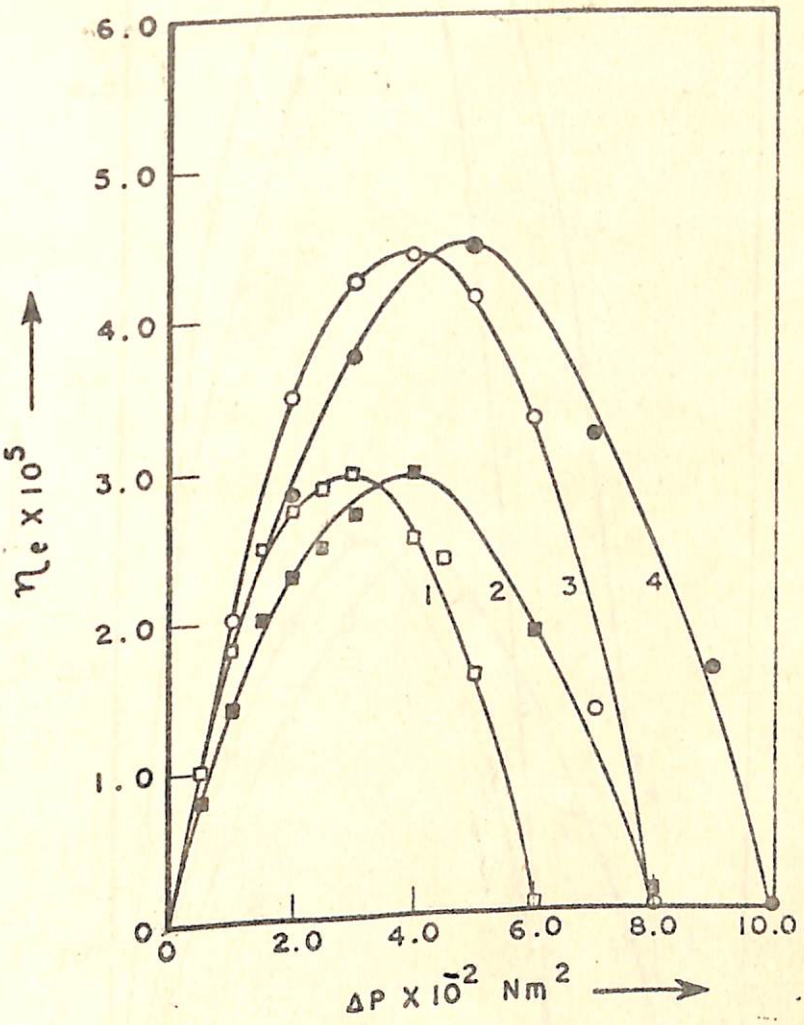

Fig. IV.10 Dependence of η_e on output force ΔP corresponding to two different input forces. The curves 1 and 2 are for sodium chloride solution of strength 2.5×10^{-4} M, the curves 3 and 4 are for sodium chloride solution of strength 1×10^{-3} M. The input forces for curves 1 and 3 are 15 volts and for curves 2 and 4 are 20 volts.

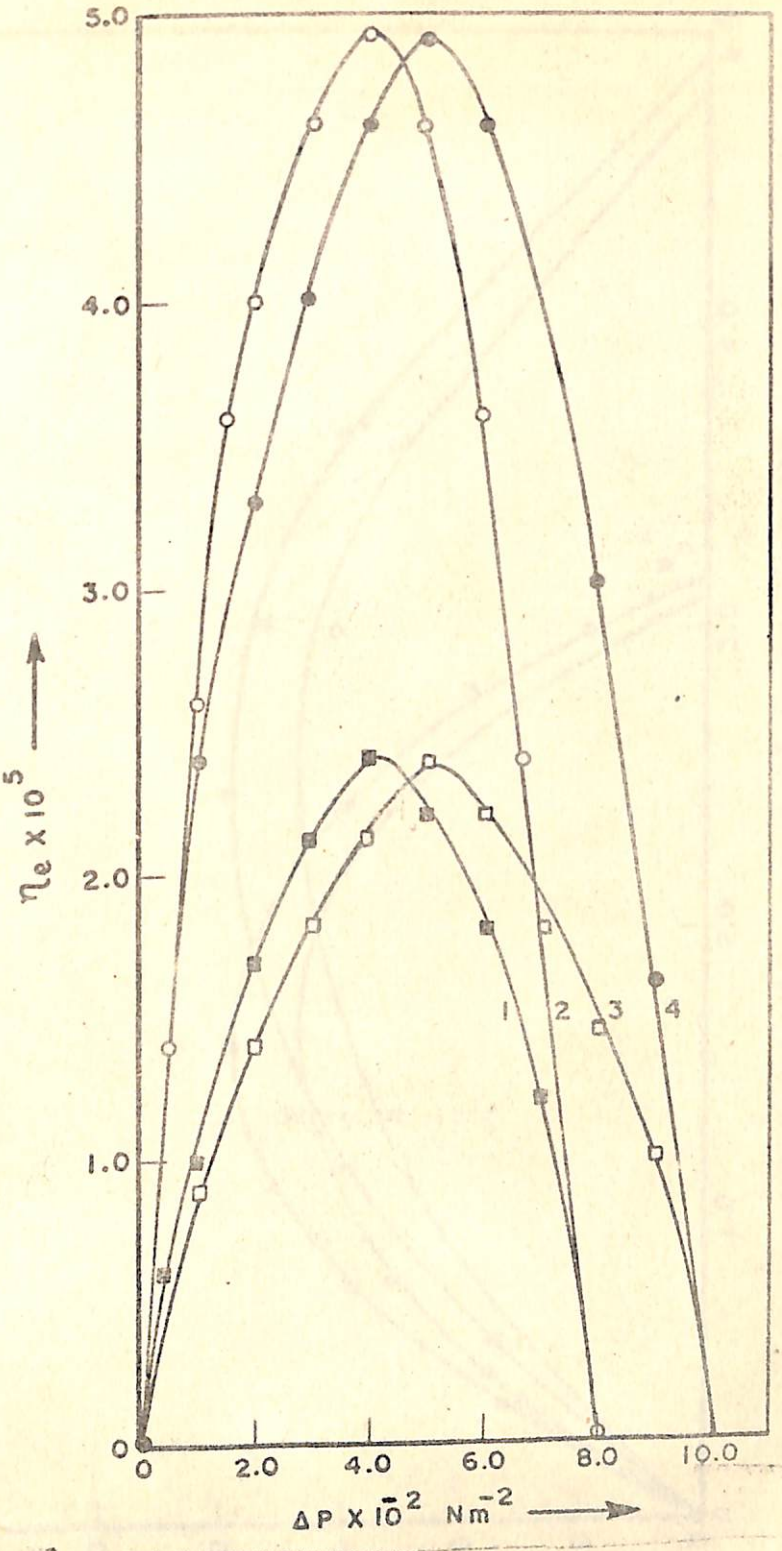

Fig. IV.11 Dependence of η_e on output force ΔP corresponding to two different input forces. The curves 1 and 3 are for sodium chloride solution of strength 0M. The curves 2 and 4 are for sodium chloride solution of strength 1×10^{-2} M. The input forces for curves 1 and 2 are 15 volts and for curves 3 and 4 are 20 volts.

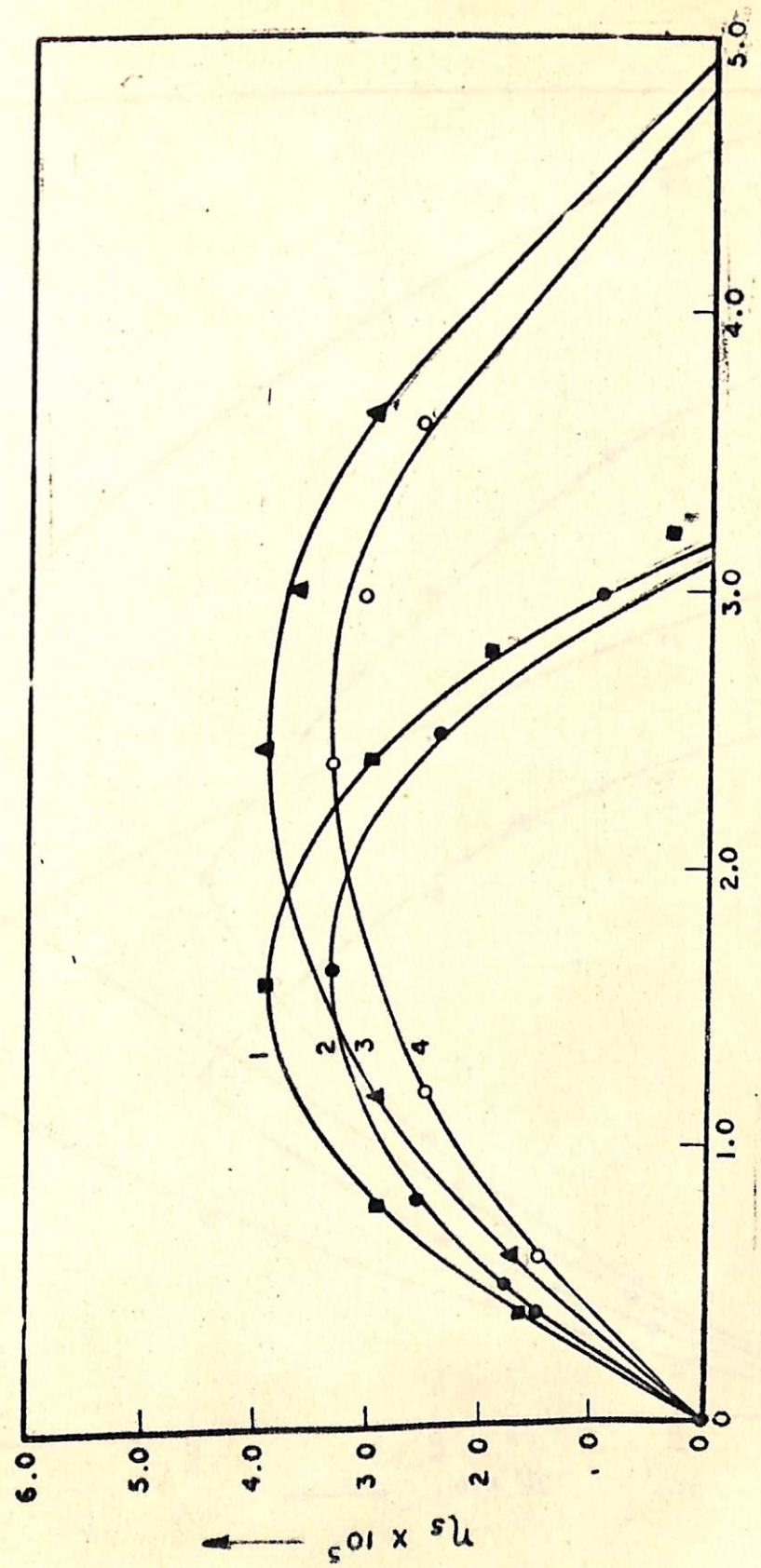

Fig. IV.12 Dependence of η_s on output forces $\Delta\phi$ corresponding to two different input forces. The curves 1 and 3 are for sodium chloride solution of strength 5×10^{-4} M. The curves 2 and 4 are for sodium chloride solution of strength 3×10^{-4} M. The input forces for curves 1 and 2 are 1×10^{-2} N m^{-2} and for curves 3 and 4 are 1.5×10^{-2} Nm^{-2}.

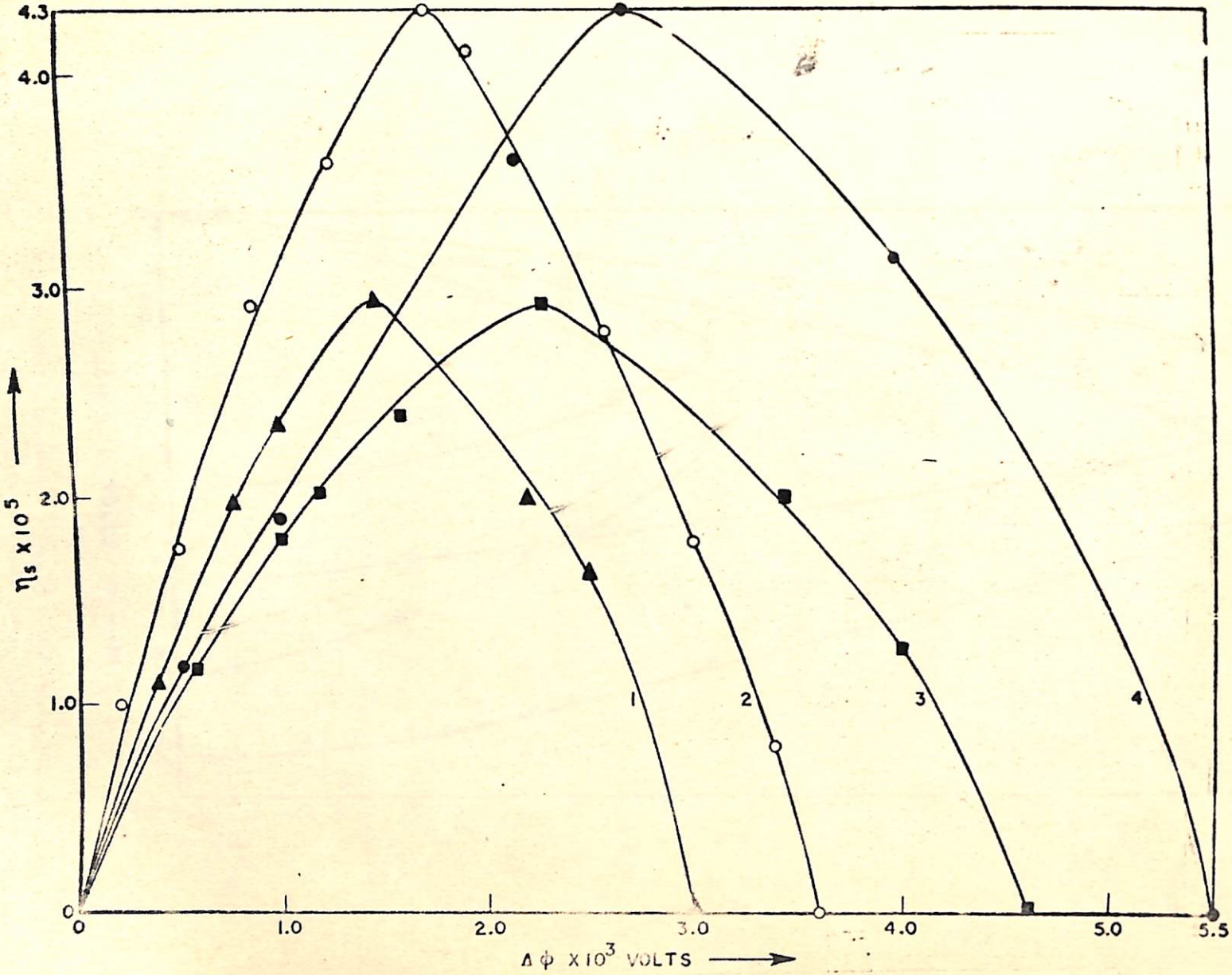

Fig. IV.13 Dependence of η_s on output forces $\Delta\phi$ corresponding to two different input forces. The curves 1 and 3 are for sodium chloride solution of strength 2.5×10^{-4} M. The curves 2 and 4 are for sodium chloride solution of strength 1×10^{-3} M. The input forces for curves 1 and 2 are 10×10^2 Nm^{-2} and for curves 3 and 4 are 15×10^2 $N\,m^{-2}$.

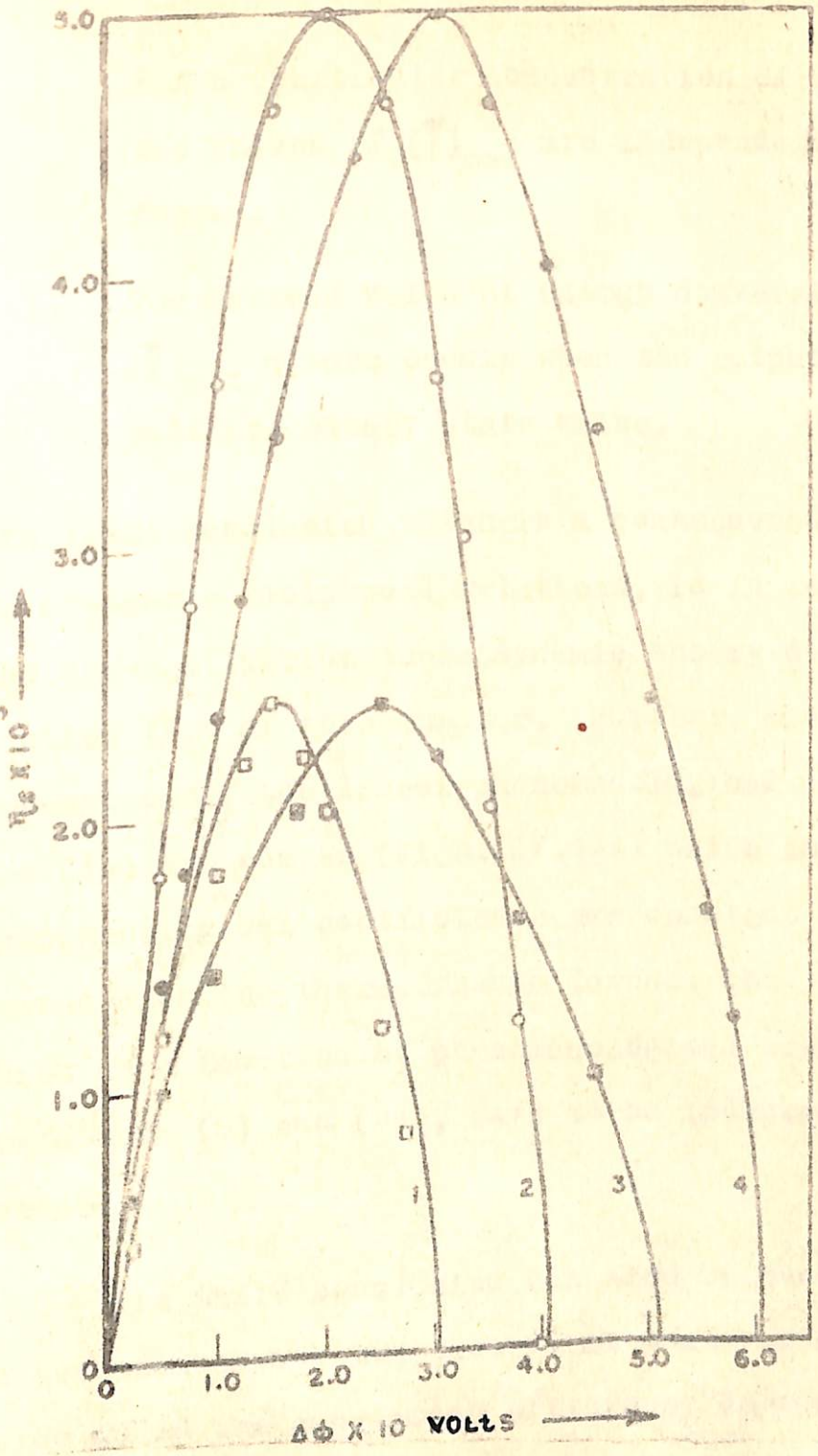

Fig. IV.14 Dependence of η_s on output forces $\Delta\beta$ corresponding to two different input forces. The curve 1 and 3 are for sodium chloride solution of strength 0 M. The curve 2 and 4 are for sodium chloride solution of strength 1×10^{-2} M. The input forces for curves 1 and 2 are 10×10^{-2} Nm^{-2} and for curves 3 and 4 are 15×10^{-2} Nm^{-2}.

2. For a particular concentration of sodium chloride the values of $(\eta)_{max}$ are independent of the input forces.

3. The maximum value of energy conversion efficiency $(\eta)_{max}$ always occurs when the output force equals half its steady state value.

The first conclusion which is a consequence of the validity of Onsager's reciprocal relations, is in accordance with the non-equilibrium thermodynamic theory described in section IV.4 of this chapter. Further, since in the present case, the linear phenomenological equations (12) and (13) are obeyed (Figs. IV.1-4) which implies that the phenomenological coefficients are constant and do not depend upon the thermodynamic forces, the values of $(\eta)_{max}$ which is a function of phenomenological coefficients only (equations (8) and (9)), have to be independent of input forces.

The third conclusion can also be shown[12,13] to be in accordance with the theory. At what value of the output force would the conversion efficiency corresponding to a fixed value of input force be maximum can be deduced by considering the equation for conversion efficiency and

phenomenological equations. Let us take a specific example of electro-osmosis, where the electrical potential difference is the input force.

The expression for electro-osmotic pressure at steady state i.e.

$$(\Delta P/\Delta \phi)_{J=0} = - \frac{L_{12}}{L_{11}} \qquad (15)$$

follows from equation (12). After substituting the value of J from equation (12) the equation (4) for electro-osmotic energy conversion efficiency reads as

$$\eta_e = \frac{(L_{11}\,\Delta P + L_{12}\,\Delta \phi)\,\Delta P}{I\,\Delta \phi} \qquad (16)$$

Since we are considering the values of η_e at fixed input force, $\Delta \phi$ and I can be treated as constants. Now applying the condition,

$$(\partial\, \eta_e / \partial\, \Delta P) = 0 \qquad (17)$$

for the maximum, one gets from equation (16)

$$\frac{2\, L_{11}\, \Delta P}{I\, \Delta \phi} + \frac{L_{12}}{I} = 0 \qquad (18)$$

which with the help of (15) transforms to

$$\Delta P = \frac{1}{2} (\Delta P)_{J_v=0} \qquad (19)$$

The equation (19) leads to the conclusion that the value of η_e corresponding to any fixed value of $\Delta\phi$ would be maximum when the output force ΔP equals half the value of electro-osmotic pressure. This conclusion is confirmed from the data plotted in Figs. IV.9 to IV.10 for aqueous sodium chloride solutions. Similar considerations would apply for η_s.

The values of $(\eta)_{max}$, for both the modes of conversions namely for electro-osmosis and streaming potential calculated using equations (8) and (9) utilising the value of the phenomenological coefficients are recorded in Table IV.5, along with the values obtained from the experimental plots (Figs. IV.9 to IV.14). The agreement between the computed values of $(\eta)_{max}$ and the values obtained from the maxima of the experimental curves (Figs. IV.9 to IV.12) is apparent from Table IV.5. This lends added support to the non-equilibrium thermodynamic theory of electro-kinetic energy conversion.

The concentration dependence of $(\eta)_{max}$ has been shown in Fig. IV.15.

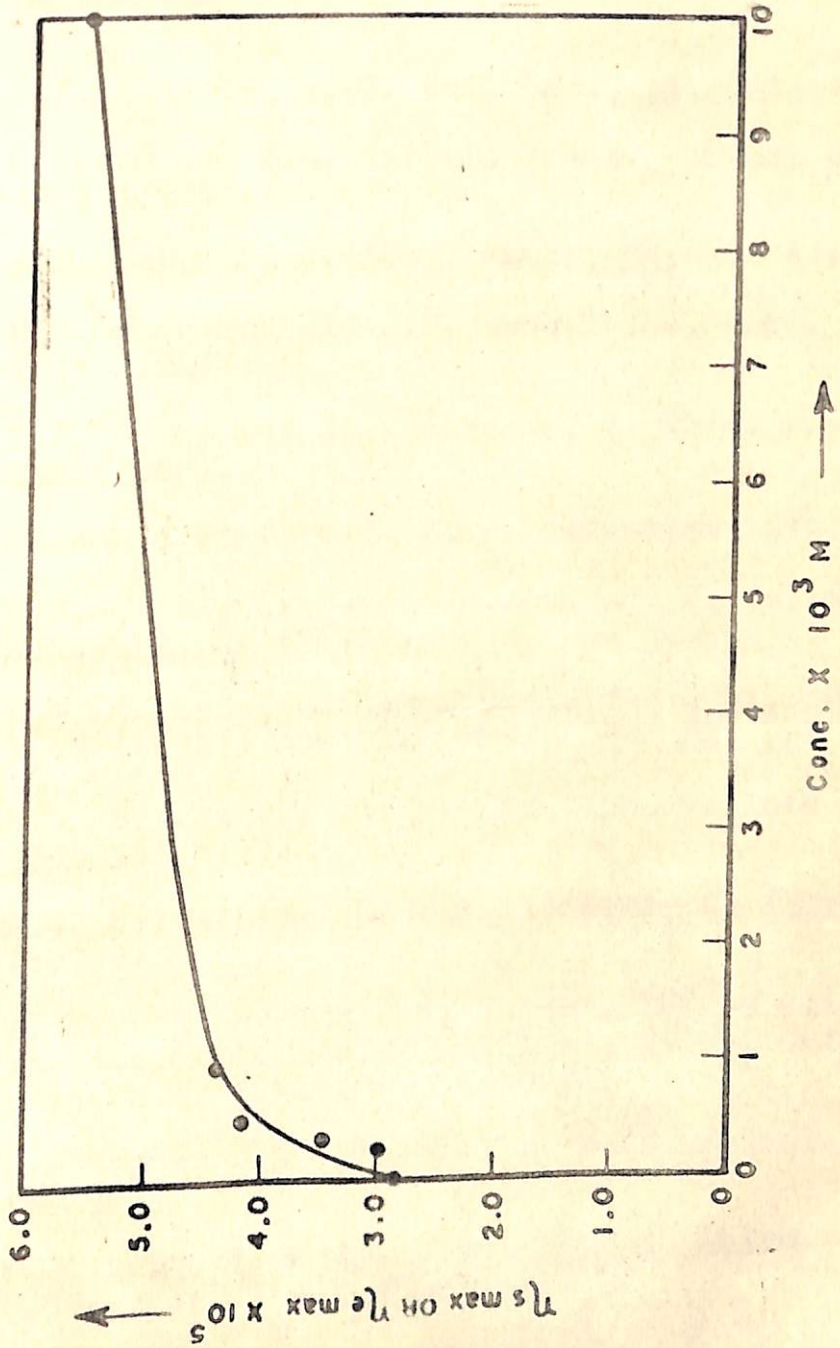

Fig. IV.15 Dependence of $(\eta_e)_{max}$ or $(\eta_s)_{max}$ with sodium chloride concentration.

IV.6 REFERENCES

1. J.F. Osterle, Appl. Sci. Res., 12, 425 (1964).
2. O.Kedem and S.R. Caplan, Trans. Faraday Soc., 61 1897 (1965).
3. J.F. Osterle, J. Appl. Mech., 31, 161 (1964).
4. F.A. Morrison and J.F. Osterle, J. Chem. Phys., 43, 2111 (1965).
5. R.J. Gross and J.F. Osterle, J. Chem. Phys., 49, 228 (1968).
6. Odum and Pinkerton, Amer. Scientist, 43, 331 (1955).
7. R.C. Srivastava and M.G.Abraham, J. Colloid Interface Sci., 57, 58 (1976).
8. W.R. Carmody, J. Amer. Chem. Soc., 51, 2901 (1929); 54 3647 (1932); See also Chem. Rev. 53, 397 (1953).
9. R.C. Srivastava and P.K.Avasthi, Kolloid Z.Z. Polym. 250, 253 (1972).
10. R.C. Srivastava and P.K. Avasthi, J. Hydrol. 20, 37 (1973).
11. A. Katchalsky and P.F. Curran, 'Non-equilibrium Thermodynamics in Biophysics', P.244, Harvard University Press, Massachusetts, 1965.
12. R.C. Srivastava and A.K. Jain; J. Hydrol., 25, 339 (1975).
13. R.C. Srivastava and A.K. Jain; J. Polym. Sci. (Polymer Physics ed.), 13, 1603 (1975).

STUDIES RELEVANT TO BIOPHYSICS

CHAPTER V

BILE SALT MICELLES AS LIQUID MEMBRANES*

---

* One paper based on this chapter has been accepted for publication and is in press with the JOURNAL OF NON-EQUILIBRIUM THERMODYNAMICS.

BILE SALT MICELLES AS LIQUID MEMBRANES

V.1 INTRODUCTION

The studies reported in this chapter are sequel to the studies on liquid membranes, described in chapter III. As mentioned in chapter III, the observation of Martin[1] that the addition of a few parts per million of surfactants like poly vinyl methyl ether to the saline feed in reverse osmosis effects a large increase in the salt retention capacity of cellulose acetate membranes with but a small decrease in the flux of product water, led Kesting et al[2,3,4] to propound a liquid membrane theory. The experiments of Kesting et al[2] and also our experiments reported in chapter III unambiguously proved the existence of a surfactant layer liquid membrane at the interface between the cellulose acetate membrane and the aqueous solution or water. It was further demonstrated that as concentration of the surfactant is increased, the cellulose acetate membrane gets progressively covered with the surfactant layer liquid membrane and at the critical micelle concentration (CMC) the coverage of the cellulose acetate membrane with the surfactant layer is complete.

Since bile salts are excellent surfactants it is logical to expect that their addition to water or aqueous solutions flowing through a membrane, would also give rise to the formation of liquid membranes at the interface between the supporting membrane and the aqueous solution. The experiments reported in this chapter have been designed to demonstrate this. The liquid membranes formed have been shown to offer resistance to both water flux and salt flux. Experiments on the hydraulic permeability and on the simultaneous transport of salt (potassium chloride in this case) and water have been performed and values of the filteration coefficient, reflection coefficient and the salt permeability coefficient for the liquid membrane have been estimated. The transport data have been further analysed in the light of Spiegler's frictional model[5] to estimate the relative magnitudes of the frictional coefficients between salt and water, water and the liquid membrane and salt and the liquid membrane.

V.2 EXPERIMENTAL

Materials: Sodium deoxy cholate (Loba Chemie, Austria), potassium chloride (BDH, Analar) and distilled water distilled once over potassium permanganate in an all glass still were used in the present experiments. The critical

micelle concentration of sodium deoxy cholate in water was determined by measuring the variation of electrical conductivity with concentration and was found to be 5 mM, which compares favourably with the values reported in literature.[6]

The Apparatus: The all glass cell used for the transport studies was similar to the one diagrammed in Fig. III.1 of chapter I. The all glass cell was separated into two compartments by a sartorius cellulose acetate millipore filter (Cat. No. 11107) of thickness 1×10^{-4} m and area 1.4×10^{-4} m^2 which in fact acted as a support for the liquid membrane.

Measurement of hydraulic permeability : The procedure adopted for the measurement of hydraulic permeability was similar to what has been described in chapter III. For the measurement of the hydraulic permeability freshly prepared aqueous solutions of sodium deoxy cholate of various concentrations ranging from zero to 7 mM were filled in the compartment C on the right hand side of the millipore filter S and distilled water was filled in the compartment D on the left hand side of the millipore filter S (Fig. III.1 of chapter III). Since the critical micelle concentration of aqueous solution of sodium deoxy

cholate as found from the electrical conductivity measurement is 5 mM, the concentration ranges from zero to 7 mM were purposely chosen so that we get data on both the lower and the higher side of CMC at which the supporting membrane is expected to be completely covered with the liquid membrane. Known pressures were applied on compartment C by adjusting the pressure head and consequent volume flux of water was measured by noting the rate of advancement of the liquid miniscus in the capillary L_1L_2 with a cathetometer reading upto .001 cms and stop watch reading upto 0.1 secs. During the volume flux measurements the electrodes E_1 and E_2 (Fig. III.1 of chapter III) were short circuited and the solution in the two compartments were well stirred using magnetic stirrers M_1 and M_2. Short circuiting of the electrodes E_1 and E_2 was done to prevent any electro-osmotic back flow due to the streaming potentials developed across the membrane.

Measurement of reflection coefficient and salt permeability :

For a system consisting of two compartments containing same binary aqueous solution of unequal concentrations and separated by a membrane, the linear phenomenological relations for the simultaneous transport of solute and solvent as obtained from non-equilibrium thermodynamic

treatment[7] have been described in chapter I (equation (31) and (32) of chapter I) which on further transformation[7,8] can be reduced to a more operational form (equation (44) and (46) of chapter I). These equations are being reproduced below for a ready reference i.e.

$$J_v = L_p(\Delta P - \sigma \Delta\pi) \qquad (1)$$

and

$$J_s = \omega \Delta\pi + \bar{C}_s (1 - \sigma) J_v \qquad (2)$$

because it is these equations which have been utilised for the evaluation of L_p, σ and ω, the three parameters which adequately describe the transport characteristics of a membrane system. The various terms occuring in equation (1) and (2) have the same meaning as in chapter I. Let us also rewrite the expression for σ and ω (equations (39), (47) and (48) of chapter I)

$$\sigma = \left(\frac{\Delta P}{\Delta\pi} \right)_{J_v=0} = - \frac{L_{PD}}{L_P} \qquad (3)$$

and

$$\omega = \left(\frac{J_s}{\Delta\pi} \right)_{J_v=0} = \bar{C}_s \left(\frac{L_P L_D - L_{PD}^2}{L_P} \right) \qquad (4)$$

for ready reference.

Values of the coefficients L_p, σ and ω were estimated in the manner described in chapter II using equation (1) according to which the plot of J_v versus ΔP is a straight line of slope L_p and intercept equal to $- L_p \sigma \Delta\pi$. Since $\Delta\pi$ is known and is more or less constant during a particular run of the experiment, L_p and σ can be conveniently estimated from the slope and intercept of such plots. In the actual experiments for the determination of L_p and σ a solution of known strength of potassium chloride prepared in a 5 mM (the CMC value of sodium deoxy cholate) aqueous solution of sodium deoxy cholate was filled in the compartment C of the cell (Fig. III.1 of chapter III) and distilled water was filled in the compartment D. The condition $\Delta P=0$ was imposed on the system by adjusting the pressure head and it was allowed to stand for some time.

As soon as recession in the capillary L_1L_2 due to osmosis was noticed known pressures were applied on the solution compartment and the rate of advancement of the liquid miniscus in the capillary L_1L_2 was noted with time. Since the back flow of water in the solution compartment due to osmosis is quite small, $\Delta\pi$ can be taken to be more or less constant during a particular run of the experiment. The data obtained in this manner for two

different values of $\Delta\pi$ are given in Table V.1 and plotted in Fig. V.1. The data for a blank experiment in which all conditions were maintained same except that no sodium deoxy cholate was used have been given in Table V.1 and plotted in Fig. V.1.

The equation (2) under the condition $J_v=0$ was the basis for the determination of the salt (potassium chloride in the present case) permeability ω. In the actual experiment for the determination of ω a solution of potassium chloride of known concentration prepared in 5 mM (the CMC value of aqueous sodium deoxy cholate) solution of sodium deoxy cholate was filled in the compartment C of the cell (Fig. III.1 of chapter III) and distilled water was filled in the other compartment of the cell (Fig. III.1 of chap.III). The condition $J_v=0$ was enforced on the system by manually adjusting the pressure head attached to the solution compartment. After a known period of time which was of the order of twelve hours or so the solutions from the two compartments were withdrawn and analysed for potassium using a flame photometer (Elico, Hyderabad Model CL 22) reading upto 2 ppm. The amount of potassium chloride lost by the solution compartment or the amount of potassium chloride gained by the water compartment divided by the

Table V.1

The volume flux data for the determination of L_p and σ using equation (1)

$\Delta P \times 10^{-2}$ N m^{-2}	$J_v \times 10^{6}$ (†) m sec^{-1}	$J_v \times 10^{6}$ (≠) m sec^{-1}	$J_v \times 10^{5}$ * n sec^{-1}
9.8	0.761	0.125	0.127
14.7	1.461	0.827	0.280
19.6	1.75	1.38	0.466
24.5	2.68	1.954	0.708
29.4	3.19	2.48	0.925

† at $\Delta\pi = 25.98 \times 10^{+2}$ N m^{-2}

≠ at $\Delta\pi = 10.38 \times 10^{2}$ N m^{-2}

* J_v values for blank experiment when no sodium deoxy cholate was used. $\Delta\pi = 25.98 \times 10^{2}$ N m^{-2}

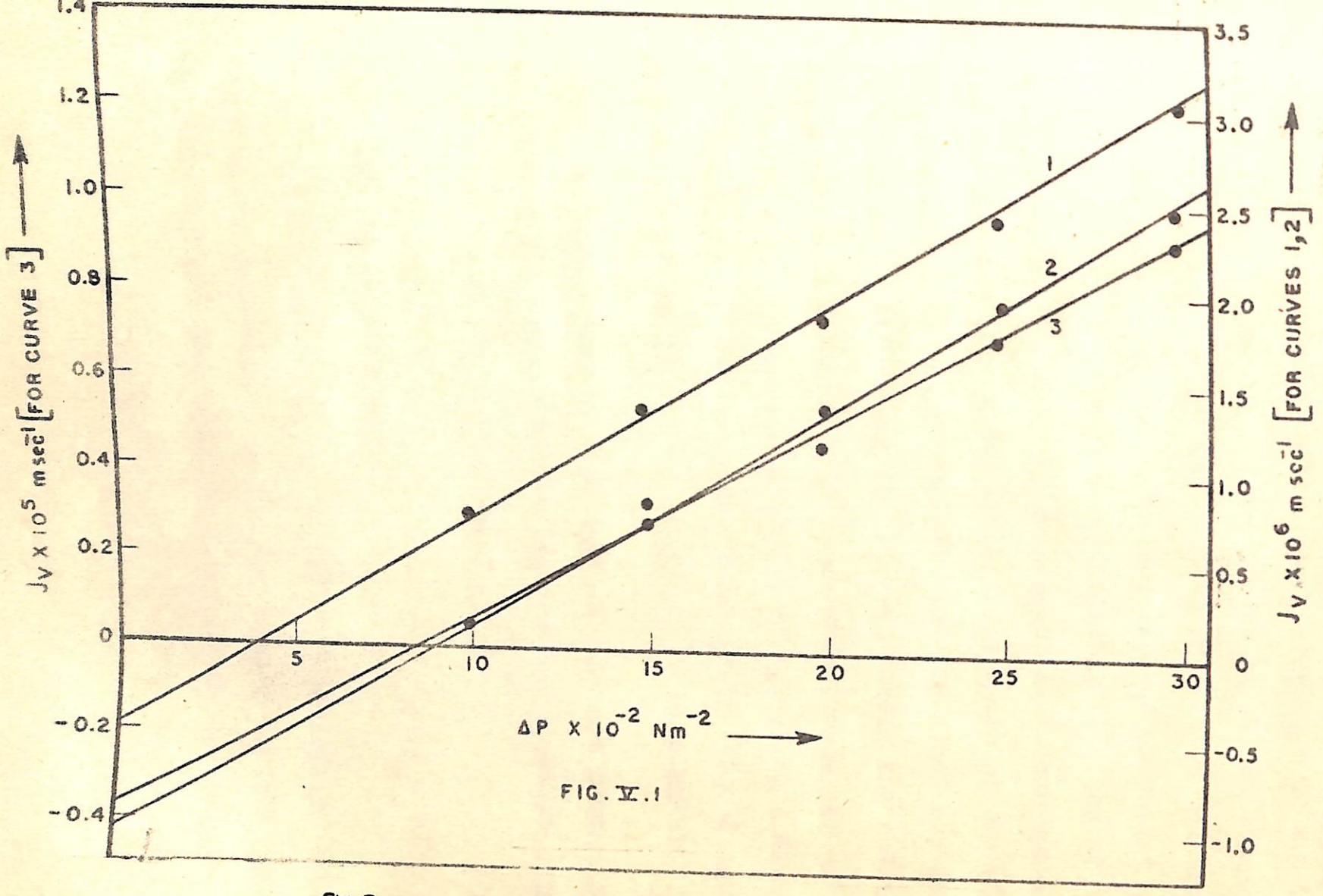

FIG. V.1

FIG. V.1 Determination of L_p and σ using equation (1). Curve 1 - $\Delta\Pi = 25.98 \times 10^2$ Nm^{-2}, Curve 2 - $\Delta\Pi = 10.38 \times 10^2$ Nm^{-2}, Curve 3 - (Blank experiment) $\Delta\Pi = 25.98 \times 10^2$ Nm^{-2}.

time gave the value of salt flux J_s. Average of the values of $\Delta\pi$ at the beginning and at the end of the experiment were considered for the calculation of ω using equation (4) Since the ionic micelles have large molecular weight their osmotic contribution will be negligible. In view of this only potassium chloride concentrations have been considered for calculating the values of $\Delta\pi$. The value of the salt permeability ω was also estimated for the blank experiment in which no sodium deoxy cholate was used. The values of L_p, σ and ω as obtained from these experiments are given in Table V.2. In the measurements of L_p, σ and ω also the solutions in the two compartments were well stirred using magnetic stirrers M_1 and M_2 (Fig. III.1 chapter III).

All measurements were made at constant temperature by placing the transport cell (Fig. III.1 of chapter III) in a thermostat set at $40 \pm 0.1^{\circ}C$.

V.3 RESULTS AND DISCUSSION

It is clear from the hydraulic permeability data for various concentrations of sodium deoxy cholate (given in Table V.3 and plotted in Fig. V.2) that the Darcy's law

$$J_v = L \Delta P \qquad (5)$$

Table V.2

The values of L_p, σ and ω and f $\Delta\pi$ for the liquid membrane as computed from the values of L_p, σ and ω for the supporting membrane, and for the supporting membrane + the liquid membrane in series.

	Sodium deoxy cholate concentration (mM)		Computed values for the liquid membrane
	0	5	
$L_p \times 10^8$ $m^3 N^{-1} sec^{-1}$	0.486(a)	0.122(a) 0.123(b)	0.162
σ	0.35 (a)	0.36 (a) 0.36 (b)	0.442
$\omega \times 10^9$ mole sec^{-1} N^{-1}	0.175(c)	0.135(d)	0.599
f_{wm} $\Delta\pi \times 10^{-2}$ $mole^{-1}$ sec^{-1} N	-	-	74.053
f_{sm} $\Delta\pi \times 10^{-7}$ $mole^{-1}$ sec^{-1} N	-	-	0.25
f_{sw} $\Delta\pi \times 10^{-9}$ $mole^{-1}$ sec^{-1} N	-	-	0.931

(a) for $\Delta\pi = 25.98 \times 10^2$ Nm^{-2} (b) for $\Delta\pi = 10.39 \times 10^2$ N m^{-2}

(c) Average value of $\Delta\pi = 14.26 \times 10^2$ N m^{-2}

(d) Average value of $\Delta\pi = 11.67 \times 10^2$ N m^{-2}

Table V.3

The Hydraulic permeability data at various concentration of Sodium deoxy cholate.

$\Delta P \times 10^{-2}$ N m^{-2}	Concentration of sodium deoxy cholate (mM)			
	0	2.5	5	7
	$J_v \times 10^5$ m sec^{-1}	$J_v \times 10^5$ m sec^{-1}	$J_v \times 10^5$ m sec^{-1}	$J_v \times 10^5$ m sec^{-1}
4.9	0.3077	0.177	0.070	0.070
9.8	0.564	0.409	0.159	0.156
14.7	0.80	0.588	0.236	0.191
19.6	1.1	0.752	0.332	0.297
24.5	1.38	1.066	0.427	0.363
29.4	1.7	1.19	0.51	0.452

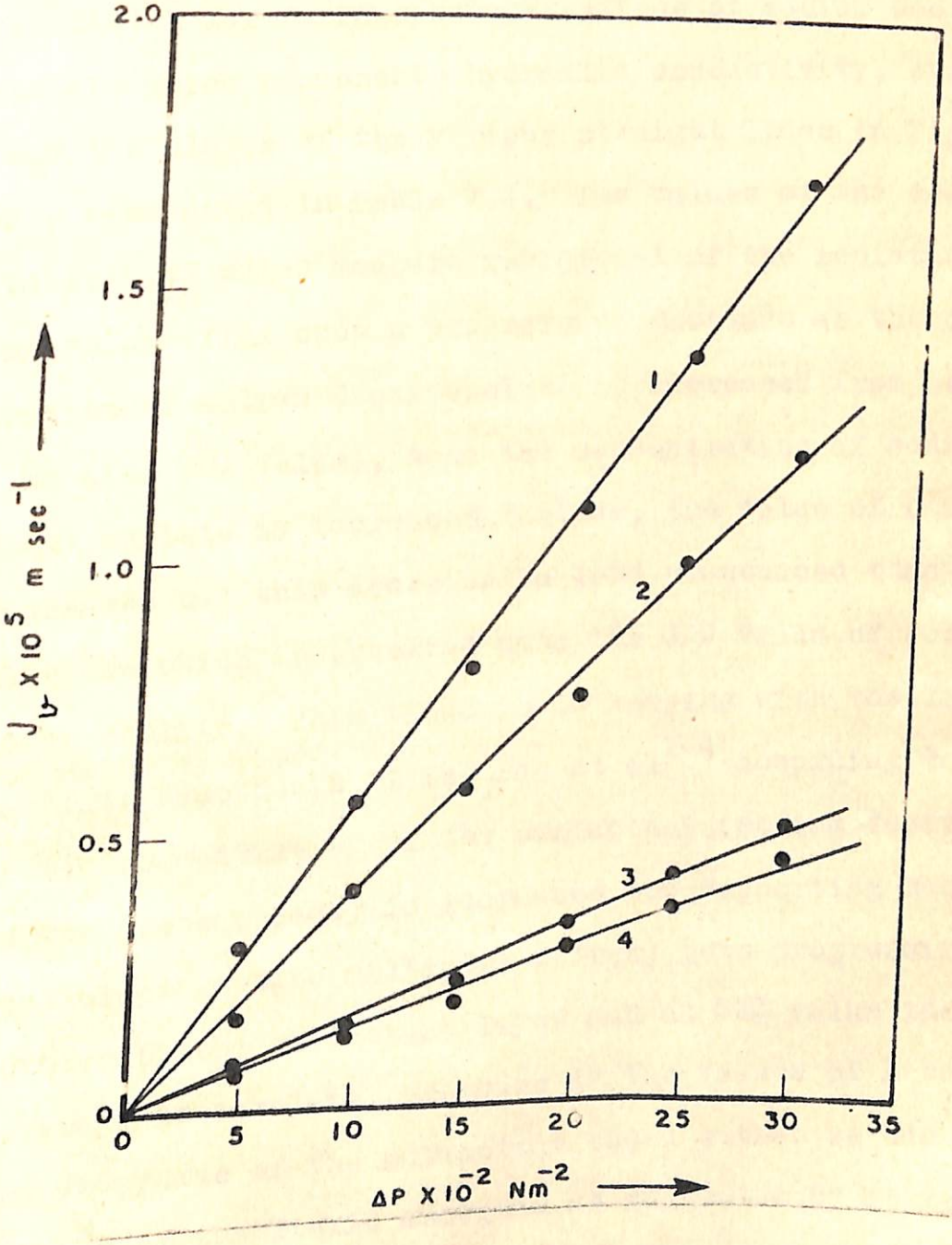

Fig. V.2 The Hydraulic permeability data. Curves 1, 2, 3 and 4 are for 0, 2.5, 5 and 7 mM of sodium deoxy cholate.

Table V.4

Values of L of various concentrations of Sodium deoxy Cholate.

	Concentration of Sodium deoxy cholate (mM)			
	0	2.5	5	7
$L \times 10^{8}$ m^{3} sec^{-1} N^{-1}	0.568	0.370	0.17	0.149

case of PVME liquid membrane. The possibility of the formation of multilayers of liquid membrane could not be investigated in this case because the aqueous solution of higher concentration of sodium deoxy cholate were not found to remain stable for more than an hour or so.

Following the analysis for mosaic[9-11] membranes in the same manner as described in chapter III, in this case also it can be possible to estimate the fraction of the total area of the supporting membrane covered with the liquid membrane at concentration lower than the CMC. For this let us consider the hydraulic permeability data for sodium deoxycholate concentrations equal to 0, 2.5 and 5 mM. Since at a concentration lower than the CMC the supporting membrane is only partially covered with the liquid membrane, the equation for volume flux of water for such a case can be written as

$$J(Y^c + Y^s) = L^c Y^c \Delta P + L^s Y^s \Delta P \qquad (6)$$

and

$$J = \left[L^c \left(\frac{Y^c}{Y^c + Y^s} \right) + L^s \left(\frac{Y^s}{Y^c + Y^s} \right) \right] \Delta P \qquad (7)$$

where the superscripts c and s respectively represent the

supporting membrane and the liquid membrane in series with the supporting membrane and Y represents the area of the membrane represented by the superscripts.

If at 5 mM concentration of sodium deoxy cholate the supporting membrane is fully covered with the liquid membrane it is logical to expect that at 2.5 mM concentration the fraction of the total area covered by the liquid membrane will be equal to half. Thus the slope L of the straight line for 2.5 mM (Fig. V.2) should be equal to $\frac{L^c + L^s}{2}$ where L^s and L^c are the values of the slopes of the straight lines corresponding to 5 mM and o mM concentrations of sodium deoxy cholate respectively. Value of the slope thus computed comes out to be equal to 0.365×10^{-8} $m^3 sec^{-1} M^{-1}$ which compares favourably with the experimental value of the slope for 2.5 mM concentration of sodium deoxy cholate (Table V.4 and Fig. V.2).

For estimating the values of L_p, σ and ω for the liquid membrane it has to be borne in mind that data corresponding to 5 mM concentration of sodium deoxy cholate is for the composite membrane consisting of the supporting membrane i.e. the cellulose acetate millipore filter and the liquid membrane in series with each other and the data from blank experiments in which no sodium deoxy cholate

was used is for the transport through the supporting membrane only. The values of L_P, σ and ω for the liquid membrane can be conveniently estimated by making use of the theory developed by Kedem and Katchalsky[7,12,13] for the permeability of series composite membrane. In dealing with series composite membrane systems it is more convenient to utilise the inverse phenomenological equations which in the present case may be written as follows.

$$\Delta P = R_P J_V + R_{PD} J_D \tag{8}$$

$$\Delta\pi = R_{DP} J_V + R_D J_D \tag{9}$$

with

$$R_{PD} = R_{DP} \tag{10}$$

on account of Onsager's theorem. The relationships between the resistance coefficients R_{ik} and the phenomenological coefficients occurring in equations (25) to (28) of chapter I are given by

$$R_P = \frac{L_D}{|L|} \tag{11}$$

$$R_{PD} = -\frac{L_{PD}}{|L|} \tag{12}$$

$$R_{DP} = - \frac{L_{DP}}{|L|} \qquad (13)$$

$$R_{D} = \frac{L_{P}}{|L|} \qquad (14)$$

where the determinant $|L| = (L_P L_D - L_{PD} L_{DP})$.

The assumptions underlying the theoretical analysis for the series composite membrane are the following:

(a) In the series arrangement the flows passing each membrane element will be the same as required for a stationary state.

(b) The forces acting on each membrane element will differ while their sum total will represent the observable macroscopic force. The thermodynamic potentials are assumed to be continuous throughout the composite structure.

(c) The linear phenomenological relations between fluxes and forces are assumed to be valid for the constituent membrane elements as well as for the series composite membrane.

As a consequence of these assumptions the following combination rules connecting the resistance coefficients for

the series composite membrane and the resistance coefficients for its constituent membrane elements would follow

$$R_P^s = R_P^c + R_P^l \tag{15}$$

$$R_{PD}^s = R_{PD}^c + R_{PD}^l \tag{16}$$

$$R_{DP}^s = R_{DP}^c + R_{DP}^l \tag{17}$$

$$R_D^s = R_D^c + R_D^l \tag{18}$$

where the superscripts s, c and l stand for the composite membrane consisting of the cellulose acetate millipore filter and the liquid membrane in a series array, the cellulose acetate millipore filter and the liquid membrane respectively. The reflection coefficient σ, from equations (8) and (9) can now be written as

$$\sigma^s = \left(\frac{\Delta P}{\Delta \pi}\right)_{J_v=0} = \left(\frac{R_{PD}^s}{R_D^s}\right) \tag{19}$$

The equation (19) on account of the combination rules (16) and (18) can be transformed into

$$\sigma^s = \sigma^c \left(\frac{R_D^c}{R_D^s}\right) + \sigma^l \left(\frac{R_D^l}{R_D^s}\right) \tag{20}$$

Using the experimentally determined values of σ^s and σ^c (Table V.2) and the equality

$$\frac{R_D^c}{R_D^s} + \frac{R_D^l}{R_D^s} = 1 \qquad (21)$$

it is possible to compute the values of σ^l from the equation (20). Value of the quantity (R_D^c / R_D^s) can be determined from equation (4) using the experimentally determined values of ω for the series membrane and the cellulose acetate millipore filter membrane (Table V.2).

Similarly for ω and L_P the following relationships can be deduced[13] from the analysis of series composite membrane given by Kedem and Katchalsky.

$$\frac{1}{\omega^s} = \frac{1}{\omega^c} + \frac{1}{\omega^l} \qquad (22)$$

$$\frac{1}{L_P^s} = \frac{1}{L_P^c} + \frac{1}{L_P^l} \qquad (23)$$

Since the values of ω^s, ω^c, L_P^s and L_P^c have been experimentally determined the values of ω^l and L_P^l for the liquid membrane can be conveniently computed using equations (22) and (23). Values of L_P^l, σ^l and ω^l thus computed for the liquid membrane are given in Table V.2.

Correlation of phenomenological coefficients with frictions between the permeating species and between the permeating species and the porous barrier through which the permeation process takes place, has been attempted by Spiegler[5]. Spiegler's frictional model[5] has been extended by Kedem and Katchalsky[7,14] to correlate the measurable quantities L_p, σ and ω with various frictional coefficients. These correlations in the present case of the liquid membrane can be written as

$$L_P^l = \frac{\varphi_w \bar{V}_w}{f_{wm}\, \Delta x} \tag{24}$$

$$\sigma^l = 1 - K \frac{f_{sw}}{(f_{sw} + f_{sm})\, \varphi_w} \tag{25}$$

$$\omega^l = \frac{K}{(f_{sw} + f_{sm})\, \Delta x} \tag{26}$$

where f represents the coefficient of friction between the species indicated by the subscripts. The subscripts s, m and w stand for the salt, the liquid membrane and water respectively and Δx represent the thickness of the liquid membrane. The quantities φ_w, $\bar{V}_w$ and K in equations (24) to (26) represent the volume fraction of water, partial

molar volume of water and the distribution coefficient of the electrolyte between the membrane phase and the aqueous phase. Since the magnitude of Δx the thickness of liquid membrane is not known, it is not possible to calculate the exact values of the various frictional coefficients. One can nevertheless have an assessment of the relative magnitudes of the various frictional coefficients from the values of $f_{\not s w}\,\Delta x$, $f_{\not s m}\,\Delta x$ and $f_{wm}\,\Delta x$ which can be conveniently calculated from the values of L_P^1, σ^1 and ω^1 (Table V.2) using equations (24) to (26). The values of the quantities ($f\,\Delta x$) thus calculated are given in Table V.2 from which it is apparent that

$$f_{\not s m} >> f_{wm} \qquad (27)$$

$$f_{\not s w} > f_{\not s m} \qquad (28)$$

The inequality $f_{\not s m} >> f_{wm}$ expresses a kinetic selectivity condition which must hold good for a salt rejecting system. The friction between salt and membrane has to be much higher than the friction between water and membrane. The inequality $f_{\not s w} > f_{\not s m}$, however, indicates that the salt and water are more strongly coupled and when one passes through the liquid membrane it drags the

other along. Thus the inequality (27) represents a condition favourable to salt rejection while the inequality (28) represents a condition that hinders it.

Before we close this section we are tempted to say a word about the physiological implications of the studies described in this chapter. Since bile salts micelles have been shown to act as membranes, an important physiological implication of this finding is that in the transport of ions etc the existence of such liquid membranes in series with the usual mucosal membranes should also be taken into account.

V.4 REFERENCES

1. F.Martin, Private communication to R.E.Kesting, March 1963 as quoted in ref. 2, see also S.T.Hwang and K.Kammermeyer, Membranes in separation, Wiley 1975 Chapter VIII page 173.

2. R.E.Kesting, W.J.Subcas ky and J.D.Paton; J. Colloid Interface Sci., 28, 156 (1968).

3. R.E.Kesting, A.Vincent and J. Eberlin; O.S.W. R and D Report 117, Aug. 1964.

4. R.E.Kesting, 'Reverse Osmosis Process using surfactant Feed Additives', OSW Patent application SAL 830 Nov. 3, 1965.

5. K.S.Spiegler; Trans. Faraday Soc., 54, 1408 (1958).

6. A.F.Hofmann and M.Donald Small; Ann. Rev. Med. 18 333 (1967).

7. A.Katchalsky and P.F.Curran; Non-Equilibrium Thermodynamics in Biophysics, Harvard University Press, Cambridge, Massachusetts, 1967.

8. O.Kedem and A.Katchalsky; Biochim Biophys. Acta, 27, 229 (1958).

9. K.S.Spiegler and O.Kedem, Desalination, 1, 311 (1966).

10. T.K.Sherwood, P.L.T. Brian and R.E.Fisher; Ind. Eng. Chem. Fundam. 6, 2 (1967).

11. F.L.Harris, G.B.Humphreys and K.S.Spiegler; Chap. 4 in membranes Separation Processes, ed. P.Meares, Elsevier Scientific Publishing Co. Amsterdam 1976.

12. O.Kedem and A.Katchalsky; Trans. Faraday Soc., 59, 1941 (1963).

13. A.Katchalsky and O.Kedem, Biophys. J., 2, 53 (1962).

14. O.Kedem and A.Katchalsky, J. Gen. Physiol. 45, 143 (1961).

CHAPTER VI

TRANS-CELLULAR OSMOSIS IN INTERNODAL CHARACEAN CELLS

TRANS-CELLULAR OSMOSIS IN INTERNODAL CHARACEAN CELLS

VI.1 INTRODUCTION

The knowledge of hydraulic conductivity of biological cell membranes (animal or plant) is important from the point of view of cell physiology. What is required here is to measure the variation of volume with time under the influence of pressure gradient. For living membranes, the use of pressure gradients generally involves serious experimental difficulties. It can be seen, however from equations (31), (32) and (39) of chapter I that if it is known or can be shown that a particular solute exhibits a value of the reflection coefficient $\sigma = 1$ for a particular membrane (that is if the membrane is strictly semipermeable towards that solute) then the volume flow developed by an osmotic gradient will be identical with that developed by a hydrostatic pressure gradient i.e. $L_P = L_{PD}$ (equation (33) of chapter I). Osmotic gradients are easily established by suitable manipulation of the solute concentration. The measurement of L_{PD} under such circumstances in fact can be used to estimate the values of hydraulic conductivity, L_P for living biological membranes. It may be emphasized here that this method of measuring L_P is based on the

assumption that (i) the linear phenomenological equations (31) and (32) of chapter I are obeyed and (ii) the solute used to establish the osmotic gradient is impermeable to the membrane i.e. $\sigma = 1$.

Using the method outlined above by Dainty and Ginzburg[1] have determined hydraulic conductivities during endo-osmosis and exo-osmosis in the internodal cells of Nitella translucens and Chara australis. They have also determined[2] independently the reflection coefficients for some solutes. Similar measurements have been done by Kamiya and Tazawa[3,4] on Nitella flexlis by means of trans-cellular osmosis. From these experiments both Dainty and Ginzburg[1,2] and Kamiya and Tazawa[3,4] concluded that the demonstrated polarity of the hydraulic conductivities in their dependence on the direction of water movement is an intrinsic characteristic of the membrane because the results could not be explained solely by the sweeping away effect[5]. More recently Steudle and Zimmermann[6] made more direct measurements of hydraulic conductivities in the internodes of Nitella flexilis and confirmed that the endo-osmotic hydraulic conductivities were not equal to the exo-osmotic hydraulic conductivities. The hydraulic conductivities were also shown to depend on osmotic

pressure differences used - an observation made earlier by Dainty and Ginjburg[1,2] as well.

In the present chapter the experiments and the data of Dainty and Ginzburg[1,2] have been re-examined. The analysis presented in the chapter reveals that the experiments of Dainty and Ginzburg[1,2] present a situation where the usual linear phenomenological equations, obtained from the non-equilibrium thermodynamic treatment[7] (equation (31) and (32) of chapter I) break down and the non-linear phenomenological equations of the kind suggested by Li[8,9] should be taken into account. In the next section the experiments and the theory used by Dainty and Ginzburg[1] is briefly summarised.

VI.2 METHOD AND THE THEORY USED BY DAINTY AND GINZBURG

The exact experimental set up used by Dainty and Ginzburg[1] is depicted in Fig. VI.1. It essentially consists of two chambers separated by a vaseline seal through which passed a long internodal characean cell. One of the compartments opens into a narrow capillary tube with an air bubble in the liquid. The volume flux through the characean cell was measured by noting the movement of this bubble against time. The other compartment is open to

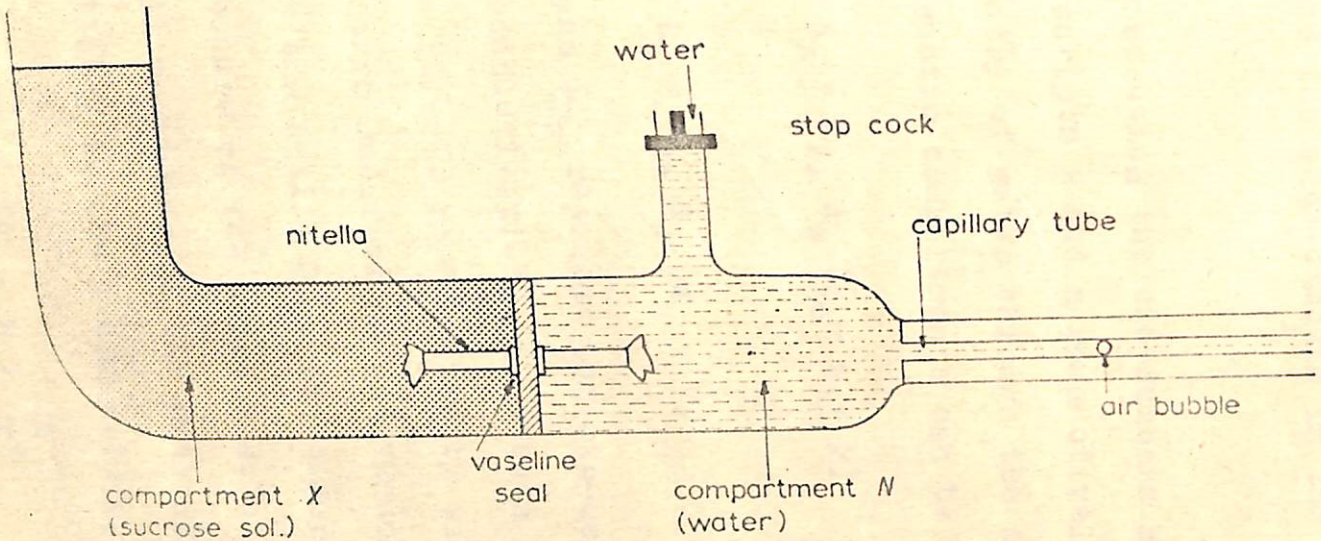

FIG 7.1 The apparatus for measuring transcellular osmosis.

the exterior and can be filled with sucrose solutions of known concentrations. The compartment containing the capillary tube was always filled with water. There was always exo-osmosis in the compartment containing sugar solution and the endo-osmosis in the compartment containing water.

Representing the exo-osmosis and the endo-osmosis by the subscripts κ and n respectively, the rate R of exit and entry of water through the cell in the exo-osmotic and endo-osmotic compartments can be written as

$$R_{\kappa} = L_{P\kappa} A_{\kappa} (\pi_o - \pi_{\kappa} + P) \qquad (1)$$

and

$$R_n = L_{Pn} A_n (\pi_n - P) \qquad (2)$$

where $L_{P\kappa}$ and L_{Pn} represent the exo-osmotic and endo-osmotic hydraulic conductivities, A stands for area of the cell in the compartments represented by subscripts, π_{κ} and π_n are the osmotic pressures of the vacuolar solutions at the two ends of the cell. P is the turgor pressure and π_o the osmotic pressure of the sucrose solution. The actual experimental recording of the rate of change of volume, R, in the capillary in the n compartment is given by

$$R = R_n + (R_{\kappa} - R_n) \frac{A_n}{A} \qquad (3)$$

where $A = A_{\pi} + A_n$ i.e. the total area of the cell. In writing equation (3) volume of the cell has been assumed to be proportional to its area. Now making use of equations (1) to (3) and assuming that there is negligible transfer of vacuolar solutes from one end of the vacuole to the other i.e. $\pi_{\pi} = \pi_n = \pi_i$ (say), Dainty and Ginzburg[1] write for the net flow

$$R = L_{P\pi} \frac{A_{\pi} A_n}{A} \pi_o + \frac{A_{\pi} A_n}{A} (L_{Pn} - L_{P\pi})(\pi_i - P) \qquad (4)$$

If $L_{P\pi} = L_{Pn}$ the equation (4) reduces to

$$R = L_{P\pi} \frac{A_{\pi} A_n}{A} \pi_o \qquad (5)$$

But if $L_{P\pi} \neq L_{Pn}$ and $R_{\pi} = R_n$ the equality which has to hold in the case of transcellular osmosis, Dainty and Ginzburg[1] using equations (1) and (2) transform equation (4) into

$$R = \frac{L_{P\pi} L_{Pn} A_{\pi} A_n}{L_{P\pi} A_{\pi} + L_{Pn} A_n} \cdot \pi_o \qquad (6)$$

In writing equation (6) the condition $\pi_{\pi} = \pi_n = \pi_i$ i.e., negligible transfer of vacuolar solutes from one end of the vacuole to the other has also been assumed.

VI.3 DISCUSSION

Dainty and Ginzburg[1,2] measured the hydraulic conductivity over a period of 30 - 60 seconds. Since cell shrinkage is over within first few seconds as shown by Dainty and Ginzburg themselves, the measurements on hydraulic conductivity were during true transcellular osmosis. Because during true transcellular osmosis R_π has to be equal to R_n, otherwise the cell would either collapse or burst, it is apparent from equations (1) and (2) that $L_{P\pi}$ cannot be equal to L_{Pn} specially for a symmetric case ($A_\pi = A_n$), since the driving forces in the two compartments are unequal. The driving forces in the exo-osmotic and in the endo-osmotic compartments being $(\pi_o - \pi_i + P)$ and $(\pi_i - P)$ respectively. It is also apparent from equations (1) and (2) that $L_{P\pi} \rightarrow L_{Pn}$ as $\pi_o \rightarrow 0$ for a symmetric case.

Since in the case of true trans-cellular osmosis $L_{P\pi}$ and L_{Pn} have to be unequal, equation (6) appears to be right equation for the calculation of L_P's. The values of $L_{P\pi}$ at various concentrations of sucrose have been calculated by Dainty and Ginzburg[1] using equation (6). The values of $L_{P\pi}$ at various concentration of sucrose

solution calculated by Dainty and Ginzburg[1] for a symmetric case ($A_\pi = A_n$) using equation (6) are given in Table VI.1. In all such calculations of $L_{P\pi}$, using equation (6), the value of L_{Pn} was assumed to be equal to the value of $L_{P\pi}$ for the lowest concentration of sucrose calculated using equation (5). This assumption appears logical in view of the fact that $L_{P\pi} \rightarrow L_{Pn}$ as $\pi_o \rightarrow o$. The variation of $L_{P\pi}$ with π_o has been plotted for a symmetric a case in Fig. VI.2 from which it is obvious that as π_o decreases the value of $L_{P\pi}$ increases and eventually as $\pi_o \rightarrow o$, $L_{P\pi} \rightarrow L_{Pn}$.

The fact that L_{Pn} is always greater than $L_{P\pi}$ and as $\pi_o \rightarrow o$, $L_{P\pi} \rightarrow L_{Pn}$ needs an explanation. Dependence of hydraulic conductivity on the direction of water movement appears to be on account of unequal shrinkage of the cell membrane in the exo-osmotic and endo-osmotic compartments. This would become clear if we look at the experimental set up used by Dainty and Ginzburg[1] (Fig. VI.1). The exo-osmotic compartment always contained sucrose solution and the endo-osmotic compartment always contained water. This means that the cell membrane in the exo-osmotic compartment gets shrunk while the cell membrane in the endo-osmotic compartment does not. As the value of π_o

Table VI.1

Values of $L_{P\pi}$ and L_{Pn} in cm sec^{-1} atm^{-1} $\times 10^5$, for Internodal Characean cell.

Chara australis

Cell No	Osmotic pressure (π_o) in atm. 2.46	4.92	7.38	9.84	12.30
	$\leftarrow L_{Pn} \rightarrow$	$L_{P\pi}$			
1.	1.05	0.76	0.82	0.67	0.57
2.	0.89	0.85	0.78	0.76	0.68
3.	1.33	-	-	1.05	1.02
4.	0.78	-	0.66	0.62	0.48
6.	0.61	0.55	0.44	-	0.38
8.	1.08	-	0.86	0.91	0.80
		Nitella transclucens			
9.	0.84	0.76	-	-	0.68

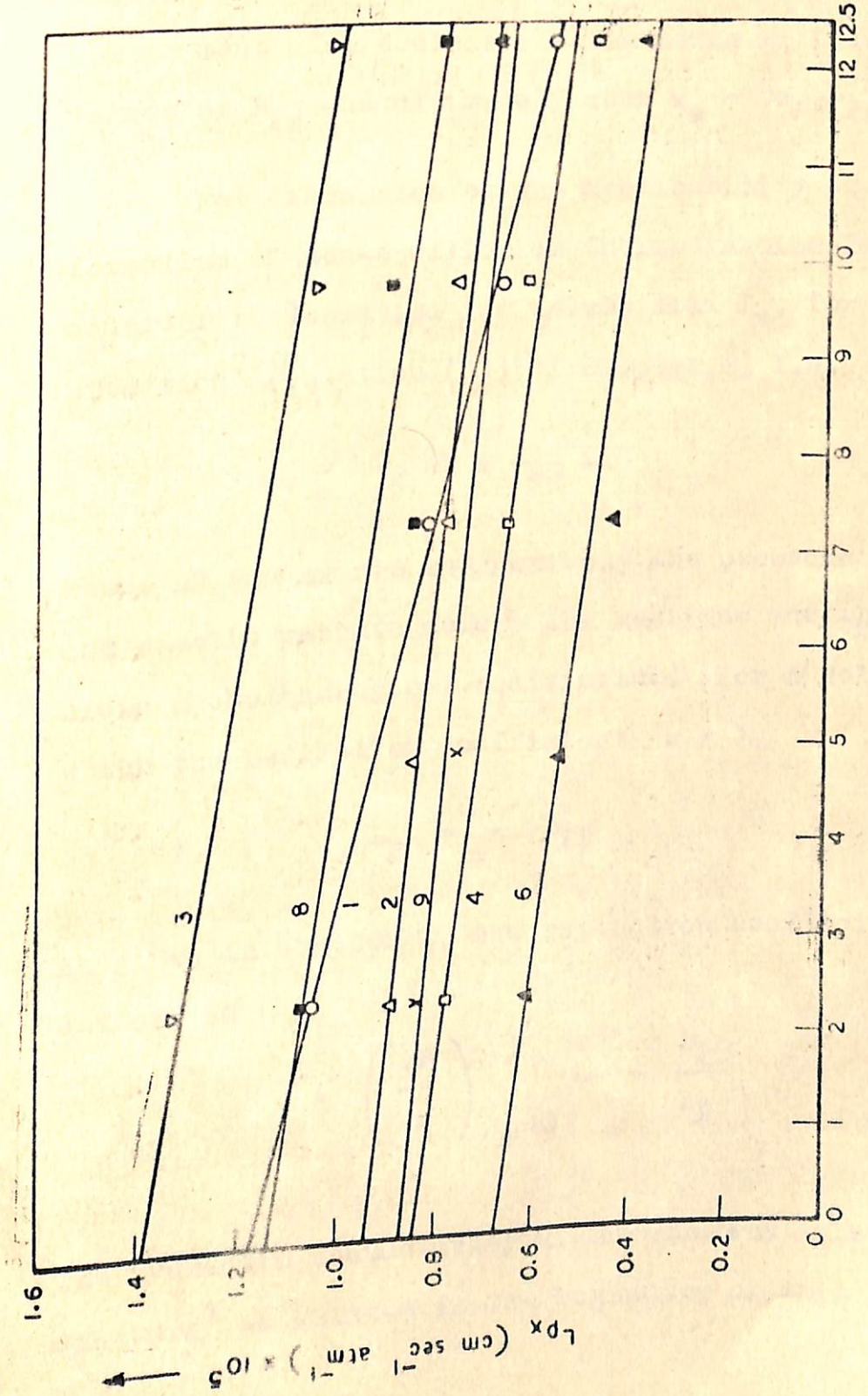

Fig. VI.2 Variation of L_{px} with Π_o for Chara Australis (curves 1, 2,3,4,5 & 8) and Nitella inslucens (curve 9). Curve numbers represent the cell number as given in Table I and II of reference *.

decreases the extent of shrinking in the exo-osmotic compartment also decreases which means an increase in the values of $L_{P\pi}$ and ultimately when $\pi_o \rightarrow o$, $L_{P\pi} \rightarrow L_{Pn}$.

For discussion on the applicability of linear formalism of non-equilibrium thermodynamics let us consider the equation for volume flux J_v, for a osmometric situation[7] (equation (31) of chapter I) i.e.

$$J_v = L_P \Delta P + L_{PD} \Delta\pi \qquad (7)$$

where ΔP and $\Delta\pi$ are respectively the pressure difference and osmotic pressure across the membrane and L_{PD} is the cross phenomenological coefficient. For a solute, for which the reflection coefficient $\sigma = 1$,

$$L_P = - L_{PD} \qquad (8)$$

As given in chapter I, the reflection coefficient σ is defined as

$$\sigma = \left(\frac{\Delta P}{\Delta\pi} \right)_{J_v=0} = - \frac{L_{PD}}{L_P} \qquad (9)$$

The hydraulic conductivity measurements by Dainty and Ginzburg[1] as pointed in the beginning of this chapter are

essentially based on equation (8). When $\Delta\pi$ is the only driving force across the membrane the equation (7) reduces to

$$J_v = L_{PD} \Delta\pi \qquad (10)$$

Now let us consider the experimental set up of Dainty and Ginzburg[1] depicted in Fig. VI.1. The thermodynamic driving forces in the exo-osmotic and the endo-osmotic compartments are $(\pi_o - \pi_i + P)$ and $(\pi_i - P)$ respectively. Thus the net driving force across the total cell membrane is π_o which induces a volume flux in the capillary attached to the endo-osmotic compartment and given by the equation (6). Thus comparing equation (6) with (10) we can write

$$L_{PD} = \frac{L_{P\pi}\, L_{Pn}\, A_\pi\, A_n}{L_{P\pi}\, A_\pi + L_{Pn}\, A_n} \qquad (11)$$

Values of the cross phenomenological coefficient at various values of π_o can be calculated from equation (11) using the values of $L_{P\pi}$ and L_{Pn} given in Table VI.1 as determined by Dainty and Ginzburg.[1]

The values of the cross coefficient thus calculated for a symmetric case ($A_\pi = A_n$) are given in Table VI.2 which have been plotted against π_o in Fig. VI.3. In all

Table VI.2

Values of the cross phenomenological coefficent, $(L_{PD})_{observed}$ for a symmetric ase at various values of the net driving force (π_0) for chara Australis

	$L_{P\pi}\, L_{Pn}\, A_{\pi}\, An\, /(L_{P\pi}\, A_{\pi} + L_{Pn}\, A_n)$			
	Osmotic pressure (π_o) in atm.			
Cell No.	4.92	7.38	9.84	12.3
1.	1.114	1.163	1.033	0.933
2.	1.098	1.050	-	0.974
4.	-	0.903	0.873	0.751
6.	0.731	0.646	-	0.592
8.	-	1.209	1.248	1.161

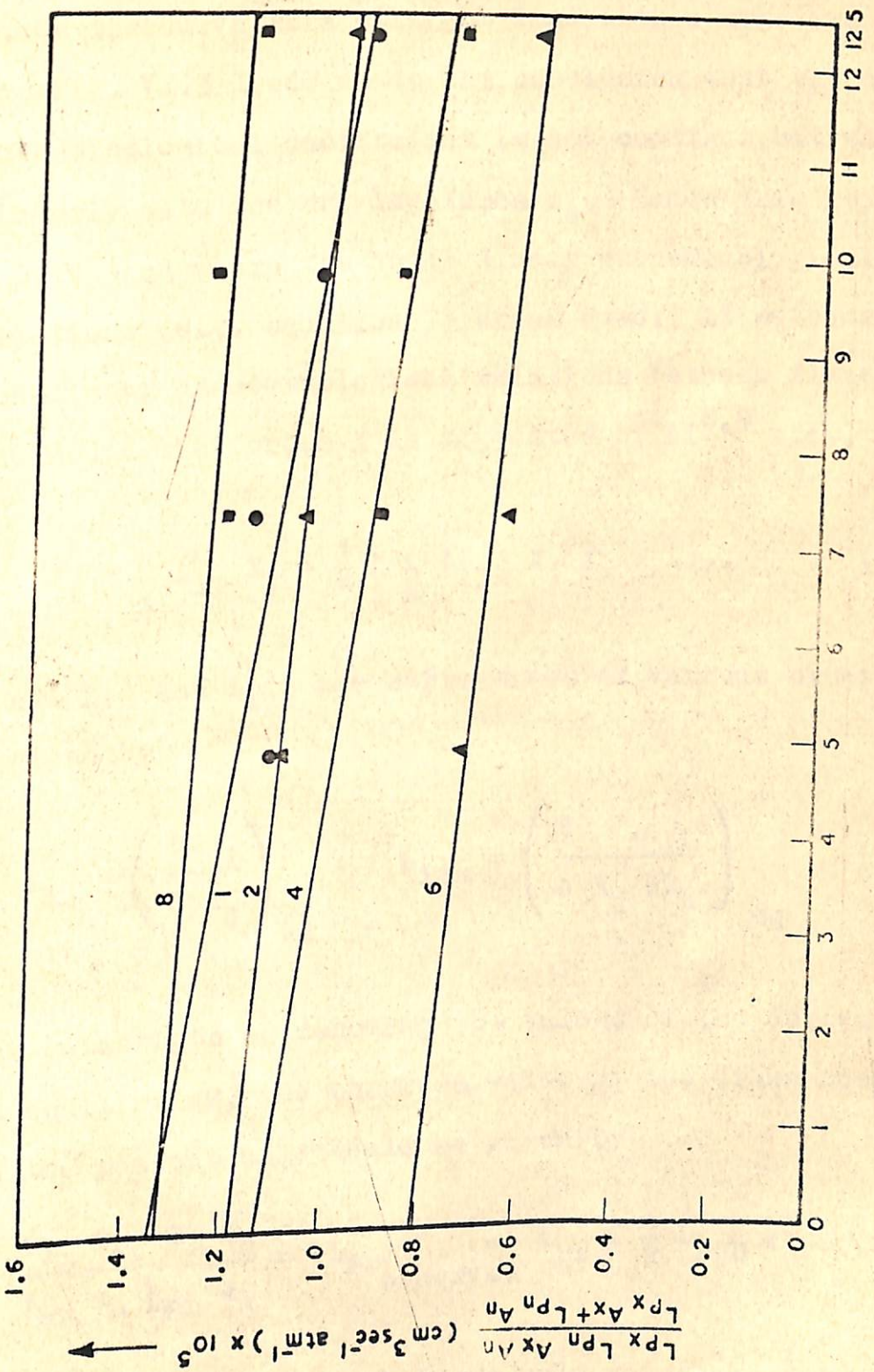

196

Fig. VI.3 Test of equation (14) for Chara Australis. Curve numbers represent the cell numbers given in reference 1.

cases the curve is a straight line with a negative slope. The Fig. VI.3 leads us to the conclusion that the cross phenomenological coefficient is not constant but varies linearly with the driving force π_o. Hence this represents a situation where the usual linear phenomenological relations (e.g. equation 7) break down. If we consider the non-linear phenomenological relations between fluxes J and thermodynamic forces X as suggested by Li[8,9] i.e.,

$$J_i = \sum_j L_{ij} X_j + \frac{1}{2} \sum_j \sum_k L_{ijk} X_j X_k + \cdots \qquad (12)$$

where L_{ij} and L_{ijk} are derivatives of various orders of J given by

$$L_{ij} = \left(\frac{\partial J_i}{\partial X_j} \right)_{eq} \quad ; \quad L_{ijk} = \left(\frac{\partial^2 J_i}{\partial X_j \, \partial X_k} \right)_{eq} \qquad (13)$$

the subscripts eq denoting the values of the derivatives at equilibrium, the observed value of the cross coefficient in the present case would be given by

$$\frac{L_{P\pi} L_{Pn} A_\pi A_n}{L_{P\pi} A_\pi L_{Pn} A_n} = (L_{PD})_{observed} = L_{PD} + \frac{1}{2} L_{PDD} \pi_o \qquad (14)$$

In writing equation (14) terms only upto second order have

been considered and L_{PDD} is the second order phenomenological coefficient. The curves in Fig. VI.3 in all cases are in accordance with equation (14). The values of second order phenomenological coefficient L_{PDD} for the various cells, calculated from the slopes of the straight lines in Fig. VI.3 are given in Table VI.3.

Another indication of the non-constancy of the cross phenomenolgocal coefficient can be had from the concentration dependence of the reflection coefficient σ of the membrane of Nitella translucens for heavy water (DHO). The values of reflection coefficient σ as obtained by Dainty and Ginzburg[2] have been plotted against π_o in Fig. VI.4. The curves in Fig. VI.4 also give indication of the break down of the usual linear phenomenological equations.

Table VI.3

Values of L_{PD} and L_{PDD} (equation 14) for different cells of Chara australis calculated from Fig. VI.3.

Cell No	$L_{PD} \times 10^5$ cm sec^{-1} atm^{-1}	$L_{PDD} \times 10^7$ cm sec^{-1} atm^{-2}
1	1.34	6.4
2	1.18	3.36
4	1.13	5.76
6	0.81	3.68
8	1.33	2.24

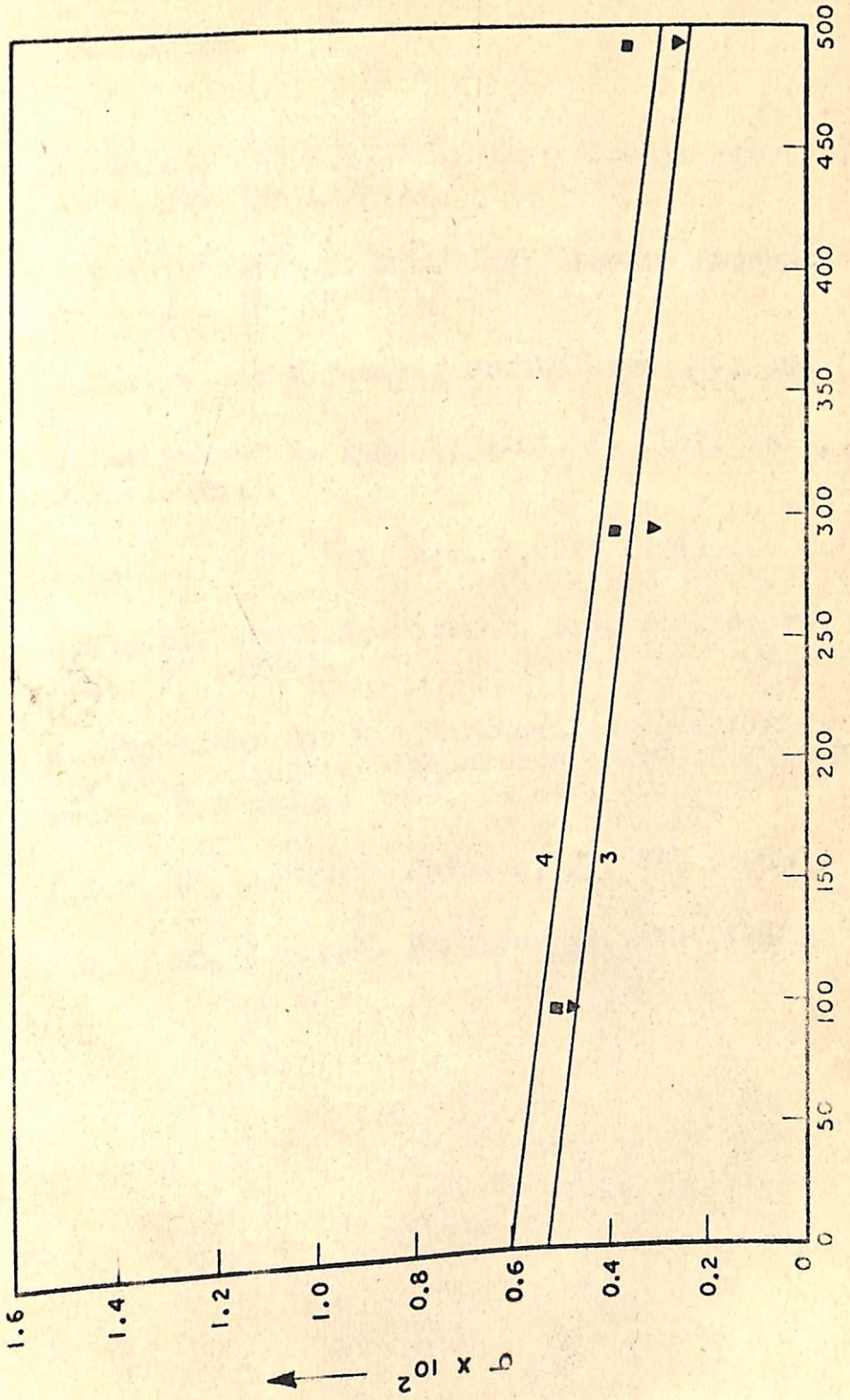

Fig. VI.4 Variation of reflection coefficient σ with Π_0 for Nitella translucens for heavy water (DHO). Curve numbers represent the cell numbers as given in reference 2.

VI.4 REFERENCES

1. J. Dainty and B.Z. Ginzburg; Biochim Biophys. Acta 79, 102 (1964).

2. J.Dainty and B.Z. Ginzburg; Biochim Biophys. Acta 79, 129 (1964).

3. N.Kamiya and M.Tazawa; Protoplasma 46, 394 (1956).

4. N.Kamiya and M. Tazawa; Aust. J. Biol. Sci., 19, 399 (1966).

5. J.Dainty; Adv. Bot. Res. 1, 279 (1963).

6. E.Steudle and U.Zimmermann; Biochim Biophys. Acta 332, 399 (1974).

7. A.Katchalsky and P.F.Curran; Non-equilibrium thermodynamics in bio-physics (Harvard University Press, Cambridge) 1965, p. 248.

8. J.C.M. Li, J. Chem. Physics, 29, 747 (1958).

9. J.C.M. Li, J. Appl. Physics, 33, 616 (1962).

CHAPTER VII

NETWORK THERMODYNAMIC MODELLING*

---

* One paper based on this chapter has appeared in the JOURNAL OF MEMBRANE SCIENCE, 3, 39-46 (1976) and the other one has been accepted for publication in the INDIAN JOURNAL OF CHEMISTRY.

NETWORK THERMODYNAMIC MODELLING

VII.1 INTRODUCTION

Network thermodynamics is a very recent development in the area of the treatment of non-equilibrium transport processes. Meixner[1,2,3] was the first to discover the connection between non-equilibrium transport processes and network theory. These ideas have recently been extended by Oster, Perelson and Katchalsky[4,5] to include the description and treatment of biological systems. The advantages of network approach and also its basic tenets and methodology have already been summarized in Chapter I.

In this chapter the network thermodynamic modelling has been attempted in the following two cases:

(i) Transport through composite membranes

(ii) Enzyme catalysed reaction.

In the former case attempt has been made to calculate the relaxation time for composite membranes consisting of a parallel and a series arrangement of two constituent membrane elements as a function of relaxation times for the constituent membrane elements. In the latter case the steady state reaction velocity and relaxation time for

a simple (single enzyme - single substrate system) enzyme catalysed reaction have been calculated. We will take up both these cases in the following sections.

VII.2 RELAXATION TIME FOR COMPOSITE MEMBRANES

The derivation of the relaxation time for membranes is usually complex. Some of the notable works in this regard are those of Daynes[6], Frish[7], Barrie[8] et al and Ash et al[9]. In the present section, an attempt has been made, utilising the formalism of network thermodynamics[4], to calculate the relaxation time for composite membranes in terms of the relaxation times for the constituent membrane elements. Two simple cases of composite membrane system have been considered. These are: (i) a composite membrane consisting of two constituent membrane elements arranged in a parallel array; and (ii) a composite membrane consisting of two membrane elements arranged in a series array.

The method developed by Oster, Perelson, and Katchalsky[4] is summarised below.

The method : Consider the simple case of a single permeant diffusing through a homogenous membrane (Fig. VII.1(a)).

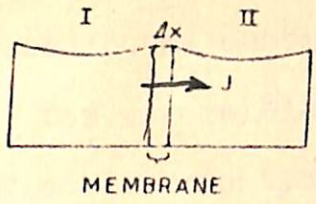

(a)

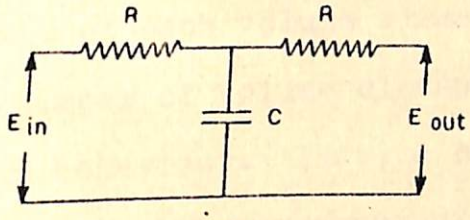

(b)

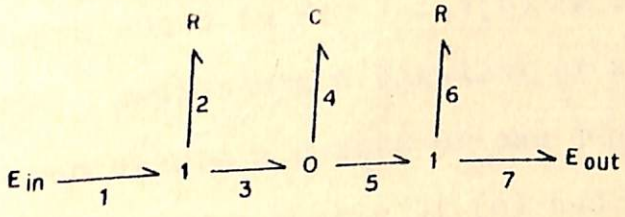

(c)

Fig.VII.1 (a) A homogeneous membrane system. J is the flux. (b) Network representation of the homogeneous membrane shown in (a). R & C are the resistance and the capacitance, respectively. (c) Bond graph representation of the network shown in (b).

We assign capcitances to the membrane as well as to the reservoirs to allow for reversible charging and discharging of the permeant. Since dissipation accompanies each flow process, a resistive element must be assigned at both the entrance and exit of each volume element of the membrane. The larger the number of volume elements, the closer we are to the continuum behaviour. Thus, a homogeneous membrane system (Fig VII.1(a)) can be represented by the network shown in Fig VII.1(a). The bond graph representation[10,11] of the network shown in Fig VII.1(b) is shown in Fig.VII.1(c) where (- 0 -) represents a parallel or a zero junction and (- 1 -) represents a series or one junction. If we represent the effort variable by (e) and the flow variable by (f), the zero junction would be defined by the condition $e_1 = e_2 = - - - = e_n$, or, since $\Sigma\, e_i f_i = 0$, $\Sigma\, f_i = 0$; and the one-junction would be defined by the condition $f_1 = f_2 = \ldots\ldots = f_n$, or, since $\Sigma e_i f_i = 0$; $\Sigma e_i = 0$. Let us assume that the bounding compartments are so large that they may be effectively time independent, that is, an infinite capacitance is equivalent to a constant effort source which has been denoted by E_{in} and E_{out} in Fig.VII.1(c). Now the governing state equation can be generated by making use of the junction rules and the nature and the manner of the elements joined. Thus, making use of the constitutive

relation for the membrane capacitor and the definition of a O-junction and a 1-junction we can write

$$C_4 \frac{de_4}{dt} = \frac{e_2}{R_2} - \frac{e_6}{R_6} \qquad (1)$$

According to the definition of a 1-junction, $e_2 = E_{in} - e_3$ and $e_6 = e_5 - E_{out}$. Further, noting that for a homogeneous membrane $R_2 = R_6 = R_m$, the membrane resistance, and C_4 is the membrane capacity C_m, equation (1) can be rewritten as

$$\frac{de_4}{dt} = \frac{1}{R_m C_m} \left[(E_{in} - e_3) - (e_5 - E_{out}) \right] \qquad (2)$$

Now identifying E_{in} and E_{out} with the chemical potentials μ' and μ'' of the permeant in the two reservoirs, we may define the average chemical potential $\langle\mu\rangle$ as

$$\langle\mu\rangle \equiv \frac{E_{in} + E_{out}}{2} = \frac{\mu' + \mu''}{2} \qquad (3)$$

Since, because of the definition of a O-junction, $e_3 = e_4 = e_5 = \mu_m$, the chemical potential of the permeant in the membrane, equation (2) with the help of equation (3) can be transformed into

$$\frac{d\mu_m}{dt} = \frac{2}{R_m C_m} \left[\langle \mu \rangle - \mu_m \right] \qquad (4)$$

From equation (4) it is obvious that the relation time τ_m for the membrane process would be given by

$$\tau_m = \frac{R_m C_m}{2} \qquad (5)$$

which has the expected form of an RC time constant familiar from network theory.

For a homogeneous membrane the magnitude of R_m evaluated[4] for an ideal permeation process is

$$R_m = \frac{RT \, \Delta x}{D_m (N_i/V)} \qquad (6)$$

where D_m is the diffusion coefficient within the membrane Δx is the membrane thickness, N_i represents the number of moles of the permeant, V is the volume of the membrane per unit area and R and T are the gas constant and temperature. Similarly, the membrane capacity C_m has been shown[4] to be given by

$$C_m = \frac{(N_i/V) \, \Delta x}{RT} \qquad (7)$$

Inserting the magnitudes of R_m and C_m into equation (5) we arrive at the well known Einstein equation for a homogeneous membrane i.e.

$$\tau_m = \frac{(\Delta x)^2}{2 D_m} \qquad (8)$$

Calculation for Composite Membranes

The parallel membrane: A parallel composite membrane consisting of two homogeneous membrane elements, say (a) and (b) is schematically represented in Fig VII.2(a), Let us now invoke the assumptions made by Kedem and Katchalsky[12] in their theory of the permeability of parallel composite membranes, which are as follows. The flows are assumed to be parallel to the x-coordinate i.e. perpendicular to the membrane surface. The forces considered are differences of potential acting across the membrane and since the same compartment maintains contact with both membrane elements on each side of the membrane, the same force which operates on the parallel composite membrane is also operative on both the constituent membrane elements. This means that the forces are perpendicular to the membrane surface and that no lateral forces have to be considered and hence no lateral flows creating internal circulations need to be

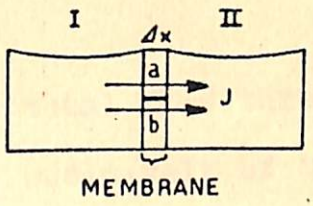

(a)

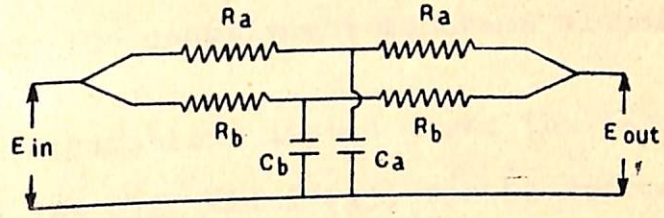

(b)

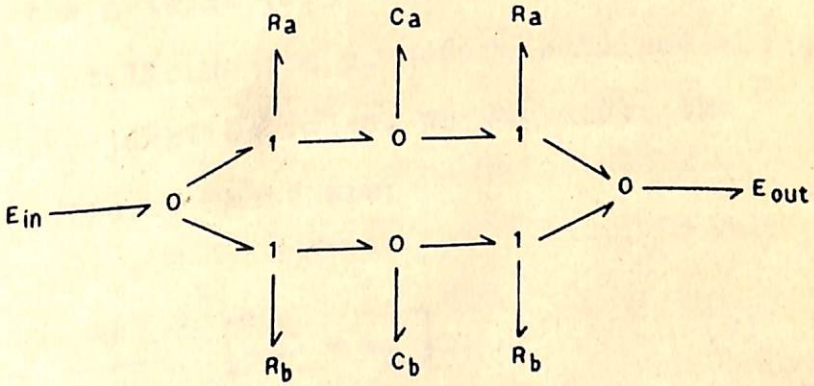

(c)

g. VII.2 (a) A parallel composite membrane, a and b represent the two constituent membrane elements . (b) Network representation of a parallel composite membrane shown in (a). (c) Bond graph representation of the network shown in (b).

taken into account. Thus, the total flow through the composite membrane is built up additively of the elementary contributions. The linear relationship between fluxes and forces is assumed to be valid for the parallel composite membrane as well as for the constituent membrane elements.

In view of the assumptions listed above the parallel composite membrane system (Fig VII 2 (a)) can be represented by the network shown in Fig VII.2(b). The bond graph representation of the network (Fig VII.2(b)) is shown in Fig VII.2(c). Now, utilising the procedure outlined above and making use of the junction rules, we can write the governing state equations. These are:

$$\frac{d\,\mu_a}{dt} = \frac{2}{R_a\,C_a}\left[\langle\mu\rangle - \mu_a\right] \qquad (9)$$

and

$$\frac{d\,\mu_b}{dt} = \frac{2}{R_b\,C_b}\left[\langle\mu\rangle - \mu_b\right] \qquad (10)$$

It is obvious from equation (9) and (10) that the parallel composite membrane system (Fig VII.2(a)) represented by the networks (Fig VII.2b or 2c) will have two relaxation times, one each for the two constituent membrane elements. Thus

$$\tau_a = \frac{R_a C_a}{2} \qquad (11)$$

and

$$\tau_b = \frac{R_b C_b}{2} \qquad (12)$$

This is also in keeping with the physical reality. The time required by the two constituent membrane elements to become saturated with the permeant would be different and hence the constituent membrane element that requires the longer time to become saturated with the permeant would determine the relaxation time for the total parallel composite membrane. Thus if $\tau_a > \tau_b$ then τ_a would be the relaxation time for the parallel membrane.

In the particular case when a=b the parallel composite membrane would become a single homogeneous membrane having a cross sectional area twice that of a single constituent membrane element. The relaxation time for such a membrane would be the same as that of the single constituent membrane element a or b i.e. $\tau_m = \tau_a = \tau_b$. This is what it should be according to the Einstein equation (equation (8)).

The series membrane: The series composite membrane consisting of two homogeneous constituent membrane elements, say a and b, is schematically represented in Fig. VII.3 a. In this case also let us bear in mind the assumption made by Kedem and Katchalsky[13] in their theory of the permeability of series composite membranes. Relevant among these for the present discussion are the following. All flows passing through the membranes are assumed to be perpendicular to the membrane. Flows through the series composite membrane as well as through the constituent membrane elements are adequately described by linear relationships between fluxes and forces. The potentials of the thermodynamic driving forces are assumed to be continuous across all boundaries in the system. This condition, first formulated by Kirkwood[14], means that approaching any point x in the system from the right or the left leads to the same potential. The physical reason for this is that if the transition layer between the two neighbouring phases (the two constituent membrane elements in the present case) is infinitely thin its resistance to flow will be zero. Hence, if the potential difference across the transition layer does not vanish, infinite local flow will develop. What is implied therefore, is that there cannot be a potential drop across the transition boundary within the series composite membrane.

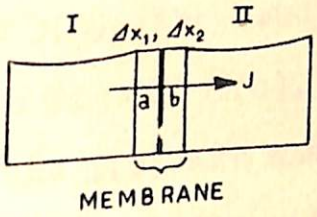

(a)

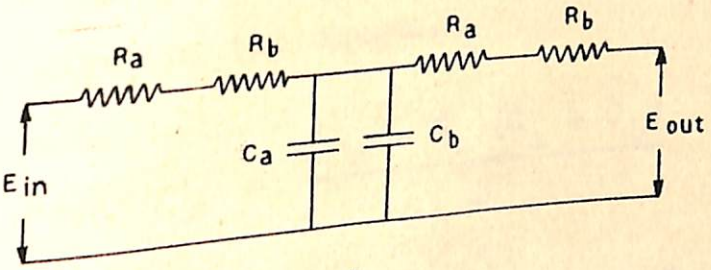

(b)

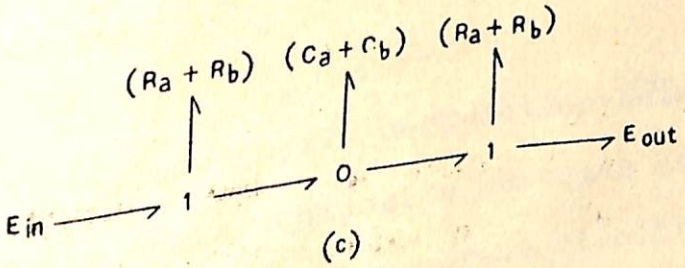

(c)

Fig. VII.3 (a) A series composite membrane, a & b represent the two constituent membrane elements. (b) Network representation of the series membrane shown in (a). (c) Bond graph representation of the network shown in (b).

In view of these assumptions the series composite membrane (Fig VII.3.a) can be represented by the network shown in Fig VII 3(b), the bond graph representation of which is shown in Fig VII 3(c). Since the networks shown in Fig VII.3(b) and 3(c) are analogous to the networks shown in Figs VII.1b and 1 c, it is easy to see that the relaxation time (τ_s) in the case of a series membrane would be given by the equation

$$\tau_s = \frac{(R_a + R_b)(C_a + C_b)}{2} \qquad (13)$$

which can be conveniently transformed into

$$\tau_s = \tau_a \left(1 + \frac{C_b}{C_a}\right) + \tau_b \left(1 + \frac{C_a}{C_b}\right) \qquad (14)$$

Equation (14) provides a correlation between the relaxation time for the series composite membrane and the relaxation time for the constituent membrane element.

In this case also, if a=b the series composite membrane would become a single homogeneous membrane whole thickness would be twice the thickness of the single constituent membrane element. It follows from equation (14) that the relaxation time for such a membrane would be

four times the relaxation time for the single constituent membrane element. This conclusion is in accordance with the Einstein equation (equation (8)).

Since the constituent membrane elements are assumed to be homogeneous equation (11), (12) or (14) can be further transformed using equations (6) and (7) to get the relationships in terms of diffusion coefficients for the constituent membrane elements.

VII.3 THE CASE OF ENZYME CATALYSED REACTION

In this section attempt has been made to utilise the formalism of network thermodynamics to calculate the steady state reaction velocity and the relaxation time for an enzyme catalysed reaction.

Let us consider the well known enzyme catalysed reaction scheme

$$E + S \underset{k_1'}{\overset{k_1}{\rightleftharpoons}} ES \underset{k_2'}{\overset{k_2}{\rightleftharpoons}} E + P \qquad (15)$$

(I) (II)

where E, S, ES and P represent enzyme, substrate, enzyme-substrate complex and product respectively. If J_1 and J_2, respectively, represent the reaction rates of the step (I)

and step (II) of the reaction scheme (15) one can write

$$\frac{d\,[E]}{dt} = J_2 - J_1 \qquad (16)$$

and

$$\frac{d\,[ES]}{dt} = J_1 - J_2 \qquad (17)$$

The reaction sites J_1 and J_2 can be written[15] in terms of the affinities A_1 and A_2 of the steps (I) and (II) of the reaction scheme (15) i.e.

$$J_1 = k_1[E]\,[S]\,\{1 - \exp\,(-\frac{A_1}{RT})\} \qquad (18)$$

$$J_2 = k_2\,[ES]\,\{1 - \exp\,(-\frac{A_2}{RT})\} \qquad (19)$$

When the reaction is close to equilibrium the equation (18) and (19) reduces to

$$J_1 = k_1[E][S]\,\frac{A_1}{RT} \qquad (20)$$

and

$$J_2 = k_2\,[ES]\,\frac{A_2}{RT} \qquad (21)$$

where R is the usual gas constant and the affinities A_1 and A_2 are defined as

$$A_1 = \mu_E + \mu_S - \mu_{ES} \tag{22}$$

and
$$A_2 = \mu_{ES} - \mu_E - \mu_P \tag{23}$$

μ being the chemical potential of the species denoted by the subscripts.

Now let us turn our attention to network modelling and analysis. Following the network thermodynamics considerations[4,5] the chemical reaction system (15) can be represented by a two-port network shown in Fig VII.4(a). The bond graph representation[10,11] of the two port network Fig VII.4(a) has been shown in Fig VII.4(b) where $(- \overset{|}{0} -)$ represents a parallel or a zero junction and $(- \overset{|}{1} -)$ represents a series or a one-junction. Applying Kirchoff voltage law and Kirchoff current law to the network shown in Fig VII.4, we can write

$$J_1 = \frac{\mu_S + \mu_E - \mu_{ES}}{R_1} \tag{24}$$

and
$$J_2 = \frac{\mu_{ES} - \mu_E - \mu_P}{R_2} \tag{25}$$

where R_1 and R_2 are the resistive elements (Fig VII.4). For the flow through the capacitors representing enzyme-substrate complex and enzyme one can write

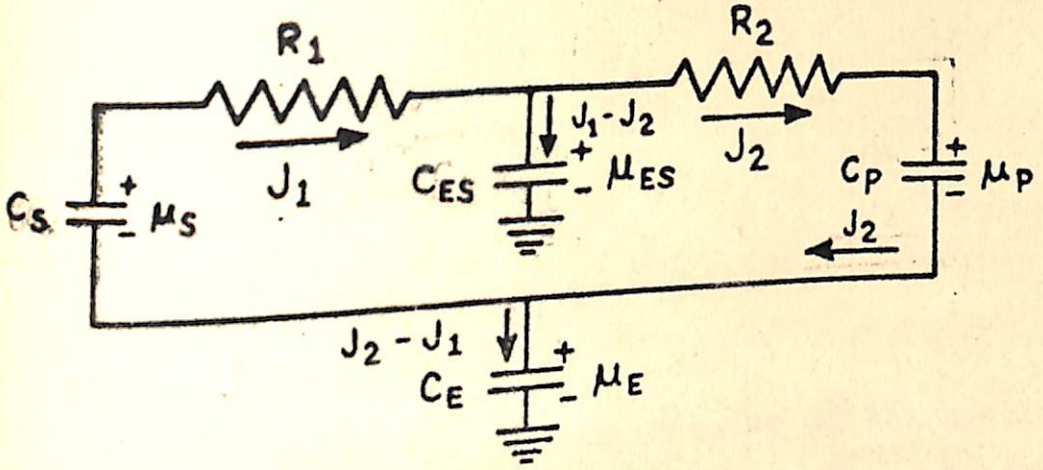

(a)

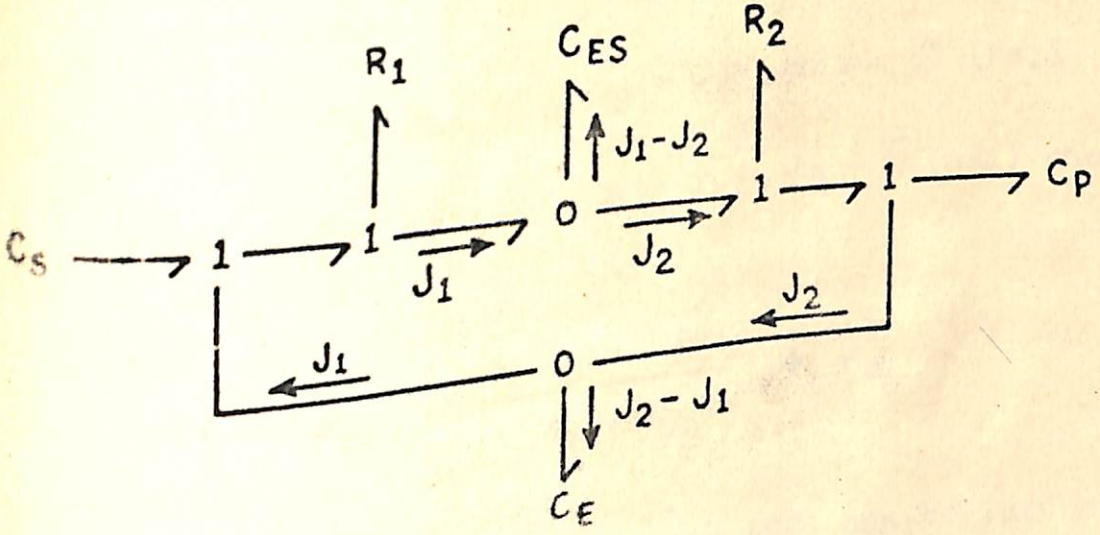

(b)

Fig. VII.4(a) A two-port network representing the enzyme catalysed reaction $E+S \rightleftharpoons ES \rightleftharpoons E+P$ R_1 and R_2 are resistances. C_S, C_{ES}, C_P and C_E are capacitances of the capacitors representing substrate, enzyme-substrate complex, product and enzyme.

(b) Bond graph representation of the network shown in (a).

$$J_1 - J_2 = C_{ES} \frac{d\mu_{ES}}{dt} \qquad (26)$$

$$J_2 - J_1 = C_E \frac{d\mu_E}{dt} \qquad (27)$$

where C stands for the capacitance of the species denoted by the subscripts. From equations (26) and (27) it follows that

$$C_{ES}\,\mu_{ES} + C_E\,\mu_E = \text{Constant} = \mu^\circ \text{ (say)} \qquad (28)$$

Since at the steady state $J_1 = J_2 = \bar{J}$ (say) one can write from equation (24) and (25)

$$\mu_{ES} = \frac{R_2\,\mu_S + R_1\,\mu_P}{R_1 + R_2} + \mu_E \qquad (29)$$

Using equation (28), equation (29) can be further transformed into

$$\mu_{ES} = \frac{R_2\,\mu_S + R_1\,\mu_P}{R_1 + R_2} \cdot \frac{C_E}{C_E + C_{ES}} + \frac{\mu^\circ}{C_E + C_{ES}} \quad \ldots\ldots \qquad (30)$$

Equation (30) gives the value of μ_{ES} at the steady state. Similarly for the value of μ_E at the steady state we can

write

$$\mu_E = \frac{R_2\ \mu_S + R_1\ \mu_P}{R_1 + R_2} \left(= \frac{C_{ES}}{C_E + C_{ES}} \right) + \frac{\mu^\circ}{C_E + C_{ES}} \quad \ldots\ldots \quad (31)$$

Now substituting the steady state values of μ_{ES} from equations (30) and (31) into equation (24) we get

$$\bar{J} = \frac{\mu_S - \mu_P}{R_1 + R_2} = \frac{A_1 + A_2}{R_1 + R_2} \quad (32)$$

Comparing equations (20) and (21) with equations (24) and (25) one can write

$$R_1 = \frac{RT}{k_1\ [E][S]} \quad \text{and} \quad R_2 = \frac{RT}{k_2\ [ES]} \quad (33)$$

Substituting the values of R_1 and R_2 from equation (33) in equestion (32) we get

$$\bar{J} = \frac{A_1 + A_2}{RT} \cdot \frac{k_1\ k_2\ [E]\ [S]}{k_2 + k_1 \frac{[E][S]}{[ES]}} \quad (34)$$

Since at steady state

$$\frac{[ES]}{[E]\,[S]} = \frac{k_1}{k_1'} \qquad (35)$$

the equation (34) can be rewritten in the form

$$\bar{J} = \frac{A_1 + A_2}{RT} \cdot \frac{k_2\,[E][S]}{K_m} \qquad (36)$$

where K_m is the well known Michaelis-Menter constant and is given by

$$K_m = \frac{k_2 + k_1'}{k_1} \qquad (37)$$

The equation (36) arrived at from network consideration, is an expression for the reaction velocity at the steady state.

Calculation of Relaxation Time: When the concentration of the substrate greatly exceeds that of the enzyme and the enzyme-substrate complex, a steady state is reached. In the steady state flow through the enzyme-substrate capacitor and the enzyme capacitor ceases (equations 26 and 27). For calculating the relaxation time for the chemical reaction system (15) one has to calculate the RC time for the network shown in Fig VII.4. Making use of the laplace

transform method[16] the RC time which equals the relaxation time for the chemical reaction system (15) can be shown to be given by

$$\frac{1}{\tau} = \left(\frac{1}{R_1} + \frac{1}{R_2}\right) \frac{1}{C_{ES}} \qquad (38)$$

Now making use of the definition[4] of the generalised capacitance i.e. in the present case

$$C_{ES} = \frac{[ES]}{RT} \qquad (39)$$

and substituting the values of R_1 and R_2 from equation (33) in equation (38) we can write

$$\frac{1}{\tau} = \frac{k_1[E][S]}{[ES]} + k_2 \qquad (40)$$

Since the equilibrium between enzyme, substrate and enzyme-substrate complex is reached very fast equation (35) can be utilised to transform equation (40) into

$$\frac{1}{\tau} = k_1' + k_2 \qquad (41)$$

which gives an expression for the relaxation time in terms of the velocity constants.

VII.4 REFERENCES

1. J. Meixner, J. Math. Phys. 4, 154 (1963).

2. J.Meixner, Arch. Ration. Mech. Analysis, 17, 278 (1964).

3. J.Meixner, Network theory in its relation to thermodynamics, in Proceedings of the Symposium on Generalised Networks, Polytechnic Press of the Polytechnic Institute of Brooklyn, pp 13-25 (1966).

4. G. Oster, A.Perelson and A.Katchalsky, Nature 234, 393 (1971).

5. G.Oster, A.Perelson and A.Katchalsky; Quart. Rev. Biophysics, 6, 1 (1975).

6. H.A. Daynes, Proc. Roy. Soc., 97A, 286 (1920).

7. H.L. Frisch, J.Phys. Chem., 63, 1249 (1959).

8. J.A. Barrie, J.D.Levi A.S.Michaels and P. Wang, Trans. Faraday Soc., 59, 869 (1963).

9. R.Ash, R.M.Basser and D.G. Palmer, Brit. J. Appl. Phys., 16, 873 (1965).

10. H. Paynter, Analysis and Design of Engineering Systems, MIT, Cambridge, Mass. (1961).

11. D. Karnopp and R. Rosenberg, Analysis and Simulation of Multiport Systems, MIT, Cambridge, Mass. (1968).

12. O. Kedem and A. Katchalsky, Trans. Faraday Soc., 59, 1931 (1963).

13. O.Kedem and A. Katchalsky, Trans. Faraday Soc., 59, 1941 (1963).

14. J.G. Kirkwood, in H.T. Clark (Ed.), Ion transport across Membranes, Academic Press, New York, 1954, P. 119.

15. I.Prigogine; Introduction of thermodynamics of irreversible processes, Wiley pp 147 (1967).

16. M.E. van Valkenburg; Network Analysis, Prentice-Hall (1974).

SUMMARY

S U M M A R Y

A concise chapterwise summary is given below.

CHAPTER I

Since the studies reported in the subsequent chapters (chapter II to VI) relate either to the phenomena of osmosis or electro-osmosis, a brief account of the non-equilibrium thermodynamic theory for both electro-osmotic and osmotic effects has been given in this chapter. A brief discussion of the phenomenological coefficients describing various osmotic effects, in terms of Spiegler's frictional model has also been given.

Since the studies reported in chapter VII relate to network thermodynamic modelling, basic tenets and methodology of network thermodynamics have been summarized in this chapter.

CHAPTER II

Substantial amount of research effort in the area of water desalination by reverse osmosis has been invested in search for suitable membranes. Since clays are known

to possess salt rejecting properties when aqueous solution of salts are forced through them, it is tempting to assess the performance and efficiency of compacted clay membranes in hyperfilteration operation.

With this object in view the experiments on simultaneous transport of salt (sodium chloride) and water through a kaolinite clay membrane reported in this chapter have been performed. For this we have designed our own osmometer. This data and the data of Letey and Kemper available in literature on the osmosis of aqueous sodium sulphate solutions through a bentonite clay membrane have been analysed in the light of non-equilibrium thermodynamics of hyper-filteration, to throw light on the salt sieving behaviour of these clays. The three parameters namely filteration coefficient L_p, reflection coefficient σ and the salt permeability ω which adequately describe the salt rejection properties of a membrane system have been evaluated for both kaolinite/sodium chloride solutions and bentonite/sodium sulphate solution systems. Utilising the data on L_p, σ and ω thus obtained the salt rejection performance of both kaolinite and bentonite clay membranes, in a hyperfilteration process has been assessed using the formalism developed by Johnson, Dresner and Kraus.

The data on L_p, σ and ω have been further utilised to assess how efficient these clay membranes would be for salt rejection in a reverse osmosis operation by using the criteria for efficient hyperfilteration membranes developed by Spiegler and Kedem from the consideration of thermodynamics of hyper-filteration. The criteria developed by Spiegler and Kedem can be stated as follows

$$f_{sm} >> f_{wm} \qquad (1)$$

$$f_{sm} >> f_{sw} \qquad (2)$$

where f stands for the coefficient of friction between the species denoted by the subscripts. The subscripts s, m and w respectively stand for salt, membrane and water. For testing the efficiency of compacted clays in reverse osmosis operation in the light of criteria of Spiegler and Kedem as stated above, the various frictional coefficients have been estimated from the experimentally determined values of L_p, σ and ω. For this the equations obtained on the basis of Spiegler's frictional model connecting L_p, σ and ω with the various frictional coefficients have been made use of.

From the values of the frictional coefficients thus estimated it has been found that the inequality (1) holds

good while the inequality (2) does not. Thus the compacted clay membranes only partially satisfy the criteria for ideal hyper-filteration membranes.

Although the compacted clays only partially satisfy the criteria for ideal hyperfilteration membranes, it has been suggested that the idea of using compacted clays as membranes in reverse osmosis operation can be given a trial because the order of magnitudes of f_{sm} and f_{sw} is more or less same. This is a significant suggestion from the point of view of reverse osmosis technology.[14]

CHAPTER III

Martin[19] observed that the addition of small amounts (of the order of a few ppm), of surfactants like poly vinyl methyl ether (PVME) to saline feed in reverse osmosis effects a large increase in the salt retention capacity of cellulose acetate membranes with but a small decrease in the flux of desalted water. The explanation of the increased permselectivity was given by Kesting et al[14] based on the hypothesis of the existence of a surfactant layer liquid membrane at the interface between the cellulose acetate membrane and the saline solution. According to Kesting's liquid membrane hypothesis as the concentration

of the surfactant is increased, the cellulose acetate membrane gets progressively covered with the surfactant layer liquid membrane and at the critical micelle concentration (CMC) the coverage of the cellulose acetate membrane with the surfactant layer is complete.

The experiments on hydraulic permeability, electro-osmotic velocity, streaming potential and current reported in this chapter lend support to Kesting's liquid membrane hypothesis. In these experiments a cellulose acetate micro-filteration membrane has been used as supporting membrane. The data have revealed that the water flux in presence of poly vinyl methyl ether does not vary proportionally with the applied pressure difference. Instead the following non-proportional exponential type of relationship

$$J_v = L_{11}[\Delta P - \Delta P_0\{1 - \exp(-\frac{\Delta P}{\Delta P_0})\}] \qquad (3)$$

where J_v is the water flux, ΔP the pressure difference, ΔP_0 is the extrapolated intercept on the ΔP-axis of the straight line portion of the J_v versus ΔP curve and the coefficient L_{11} measures the hydraulic conductivity, has been shown to describe the hydraulic permeability data. In the case of electro-osmotic velocity and streaming current, however, the usual linear relationships between

fluxes and the res pective driving forces have been found to be valid. The non-ideal flow behaviour (equation 3) appears to be the result of the flow through the PVME liquid membrane formed in series with the cellulose acetate microfilteration membrane as hypothesised by Kesting et al because the volume flux through the cellulose acetate microfilteration membrane was found to obey the ideal Darcy's law. A more definite indication of the formation of the liquid membrane is obtained from the gradation in the values of coefficient L_{11} as the concentration of PVME is increased from zero to twelve ppm - twice the CMC value (6 ppm) of PVME. Values of the coefficient L_{11} which measure conductivity to volume flow of water, show a progressive decrease as the concentration of PVME is increased from zero to six ppm (the CMC value). When the concentration of PVME is increased further the value of L_{11} also decreases but this decrease is less pronounced than the decrease which is observed upto six ppm - the CMC value for aqueous PVME. Similar trends were observed in the values of the coefficients measuring electro-osmotic velocity and streaming current. These trends are in keeping with the liquid membrane hypothesis of Kesting et al according to which, as concentration of the surfactant (PVME in the present case)

is increased the supporting membrane (the cellulose acetate microfilteration membrane) gets progressively covered with the surfactant layer liquid membrane, and at the CMC the coverage is complete. The decrease in the values of L_{11} beyond the CMC was ascribed by Kesting et al [10-1] to densing of the liquid membrane which at the CMC is fully developed and completely covers the supporting membrane.

The analysis of the data on electrical resistance and salt permeability, however, indicated that when concentration of the surfactant is increased beyond its CMC value, the increased resistance to flow is not on account of densing of the liquid membrane as proposed by Kesting et al [10-1] but due to the formation of multilayers of the liquid membrane.

The analysis for masaic membrane model [1-20] has been utilised to demonstrate that when concentration of the surfactant is half its critical micelle concentration (CMC) the area of the supporting membrane covered with the liquid membrane is half the area covered at CMC. At CMC the supporting membrane is fully covered with the liquid membrane.

CHAPTER IV

Experiments on electro-osmosis of aqueous solution of sodium chloride through a cellulose nitrate millipore filter membrane have been performed. The data obtained have been utilised to calculate the efficiencies of electro-kinetic energy conversion for both the modes of conversions namely electro-osmosis and streaming potential in addition to verifying the linear phenomenological relations. The results thus obtained have been shown to be in accordance with the non-equilibrium thermodynamic theory of electro-kinetic energy conversion [21-23]. The data reveal that in all the cases the following three conclusions i.e.

1. For a particular concentration of sodium chloride solution $(\eta_e)_{max}$ the optimum value of energy conversion efficiency for electro-osmosis was always equal to the value of $(\eta_s)_{max}$ the optimum value for energy conversion efficiency for streaming potential.
2. For a particular concentration of sodium chloride the values of $(\eta)_{max}$ the optimum value of energy conversion efficiency are independent of the input forces.
3. The maximum value of energy conversion efficiency $(\eta)_{max}$ always occurs when the output force equals half its steady state value.

derived from the non-equilibrium thermodynamic theory of electro-kinetic energy conversion hold good.

The data also reveals the concentration dependence of the phenomenological coefficients and also that $(\eta)_{max}$ with concentration.

CHAPTER V

The studies reported in this chapter are inspired by the studies on liquid membranes described in chapter III. Since bile salts are excellent surfactants, it is logical to expect that their addition to water or aqueous solution flowing through a membrane, would also give rise to the formation of such liquid membranes as detected in the experiments on poly vinyl methyl ether reported in chapter III. The experiments reported in this chapter have been designed to demonstrate this. The bile salt used in these studies is sodium deoxy cholate.

It has been demonstrated that when bile salts, are added to water or aqueous solution flowing through a membrane cellulose acetate millipore filter in the present case, a surfactant layer liquid membrane is formed at the interface between the supporting membrane i.e. the cellulose acetate

millipore filter and the aqueous solution. The data reveal that as the concentration of the surfactant is increased the supporting membrane gets progressively covered with the liquid membrane and at critical micelle concentration (5 mM in this case) coverage of the supporting membrane with the liquid membrane is complete. Area of the supporting membrane covered at concentration below the critical micelle concentration has been estimated and it has been concluded that when concentration of the surfactant is half the critical micelle concentration (CMC), the area covered is half the area covered at CMC. The liquid membranes developed have been shown to offer resistance to both water flux and salt flux.

Values of the filteration coefficients, reflection coefficient and the salt permeability for the liquid membrane have been estimated. Relative magnitudes of the frictional coefficients between salt and water, salt and the liquid membranes and water and the liquid membrane have also been estimated using Spiegler's frictional model for membrane transport.

A significant physiological implication of the studies described in this chapter is that in the transport of ions

etc. the existence of such liquid membranes in series with the usual mucosal membranes should also be taken into account.

CHAPTER VI

Experiments and the data of Dainty and Ginzburg on the hydraulic conductivity of internodal characean cells have been re-examined. The analysis has led to two significant conclusions. These are:

1. The experiments of Dainty and Ginzburg represent a situation where the linear formalism of non-equilibrium thermodynamics breaks down and the non-linear phenomenological relations of the kind suggested by Li should be taken into account.
2. The dependence of hydraulic conductivity on the direction of water movement, is on account of unequal shrinkage of the cell membrane in the exo-osmotic and endo-osmotic compartments. Thus the fact that exo-osmotic hydraulic conductivity is not equal to endo-osmotic hydraulic conductivity is not an intrinsic property of the cell membrane.

CHAPTER VII

In this chapter the network thermodynamics modelling ' has been attempted in the following two cases:

1. Transport through composite membranes
2. Enzyme catalysed reaction.

Equivalent electrical networks and the corresponding bond graphs for both the cases mentioned above have been prepared.

In the former case relaxation times for the composite membrane consisting of a parallel and a series arrangement of two constituent membrane elements have been calculated as a function of the relaxation time for the constituent me mbrane elements. In the case of parallel composite membrane it has been shown that the constituent membrane element having higher relaxation time determines the relaxation time for the total parallel composite membrane. In the case of series composite membrane the following relationship has been deduced

$$\tau_s = \tau_a \left(1 + \frac{C_b}{C_a}\right) + \tau_b \left(1 + \frac{C_a}{C_b}\right) \qquad (4)$$

where τ and C represent the relaxation time and the

capacitance for the membranes denoted by the subscripts. The subscripts s denotes the series composite membrane and a and b denote the two constituent membrane elements.

In the latter case expression for the steady state reaction velocity and relaxation time for a simple enzyme catalysed reaction (single enzyme - single substrate system) has been deduced. The results thus obtained using network thermodynamic formalism match with those obtained using usual methods of chemical kinetics and statistical consideration.

LIST OF PUBLICATIONS

1. Salt sieving by compacted clays, Indian J. Chem. 16A, 920-924 (1978).

2. Relaxation time for composite membranes, J. Membrane Sci., 3, 39-46 (1978).

3. Bile salt micelles as liquid membranes, J. Non-equilib. Thermodyn. (in press).

4. Electro-osmosis of water through liquid membranes, J. Colloid Interface Sci. (in press)

5. Permeability of liquid membranes, Indian J.Chem. (accepted).

6. Network modelling of enzyme catalysed reaction, Indian J. Chem. (accepted).

7. Trans-cellular osmosis in Internodal characean Cells, Proc. Indian Acad. Sci. (communicated).

8. Electro-osmosis of saline water through a cellulose-nitrate millipore filter membrane - Studies on electro-kinetic energy conversion, Electrochimica Acta (communicated).

9. Formation of multilayers of liquid membrane at the Cellulose acetate membrane/water interface, Desalination (communicated).